ALTERED AIRWAY SMOOTH MUSCLE CONTRACTILE FUNCTION IN THE PRESENCE OF AIRWAY EPITHELIUM AND THE INFLUENCE OF TGF-β1

by

Jonathan Tjong

Submitted in partial fulfilment of the requirements
for the degree of Master of Applied Science

at

Dalhousie University
Halifax, Nova Scotia
May 2017

Table of Contents

List of Tables

List of Figures

Abstract

Airway smooth muscle (ASM) contraction is a major contributor to bronchoconstriction, the narrowing of the airways observed in asthmatic airways. *In vitro,* ASM cells demonstrate the capacity to switch between more proliferative and more contractile phenotypes, and changes to ASM contractile function, potentially as a consequence of this phenotypic switching, may play a significant role in the exaggerated airway narrowing observed in asthma. *In vivo,* airway epithelial (AE) cells are topographically close to the ASM and may modulate and regulate ASM phenotype and function that could be dysregulated in asthma. One important mediator increased in asthma is TGF-β1, which influences AE cell phenotype and thus possibly affects AE cell effects on ASM.

In this work, we investigated the effects of AE, with and without the influence of TGF-β1, on ASM contractile function. After examining the response of AE and ASM to TGF-β1 individually, one-way and two-way communication modes between the cell types were established using conditioned media and co-culture systems as routes of exposure, respectively. Cell stiffness and changes in cell stiffness in response to KCl-induced contraction, as well as protein expression, were used to assess changes in ASM contractile function.

We found that the addition of AE-conditioned media to ASM dramatically increased ASM expression of myocardin, but interestingly this was not accompanied by increases in contractile function or in the expression of contraction-associated proteins in the ASM. In contrast, ASM cells in co-culture with AE did not show the same dramatic increase in myocardin expression observed with AE-conditioned media exposure. In both conditioned media and co-culture experiments however, we found that ASM stiffness was consistently decreased as a response to AE exposure; ASM contractility also decreased, but only via co-culture. These decreases in stiffness were also consistently accompanied by a decrease in the expression of the smMHC motor protein for both conditioned media and co-culture experiments. When TGF-β1 was added to ASM cells, calponin expression in ASM increased, independent of whether AE cells were present. Interestingly, only the addition of TGF-β1 into an AE-ASM co-culture led to the increased expression of some canonical markers for a contractile ASM phenotype, although this effect was divorced from any functional increase in ASM contractility. Overall, we show that AE cells had a relaxing effect on ASM cells and attenuated contractile function, likely due in part to the consistently suppressed expression of smMHC. These results demonstrate that AE plays an important role in regulating ASM contractile function and phenotype in culture, and that TGF-β1 may alter this AE-ASM interaction. Taken together this suggests that AE-ASM intercellular communication can play an important role in the regulation of ASM function that may be potentially altered in asthma.

List of Abbreviations Used

16HBE14o-	Human bronchial epithelial cell line 16HBE14o-
AA	Arachidonic acid
ACh	Acetylcholine
AE	Airway epithelium
ALI	Air-liquid interface
Alk1, 2, 5	Activin receptor-like kinase 1/2/5
ANOVA	Analysis of variance
ASM	Airway smooth muscle
AU	Arbitrary units
BAL	Bronchoalveolar lavage
BC3H1	Mouse brain tumor cell line BC3H1
BMP	Bone morphogenic protein
BSA	Bovine serum albumin
Ca^{2+}	Calcium (II) ion
CaM	Calmodulin
CAR	Coxsackievirus and adenovirus receptor
CB	Cytoskeleton buffer
c_{bead}	Bead constant
CI	Confidence interval
CM	Conditioned media
CNN1, 2, 3	Gene coding for calponin 1/2/3
COX-2	Cyclooxygenase-2
DAPI	4',6-diamidino-2-phenylindole
ddH_2O	Double-distilled H_2O
DMEM	Dulbecco's modified Eagle's medium
ECM	Extracellular matrix
EDA-fibronectin	Extracellular domain A-containing fibronectin
EDM	Euclidean distance map

EGF	Epithelial growth factor
EMT	Epithelial-mesenchymal transition
EpDRF	Epithelium-derived relaxing factor
ERK	Extracellular signal-regulated kinase
F-, G-actin	Filamentous/Globular actin
F12	Ham's F12 medium
FBS	Fetal bovine serum
FEV	Functional expiratory volume
FEV1	Functional expiratory volume over 1 second
FGF	Fibroblast growth factor
FOXA1/2, C2, O	Forkhead box protein A1/A1/C2/O
FSP	Fibroblast-specific protein
G*	Complex modulus G
G'	Storage/elastic modulus G
G''	Loss/inelastic modulus G
GABA	Gamma-amino butyric acid
GPCR	G-protein coupled receptor
H1	Histamine H_1 receptor
HASM	Human airway smooth muscle
HB-EGF	Heparin-binding EGF-like growth factor
HCl	Hydrochloric acid
HDM	House dust mite
$H_z(t)$	Time-varying magnetic field
IF	Intermediate filament
IgE	Immunoglobulin E
IL	Interleukin
IP_3	Inositol triphosphate
IR	Infrared
IT	Insulin/transferrin-supplemented media
JNK	c-Jun N-terminal kinases

kDa	Kilodalton
Ki67	Antigen identified by monoclonal antibody Ki-67
LAP	Latency-associated peptide
LTBP	Latent TGF-β binding protein
M	Magnetic moment vector
mAB	Monoclonal antibody
MAP, MAPK	Mitogen-activated Protein Kinase
MEF2C	Myocyte-specific enhancer factor 2C
MET	Mesenchymal-epithelial transition
MHC	Myosin heavy chain
MLC	Myosin light chain
MLC_{20}	Myosin light chain (20 kilodalton regulatory subunit)
MLCK, MYLK	Myosin light-chain kinase
MLCP	Myosin light chain phosphatase
MMP	Matrix metalloproteases
M-RIP, MPRIP	Myosin phosphatase Rho-interacting protein
MYH11	Myosin-11, Smooth muscle myosin heavy chain
NHBE	Normal human bronchial epithelium
NO	Nitric oxide
OMTC	Optical magnetic twisting cytometry
p120-	Catenin delta-1
p38	p38 mitogen-activated protein kinase
p53	Cellular tumor antigen p53
PBS	Phosphate buffered saline
PCNA	Proliferating cell nuclear antigen
PIP_2	Phophatidylinositol 4,5-bisphosphate
px	Pixels
RGD	Arginine-Glycine-Aspartate
RhoA	Ras homolog gene family, member A
ROCK	Rho-associated protein kinase

ROI	Region of interest
RT	Room temperature
SD	Standard deviation
SEM	Standard error of the mean
shRNA	short hairpin RNA
SM-1, 2, A, B	Smooth muscle myosin heavy chain isoform 1/2/A/B
Smad1, 2, 3, 5, 8	Mothers against decapentaplegic homolog 1/2/3/5/8
smMHC	Smooth muscle myosin heavy chain, Myosin-11
SNR	Signal-to-noise ratio
SRF	Serum response factor
SV40	Simian vacuolating virus 40
T	Tesla
T25/75	Tissue culture flask (25 cm^2, 75 cm^2)
TEAD1/2	TEA domain family member 1/2
TEER	Transepithelial electrical resistance
TGF-β RI, II, III	TGF-β receptor I/II/III
TGF-β1, 2, 3	Transforming growth factor beta 1/2/3
Th17	T-helper type 17
Th2	T-helper type 2
$T_s(t)$	Specific torque
V_{max}	Maximum velocity of shortening
α-SMA	Alpha smooth muscle actin

Chapter 1: Introduction

1.1 Asthma

Asthma is a disorder of the airways that can be characterized by airway inflammation, hyperresponsiveness, and remodeling, ultimately leading to airway narrowing. While asthma is often treatable and can be well-controlled, without a clear or complete picture of how asthma develops, it is also both unpreventable and incurable[1]. At present, the management of asthma predominantly utilizes β_2-adrenergic agonists, which work directly on the airway smooth muscle to cause relaxation, and treatments that focus on the inflammatory aspect of the disease (classically glucocorticoids, and more recently anti-IgE and anti-leukotriene agents) to limit the chronic inflammation of the airways[1,2]. Unfortunately, asthma is a heterogeneous and complex disease, with multiple potential phenotypes and etiologies, and current treatments are not universally efficacious, nor do they effectively alter the course of the disease[3]. Improving the treatment of asthma will require a better understanding of the interrelated mechanisms of inflammation, hyperresponsiveness, and remodeling and their roles in the disease.

In the inflammatory component of the disease, it is hypothesized that for a large subset of patients, sensitization to an allergen is mediated by T-helper type 2 (Th2) cells and the associated cytokines interleukins (IL)-4, IL-5, and IL-13, which lead to B-cell production of immunoglobulin E (IgE) and the recruitment of eosinophils typical of allergic asthma[4–6]. Other inflammatory pathways may be active in some phenotypes of asthma (such as in late-onset asthma), which can be non-atopic (i.e. not associated with allergen exposure), or may involve alternate mediators, including Th17 cells, IL-17, and neutrophilic inflammation, suggesting a diverse heterogeneity within asthma[1,4,7]. Airway hyperresponsiveness is strongly associated with asthma, and is an increased sensitivity of the airways to stimuli, which may be described as a

leftward shift of the dose-response curve of a bronchial challenge (e.g. methacholine or histamine) and the resulting excessive airway narrowing due to airway smooth muscle contraction, which results in an increased maximum response by the airways, reducing the diameter of the airways by a greater magnitude compared to normal airways[8–10]. Also associated with asthma is airway remodeling, which refers to structural changes to the cellular organization of the airways, and can involve the hypertrophy or hyperplasia of the cells in airway tissues, as well as changes to the extracellular matrix (ECM), and even angiogenesis[11–13]. Indeed, a commonly found feature in asthma is the thickening of the airway walls as a result of remodeling[14,15]. These components of asthma are hypothesized to have close and complex links to one another; for instance, eosinophilic inflammation can result in damage to the structural integrity of the epithelial layer, which normally acts as a physical barrier[10,16]. Disruption of this barrier function may then allow an increase diffusion rate of spasmogens into the airway walls, altering airway responsiveness[10,17].

1.2 Transforming Growth Factor-β1 (TGF-β1)

1.2.1 Background

TGF-β1 is a signaling protein that is widely expressed in multiple tissues, and while it is thought to be involved in a variety of respiratory and other disease processes, in the airways in asthma, it is thought to play a role in airway remodeling. Its active form is a 25 kDa protein that is composed of two identical 12.5 kDa subunits linked by cysteine bonds, forming a homodimer[18]. However, it is typically present in its inactive form, non-covalently complexed with latency-associated peptide (LAP), another dimeric protein which is, interestingly, the N-terminal region of the TGF-β1 pro-peptide prior to post-translational cleavage[19,20]. The TGF-β1-LAP complex can also in turn be bound to latency binding proteins (LTBP), large 125-210 kDa

proteins that associate with the extracellular matrix (though binding to LAP is sufficient to inactivate TGF-β1)[19,21]. These are referred to as small and large latent TGF-β1 complex, respectively[19]. The multiple isoforms of LTBP may differentially localize TGF-β to specific regions in the ECM, and this localization may be important, as knockouts for some LTBP isoforms in murine models show changes in phenotype similar to changes that might be expected as a result of altered TGF-β signaling[22,23]. Consequently, the ubiquity of TGF-β1 and its receptors in tissues suggests that the post-translational release of TGF-β1 from these complexes plays a large role in the regulation of active TGF-β1[19].

In mammals, three isoforms of the TGF-β family are primarily present: TGF-β1, TGF-β2, and TGF-β3. They are the result of separate but similar genes, rather than alternative splicing, though any of these three isoforms have the ability to bind to the TGF-β specific signaling receptors[24]. However, subtle differences between the TGF-β ligand isoforms do exist; for instance, TGF-β2 has a significantly lower affinity for the TGF-β RII receptor compared to the β1 and β3 ligands, unless the receptor TGF-β RIII (also known as betaglycan) is also present on the cell membrane[24–27]. Additionally, knockout mice for each of the three TGF-β isoforms indicate that the absence of any of these ligands have significant deleterious effects *in vivo*, despite their interchangeable binding[28–31]. It is also worth noting that the three TGF-β isoforms belong to a larger group of ligands that include BMPs (bone morphogenic proteins), Activin, and other signaling proteins, and are sometimes collectively referred to as the TGF-β superfamily of ligands; however, for this proposal TGF-β will simply refer to the three initially mentioned isoforms.

As with the superfamily of TGF-β ligands there is also a 'superfamily' of TGF-β receptors. Structurally and functionally, these receptors are typically transmembrane, homodimeric, serine-threonine kinases[32]. They can be classified into either type II (RII) or type I (RI) receptors,

which form homodimers that can then associate in an activated receptor complex consisting of both type RII and RI homodimers[32]. The canonical receptors for TGF-β are, specifically, the TGF-β RI receptor (also commonly known as the Alk5 receptor in literature), and the TGF-β RII receptor[25]. TGF-β ligands activate their signaling pathway by first binding to the TGF-β RII receptor, which subsequently recruits a TGF-β RI (Alk5) receptor to form a stable complex in which the TGF-β RI receptor is then phosphorylated[25,33]. Interestingly, TGF-β bound to the TGF-β RII receptor can also activate other type I receptors, such as Alk1 and Alk2[25]. This has the effect of activating alternate intracellular signaling pathways. For instance, the inclusion of the Alk5 receptor may activate the Smad2/3 pathways, whereas the Alk1 and Alk2 receptors can activate the Smad1/5/8 pathways[32]. In order to obtain specificity in the cellular response, extensive regulation at each level of the pathway must occur, which can include the activation of the TGF-β ligand, receptor availability, intracellular regulation of the Smad pathway, and cell and context specific transcription factors[34]. TGF-β may also act on a number of non-Smad pathways. For instance, the MAP kinase pathways for JNK and p38 can act independent of Smads to induce apoptosis, while other pathways, such as the MAP kinase Ras-Erk pathway may cooperate with Smads to induce epithelial-mesenchymal transition in epithelial cells[35–38].

The activation of TGF-β from its inactive, ECM-bound form to its active form can be the result of multiple potential processes, including the action of trombospondin-1, plasmin, and MMP-9, among a myriad of proteins that can play a role in tissue growth and repair[39–42]. With respect to cells from the airways, wounding of bronchial epithelial cells led to conversion of latent TGF-β1 and 2 into their active forms, and the presence of active TGF-β1 enhanced epithelial cell migration in the subsequent repair process[43]. Additionally, TGF-β may be activated by several integrins, proteins on the cell surface that facilitate binding to the ECM, including the

αVβ5 integrin, which is present on ASM cells and, interestingly, can facilitate TGF-β activation by the contractile agonists lysophosphatidic acid (LPA) and methacholine[44,45].

1.2.2 Elevated TGF-β1 in Asthma

Although the increased expression of TGF-β1 in asthma has in the past been debated, the current preponderance of evidence suggests that it is indeed elevated[24]. In the induced sputum samples of asthma patients followed longitudinally, Nomura et al. observed an increase in TGF-β positive cells as functional expiratory volume (measured as %FEV1, i.e. actual FEV over one second as a percent of expected FEV) decreased[24,46]. Elevated TGF-β1 concentrations were also observed in the bronchoalveolar lavage (BAL) fluid of asthma patients 24 hours after segmental allergen challenge[47]. In addition, the level of active TGF-β1 in the BAL fluid of patients with acute severe asthma (i.e. an exacerbation of asthma) is dramatically increased compared to both control subjects without asthma and subjects with stable asthma, further suggesting that TGF-β1 may also be transiently increased within asthma[24,48]. More recently, the use of a less invasive sampling technique by Matsunaga et al. utilizing exhaled breath condensate, which avoids excess mechanical stimulation of the airways during sample collection, saw elevated levels of several growth factors and cytokines, including TGF-β, when comparing patients with stable asthma to controls[24,49]. Further evidence for the presence of TGF-β comes from studies of the downstream TGF-β effector pathways, such as the increase in phosphorylated (and therefore activated) Smad2 in subjects with asthma and atopic asthma following allergen challenge[50–52]. We are currently interested in examining the role of increased TGF-β1 in the airway tissues, specifically the airway smooth muscle and the airway epithelium. Both tissues can undergo dramatic changes in asthma, and our overarching goal is to investigate whether the dysregulation of TGF-β1 in asthma may contribute to these changes.

1.3 Airway Smooth Muscle Cells

Airway smooth muscle (ASM) cells play a major role in the pathology of asthma, most notably through its role in bronchoconstriction in acute asthma. *In vivo* contraction occurs when an agonist binds to G-protein coupled receptors (GPCRs, e.g. histamine binding to the H1 receptor), leading to a intracellular cascade resulting in the cleavage of PIP_2 to release IP_3, which opens calcium channels on the membrane of the sarcoplasmic reticulum (SR) induces intracellular Ca^{2+} ion release from the SR[53]. Ca^{2+} binding to calmodulin activates myosin light-chain kinase (MLCK) which goes on to phosphorylate the 20 kDa myosin light chain (MLC_{20}) and contribute to the crossbridge cycling needed for muscle contraction[53,54]. In our cell culture models, to be introduced below, KCl will generally be used to directly trigger membrane depolarization. The ratio between extracellular and intracellular K^+ concentrations contributes significantly to the resting membrane potential of cells due to the permeability of the cells to K^+. Assuming the contribution of K^+ permeability predominates at rest, the typical intracellular concentration of K^+ in a mammalian cell at 139 mM with a typical extracellular concentration of K^+ at 4 mM can result in a membrane potential of approximately -94.8 mV (via the Nernst equation, shown below where R = 8.314 $J \cdot K^{-1} \cdot mol^{-1}$, T = 310.15 K, z = 1, and F = 96 485 $C \cdot mol^{-1}$)[55].

$$V = \frac{RT}{zF} \ln \frac{[K^+_{extracellular}]}{[K^+_{intracellular}]}$$

With an increase in extracellular K^+ concentration (in our case, an isotonic KCl solution at 80 mM added at a 1:2 ratio to cell culture media, resulting in a final extracellular concentration of approximately 27 mM of K^+) would result in a depolarization of the membrane potential to approximately -43.8 mV. This depolarization would subsequently lead to the opening of voltage-dependent calcium channels, allowing Ca^{2+} influx, thereby bypassing the need for GPCR activation[54].

Smooth muscle cells (SMC) have a degree of phenotypic plasticity and may adopt a span of phenotypes, ranging from a 'synthetic/proliferative' to a 'contractile' phenotype, in response to external environmental cues[56,57]. This phenotypic plasticity is distinct from the property of mechanical plasticity also observed in SMCs (where cytoskeletal rearrangement in SMCs contribute to the maintenance of the tension-generating capacity of individual cells)[56,58]. SMCs taking on a more synthetic/proliferative phenotype express fewer contractile proteins and have a greater volume fraction of organelles associated with synthesis. In contrast, SMCs that take on a more contractile phenotype have a more elongated, spindle-shaped morphology and develop contraction-associated features, including contractile filaments and receptors to potential contraction-inducing agonists[56,57]. Interestingly, both *in vivo* and *in vitro*, any population of SMCs are heterogeneous, with the potential for distinct subpopulations of SMCs[56].

1.3.1 Airway Smooth Muscle in Asthma

As a result of remodeling in the asthmatic airways, the ASM layer is noticeably thicker compared to normal airways, likely as a result of hyperplasia of the ASM cells[11]. Increased proliferation of ASM cells in asthmatic airways has been demonstrated *in vitro* through cell counts and tritiated thymidine assays of cultured primary cells from patients with asthma, as well as *in vivo* by detection of cell proliferation markers PCNA and Ki67[59,60]. It may follow that a thicker ASM layer would have a larger cross-sectional area and could contract with a greater total force in response to a spasmogens, thereby contributing to airway hyperresponsiveness[61]. However, since more ASM cells, like other SMCs, have a degree of phenotypic plasticity, ASM cells in asthma may not necessarily generate more force per cell to contribute to airway hyperresponsiveness; hyperplastic ASM may then generate less force per cell, while still being more contractile as a whole[56].

Although it is debatable if ASM cells in asthma contract with greater force per cell compared to normal ASM cells[62], the ASM in asthmatic airways can contract with a greater velocity of shortening (V_{max}) and greater degree of shortening, compared to normal airways[63]. The increase in V_{max} may directly translate into a greater magnitude of contraction (i.e. Δ length, and not necessarily an increase in total force) which contributes to an overall narrower airway[64]. This increase in V_{max} and magnitude change in length in asthma has been observed at the level of a single cell and with ASM tissue strips, with the effect being preserved even under an oscillating load[65,66].

Where does this increase in V_{max} come from? One possibility that has been put forth is that an increase in the concentration of MLCK increases the rate of cross-bridge cycling, thereby increasing V_{max}. This hypothesis is primarily supported by linear correlations observed between V_{max} and MLCK levels, as well as increased MLCK measured in asthmatic patients, but whether this mechanism actually occurs remains controversial[67–69]. Alternatively, an increased expression of a faster-cycling smooth muscle myosin isoform may also contribute to increased V_{max}[69]. In motility assays, the purified myosin of hyperresponsive Fisher rats (which had a higher amount of the myosin isoform SM-B) could propel actin filaments faster than the purified myosin of hyporesponsive Lewis rats[69]; additionally, an SM-B knockout in another rodent model found a corresponding decrease in shortening velocity[70].

1.3.2 Effects of TGF-β1 on Airway Smooth Muscle

The direct application of TGF-β1 to ASM cells in culture can lead to a variety of consequences that may be applicable to asthma. Increased proliferation of ASM cells upon exposure to TGF-β1 has been shown to occur in a dose-dependent manner[71,72]. The effect of TGF-β1 on ASM cell proliferation acts along certain MAPK pathways, including ERK, JNK, and

p38, but likely not through Smad pathways[71,72]. Interestingly, TGF-β also led to the increased expression of α-smooth muscle actin (α-SMA), an increase in short-isoform MLCK (which is classically-associated with contraction, unlike its longer isoform), and an increase in smooth muscle myosin heavy chain (smMHC) in a proportion of exposed cells[73,74]. Finally, TGF-β regulates ASM cell synthesis of ECM proteins, the deposition of which would play a major role in airway remodeling[75,76].

1.4 Airway Epithelial Cells in Asthma

The airway epithelium (AE) is a pseudostratified layer of multiple epithelial cell types that line the luminal surface of the airways. This layer takes on the appearance of a stratified epithelium with multiple cell layers because their nuclei may be positioned at different 'depths', but all cells maintain some contact with the basal lamina and are thus formally composed of a single layer, albeit with some cells that are not exposed to the lumen. Their location on the luminal surface provides a crucial barrier function between the external environment and the underlying cells. Tight junctions and adherens junctions between the airway epithelial cells help maintain a continuous, impermeable physical barrier and maintain an apical-basal polarity with regard to the distribution of membrane proteins on the AE cells[77,78]. The composition of the AE layer is not homogenous; it is comprised of a number of AE cell subtypes with varying functions. Goblet cells secrete mucous into the luminal space, while ciliated AE cells transport the mucous (and any undesired particles trapped in the mucous) up from the bronchi into the throat through concerted ciliary beating[77,78]. Club cells, another type of AE cell, may be able to break down foreign molecules via a cytochrome P450 system and can also act as a progenitor cells in the small airways[77]. Finally, basal AE cells, which in accord with their namesake are typically found basal to the other AE cell types, mainly provide a contiguous barrier, serve as primary attachment points to the basement membrane for other AE cell types, and play the role of

progenitor cells in the larger airways[77]. These individual cell functions highlight the multiple modes of protection the airway epithelium provides.

Changes to the airway epithelium can occur in asthma, which may impair the normal protective function of the epithelium. Histological examinations of biopsied tissue show extensive damage in asthmatic epithelium, along with the loss of cell-cell desmosomal contacts, and the supplanting of mature columnar cells with basal cells[79,80]. Furthermore, it is also possible that the damage observed in asthmatic epithelium is an artifact of the biopsy procedure, in which case, would suggest that the airway epithelium is not simply damaged in asthma but is more susceptible to damage[79]. This would be consistent with the observed loss of desmosomes and the pseudostratified nature of the airway epithelium, since while basal cells may be firmly bound to the basement membrane via hemidesmosomes, basal cell attachments to other AE cells via desmosomes would be compromised. AE cells in asthma also have reduced expression of E-cadherin, which contribute to adherens junctions[3]. The loss of tight junctions and adherens junctions would then limit the effectiveness of the epithelial barrier, allowing antigens to infiltrate the underlying layers. Interestingly, the addition of TGF-β1 to AE cells in culture can trigger a phenomenon known as epithelial-mesenchymal transition (EMT), the markers of which include reduced cell-cell contacts and decreased E-cadherin[81].

1.5 Epithelial-Mesenchymal Transition

Epithelial-mesenchymal transition (EMT) is a process whereby epithelial cells undergo a phenotypic shift, losing the typical characteristics of epithelial cells while developing the properties of mesenchymal cells[82]. EMT may be categorized into three types: type I is associated with development (e.g. embryogenesis), type II is associated with wound healing and fibrosis, and type III is associated with the metastasis of neoplasms[83]. We are primarily interested in type

II EMT. In EMT, cell-cell contacts (e.g. tight junctions, desmosomes, adherens junctions, and gap junctions) of the epithelial cells are lost, along with their apical-basal polarity[82]. The mesenchymal properties gained, including a front-rear polarity, cytoskeletal rearrangement, and the expression of proteins such as matrix metalloproteases (MMP), contribute to greater motility for these cells[37,82,84,85].

While the downregulation of E-cadherin in the airway in the airway epithelium is a useful negative marker for the loss of cell-cell connections that is indicative of EMT, the presence of positive markers can help confirm EMT, which may in some circumstances occur only partially[82,86]. In AE cells, these positive mesenchymal markers include vimentin, fibroblast-specific protein 1 (FSP1), α-SMA, and EDA-fibronectin[86]. Morphologically, AE cells undergoing EMT also lose their typical cuboidal, cobblestone-like shape and take on a more spindle-shaped appearance[86]. The production of pro-collagen I by AE cells undergoing EMT, coupled with their ability to infiltrate the basement membrane, may also potentially contribute to the subepithelial fibrosis seen in airway wall thickening, as mesenchymal cells resulting from EMT are hypothesized to contribute to fibrosis in the asthmatic airway[86,87].

Not all AE cells may undergo EMT, and other events may occur in this transition that can affect other airway cells, including the airway smooth muscle. Because EMT involves a dramatic phenotype switch, it follows that cells with higher plasticity may undergo EMT more readily. The induction of EMT with TGF-β1 in normal differentiated AE cells, for instance, showed that only the progenitor basal cells began expressing mesenchymal markers[81]. In contrast, when AE cells from asthmatic subjects were exposed to TGF-β1, mesenchymal markers appeared in cells throughout the entire AE layer[81]. This can may additional consequences for AE cells in the asthmatic airway, as typically, differentiated ciliated cells are lost, and while there is some goblet cell metaplasia, overall, the proportion of basal cells (or progenitor cells) increased[79,86,88].

Therefore, in addition to asthmatic airways having an elevated level of TGF-β, there may be a larger relative proportion of AE cells in asthmatic airways that are susceptible to the influence of TGF-β.

1.6 AE-ASM Signaling

A central objective in studying AE cells alongside ASM cells is to demonstrate how the two cell types may communicate and how dysregulated communication to and from the altered cells can have implications, particularly in asthma. It may be useful to think of AE cells and ASM cell as analogous to their vascular counterparts: the vascular endothelium and vascular smooth muscle. In the vascular system, endothelium releases transmitters such as nitric oxide (NO) to modulate (and in this case, relax) smooth muscle tone. In the airways, AE cells may release a number of epithelium-derived relaxing factors (EpDRF) that contribute to ASM relaxation, including NO and arachidonic acid (AA) derivatives via COX-2 that can act directly on the smooth muscle[89,90], and neurotransmitters such as acetylcholine[91] and γ-amino butyric acid (GABA)[92,93] that may act indirectly and directly on ASM relaxation, respectively. The airway epithelium can also release a number of cytokines, which non-exhaustively include proinflammatory cytokines, various interleukins, as well as several growth factors (e.g. TGF-β, EGF, HB-EGF, FGF)[94,95]. These may indirectly induce intermediary cell types, such as those in the subepithelial layer, to produce bronchoactive molecules (e.g. NO or AA derivatives)[89], but given the knowledge that growth factors such as TGF-β1, which are elevated in asthma, can alter ASM cell phenotype, it may also be reasonable to posit that this and other growth factors released by AE cells may together affect ASM cell phenotype and alter contractile function. It is important to note that factors released by epithelial cells in asthma or otherwise can have an acute or a more long-term action; molecules such as NO act acutely to modulate ASM tone and are soon eliminated, while growth factors that alter phenotype would have a more long-term effect. Furthermore,

the growth factors that can be released by AE may generate autocrine signaling, particularly when the AE are in a state of repair in response to perceived wounding[94]. A chronic wound state in the airways is a proposed model for the development of asthma[94,96]. An epithelium-mediated cycle of repair and remodeling may therefore expose multiple cell types to elevated levels of growth factors, including TGF-β1.

1.7 Proteins of Interest

To characterize the potential changes to our cells, we will examine changes to the relative expression of a number of proteins. In brief, the first six proteins listed are contraction-associated proteins expressed in smooth muscle. Some, including myocardin, smooth muscle myosin heavy chain, and myosin light chain kinase, have been used as markers for a switch in smooth muscle cell phenotype. We also look at two epithelial cell proteins, used as markers for EMT transition in epithelial cells.

1.7.1 Myocardin

Although its namesake may suggest it is exclusive to cardiac muscle cells, myocardin is a protein that is also expressed in smooth muscle cells and transiently in skeletal muscle during development[97,98]. Myocardin acts as a transcriptional co-factor, associating with serum response factor (SRF) to direct binding of the SRF transcription factor to the CArG [$CC(A/T)_6GG$] box sequence motif[97]. CArG box sequence motifs can be found at the 5' promoter region and/or on introns near the 5' promoter of several smooth muscle genes associated with contraction; this includes genes for smooth muscle α-actin (SM α-actin), smooth muscle myosin heavy chain (SM-MHC), myosin light-chain kinase (MLCK), and calponin[99–102]. SRF is not specific to smooth muscle, so the interaction between myocardin and SRF is critical in regulating binding to smooth muscle gene CArG domains[103,104]. The CArG domains in many smooth muscle genes are present in pairs;

myocardin has the ability to homodimerize, and therefore, a mechanism exists in which myocardin-SRF can distinguish genes with paired CArG domains from genes with only one[104]. Indeed, when myocardin is prevented from dimerization, expression of the above smooth muscle gene transcripts are greatly diminished[104].

The myocardin gene, in turn, has a number of upstream binding sites for several transcription factors, including MEF2C, FOXO, and TEAD1/2[105–109]. Interestingly, some of these proteins may even be able to bind to the myocardin protein itself or to SRF, suppressing myocardin activity and thereby diminishing smooth muscle gene expression[108,109]. These multiple levels at which the activity of myocardin is modulated may play an important role in the characteristic phenotypic plasticity (i.e. synthetic/proliferative versus contractile states) of smooth muscle. In fact, in cardiomyocytes, where dedifferentiation of mature cells is not observed, cardiac isoforms of myocardin (which result from alternative splicing) are, instead, able to positively maintain their own expression via feedback loop; thus, the absence of such a feedback loop in smooth muscle is also consistent with smooth muscle's characteristic phenotypic plasticity[105,110].

The degree to which myocardin induces smooth muscle differentiation may be graded. When tumor-derived fibroblasts were induced to express myocardin protein via adenoviral transduction, the level of expression of downstream proteins such as MLCK appeared to positively correlate with the number of myocardin-encoding adenovirus[111]. In addition, cells transduced with myocardin also appear to gain contractile ability, shortening in response to KCl stimulation[111]. This suggests the expression of myocardin may be associated with a more physically contractile cell.

1.7.2 Smooth Muscle Myosin Heavy Chain

Myosins are a type of motor proteins that allow the conversion of the energy from ATP into mechanical force. While number of different classes of myosin exist, the most commonly studied and well-understood are myosin I, myosin II, and myosin V[55]. Many myosins have a variety of roles related to motion within the cell; for instance, the myosin I and V families contain myosins responsible for organelle and vesicle transport[55]. Smooth muscle myosin (SM myosin) belongs to the myosin II family, which also encompasses other myosins commonly known for muscle contraction (e.g. in skeletal muscle).

The functional unit in molecules of the myosin II family typically consist of two myosin heavy chains (MHCs), each of which consists of the head, neck, and tail regions[112]. The head region can bind to actin and contains the region with Mg-ATPase activity. The neck region acts as a lever arm, and the tail region in myosin II allows multiple myosin functional units to associate in order to form filaments[112]. In addition to the MHCs, the myosin functional unit also contains two pairs of myosin light chains (MLCs), separate but closely associated proteins, which localize near the head/neck region of the MHCs[113]. The light chain pairs consist of a "regulatory" light chain and an "essential" light chain (termed "essential" not because it is necessary for myosin function, but because it is difficult to remove even under laboratory conditions)[113].

The predominant "contractile" myosin heavy chain in smooth muscle, MYH11, is distinct and encoded separately in the genome from other MHCs, such as that found in skeletal muscle[114,115]. Further specialization of myosin is achieved by the various MHC and MLC isoforms resulting post-translational modifications (e.g. alternative splicing). This may have a profound impact on the aggregate muscle function. For comparison, in skeletal muscle, certain MHC and MLC isoforms are more prevalent in certain muscle cells, giving rise to the differences between

type I versus type II muscle fibers[116]. In smooth muscle, alternative splicing of the smooth muscle myosin heavy chain (smMHC), resulting in changes at the C- or N-termini, result in the SM-1 and SM-2 isoforms, or the SM-A and SM-B isoforms, respectively (and it may of note that SM-B has a greater V_{max} and may contribute to hypercontractility)[64,69]. In addition, smooth muscle MLCs consist of a 17 kDa "essential" unit (with two possible isoforms, MLC_{17a} and MLC_{17b}) and a 20kDa "regulatory" unit (MLC_{20})[64]. While the role of MLC_{17} is not well-understood, it may be associated with the V_{max} of the muscle; on the other hand, MLC_{20} is the light chain that can be phosphorylated by MLCK, resulting in the activation of the myosin unit[64].

1.7.3 Calmodulin

In smooth muscle, the influx of Ca^{2+} into the cytosol allows Ca^{2+} interaction with the protein calmodulin (CaM), which is necessary for the activation of MLCK and eventual cell contraction. Three separate genes with highly divergent sequences code for human CaM, yet produce identical protein products (via degenerate codons)[117]. It is a small, versatile protein with and can interact and associate with a considerable variety of proteins, MLCK being one of them[118,119]. The mechanisms through which CaM responds to Ca^{2+} is complex and highly dependent on context. For instance, in response to an increase in intracellular [Ca^{2+}], CaM can either activate or deactivate an associated protein, by either increasing affinity and association or by decreasing affinity and dissociation, depending on the identity of the target protein and the conformational state of CaM (which itself depends on which of the four Ca^{2+} binding sites on CaM are occupied by Ca^{2+})[119].

In the case of MLCK, CaM associates weakly with an inactive MLCK at low [Ca^{2+}]; the association with MLCK causes an increase in Ca^{2+} ion affinity in the two C-terminal Ca^{2+} binding sites, so that the sites can be occupied even while the CaM-MLCK complex is inactive[118,120]. The

two remaining N-terminal binding sites on CaM have faster binding kinetics to Ca^{2+} compared to the C-termini sites, meaning that CaM in this state may more readily respond to transient changes in Ca^{2+} concentrations, a feature that is potentially of benefit when considering smooth muscle contraction[120].

1.7.4 Myosin Light Chain Kinase

Myosin light chain kinase (MLCK) refer to contraction-associated proteins found in skeletal, smooth, and cardiac muscle tissues. For our purposes, we are interested in MLCK proteins from smooth muscle, which are encoded by the *mylk1* gene. The *mylk1* gene, in turn, encodes 3 potential protein products: a 210-kDa long isoform (also described in literature as "non-muscle" MLCK), a 130-kDa short isoform (sometimes described as "smooth muscle" MLCK), and much smaller 17-kDa fragment of the C-terminal that does not have kinase activity (known as telokin)[73,121]. The three different classes of MLCK proteins are a result of transcriptional control by different promoters on the *mylk1* gene; further post-transcriptional modifications can result in additional variants[121].

The 130-kDa "short-isoform" MLCK can be found in most tissues, but we are primarily interested in its presence and function in smooth muscle cells. Of the three *mylk1* products, this short-isoform MLCK is the isoform that is typically associated with smooth muscle contraction, acting as a kinase with Ca^{2+}/CaM activation in order to phosphorylate MLC_{20} and allow crossbridge cycling[73]. All three isoforms can be found in smooth muscle, with the short-isoform MLCK being largely dominant in *ex vivo* smooth muscle tissue[73,122]. However, as smooth muscle cells are cultured, the expression of short-isoform MLCK decreases dramatically with increasing passage number[122]. This is in line with the observation that MLCK is upregulated in mature ASM

while less abundant in proliferating ASM, and therefore it may be useful as a marker for differentiated smooth muscle[123,124].

1.7.5 Myosin Phosphatase Rho-interacting Protein

Myosin phosphatase Rho-interacting protein (M-RIP) is a protein that binds to both myosin light chain phosphatase (MLCP) and the GTPase RhoA[125]. M-RIP localizes MLCP to actin-myosin stress fibers in smooth muscle cells, which may facilitate MLCP dephosphorylation of myosin light chain (via termination of cross-bridge cycling leading to relaxation), though it should be noted that M-RIP itself does not influence the activity of MLCP, only its localization[125,126]. Reduced M-RIP expression via RNA silencing led to an increase in the number of stress fibers, as MLCP is prevented from dephosphorylating myosin light chain, and phosphorylated myosin light chain can stabilize stress fibers[126]. On the other hand, RhoA, which activates Rho-associated protein kinase (ROCK), leads to inhibition of MLCP activity (thus preserving a contractile state), although RhoA does not appear to rely solely on M-RIP for stress fiber localization[127]. Again, M-RIP itself does not appear to influence RhoA activity, only its localization to stress fibers[127]. Taken together, M-RIP may therefore allow regulation of MLCP by RhoA/ROCK at the stress fibers of smooth muscle cells.

1.7.6 Calponin

Calponin is an actin-binding protein found primarily in smooth muscle tissues, although it can also be present in other non-muscle tissues[128]. There are three isoforms of calponin, simply numbered 1/2/3, which vary in size from 33.2 kDa to 36.4 kDa in humans, and are encoded by three separate genes[128]. All three isoforms have two actin-binding sites, one of which has the effect of inhibiting actin-myosin ATPase activity, while the other site can reverse

this inhibition[128,129]. In addition, calponin binding to actin also slows the rate of filamentous actin depolymerization[128]. Altogether, this points to a regulatory role of actin in smooth muscle.

Calponin 1 is unique to smooth muscle tissue and its primary role appears to be the regulation of smooth muscle contractility[128]. When calponin 1 is dephosphorylated, it can bind to actin, which leads to the inhibition of contractility via inhibition of actin-myosin ATPase activity, but when it is phosphorylated (e.g. via protein kinase c) or if it interacts with Ca^{2+}-CaM, binding to actin may be inhibited, thereby diminishing the inhibitory activity of calponin 1[130–132]. The presence of calponin 1 may be indicative of a mature smooth muscle phenotype that is differentiated and contractile. *CNN1*, the gene that encodes calponin 1, is downregulated when smooth muscle cells enter/re-enter the cell cycle, and it may be upregulated in adult smooth muscle cells (based on expression patterns throughout development)[133,134].

Calponin 2 may be expressed in several non-muscle tissue types, where it plays a role in regulating cell motility through regulation of the actin cytoskeleton. In neural crest cells, for instance, a knockdown of *CNN2*, which encodes calponin 2, led to defects in the directionality of cell protrusions[135]. Interestingly, *in vitro* calponin 2 expression may be influenced by cytoskeletal tension; in 3T3 fibroblasts treated with blebbistatin (to eliminate cytoskeletal tension) had diminished calponin 2 expression, as did cells cultured on softer polyacrylamide gels (versus stiffer gel matrices)[136]. In smooth muscle, calponin 2 expression increases when cells are more proliferative and decreases in more quiescent cells, a behavior opposite that of calponin 1[128,137].

The sequence and structure of calponin 3 is notably more divergent from that of calponin 1 or 2[128]. It may be expressed in non-smooth muscle cells including neurons and glia, and while it is suggested that calponin 3 may play a role in neural tissue plasticity[138], the protein is currently not well-characterized and further study is likely needed. Calponin 3 interacts only

weakly with actin-myosin ATPase and likely does not play a role in the regulation of this aspect of cell contractility[139].

1.7.7 Epithelial Cell Proteins – Vimentin

Vimentin has the ability to influence cell morphology simply by its presence or absence; exogenous and forced expression of vimentin can induce mesenchymal-like morphology, while vimentin knockouts or silencing leads to epithelial-like cell shapes[140]. In a further departure from typical epithelial behavior, vimentin interaction with motor proteins may contribute to cell motility[82,140]. With respect to TGF-β1, multiple transcription factors may be influenced by the growth factor and lead to the upregulation of vimentin; in more detailed studies, a decrease in FOXA1/2 in response to TGF-β1 was associated with an increase in vimentin expression, while an increase in FOXC2 in response to TGF-β1 appears to be associated with increased vimentin expression and cell motility[82,141,142]. An increase in cell motility is useful in cases where the epithelium undergoes wound healing, and both TGF-β1 and vimentin contribute to this process. Mechanically wounded epithelium can lead to an autocrine increase in TGF-β1 expression, and exogenous TGF-β1 can enhance this repair process, while TGF-β receptor inhibition can hinder wound closure[143]. Similarly, overexpression of vimentin can increase wound repair, while shRNA knockdowns of vimentin inhibited wound repair[144].

1.7.8 Epithelial Cell Proteins – E-cadherin

E-cadherin is a junctional protein that is associated with a polarized epithelial cell phenotype; its extracellular region binds to other cadherins on adjacent cells to form part of the structure that composes adherens junctions[145]. While it belongs to a family of cell surface adhesion proteins, the cadherins, E-cadherin is most commonly associated with epithelial tissues, where it is an important participant in cell-cell adhesion and facilitates the formation of

other intercellular junctions, such as tight junctions[145,146]. It is a transmembrane protein; its intercellular region forms homotypic associations with other E-cadherins on other cells, while its intracellular domain is associated with other proteins, such as β-catenin and p120-, which in turn interact with proteins inside the cell (which, interestingly, include structural proteins, i.e. the actin cytoskeleton)[147]. During EMT, E-cadherin is downregulated as cells lose normal epithelial cell characteristics, and therefore, it is commonly used as a marker for intact, normal epithelium[82,86].

1.8 Optical Magnetic Twisting Cytometry

Optical magnetic twisting cytometry (OMTC) is a method used to assess cell stiffness. In this technique, ferrimagnetic beads (approx. 4.5μm in diameter) are coated with RGD (Arg-Gly-Asp)-containing peptides that are recognized by integrins on the outer surface of a cell (resulting in beads binding to the cell surface)[148,149]. The beads are magnetized with a strong magnetic pulse (approx. 100 mT for 1 ms) in the horizontal plane, resulting in beads with some magnetic moment vector (M)[150]. They are then subjected to a smaller, uniform, sinusoidally-oscillating magnetic field in the vertical direction (3.390 mT/A, with a peak current of 1.5 A in our protocols); the field at this strength is insufficient to re-magnetize the beads and, instead, exerts a torque on the beads[149].

Part of this torque depends on the amount of magnetized material in the bead, which corresponds directly with the size of the beads, and therefore, the bead volume. This is determined empirically for each batch of manufactured beads by placing magnetized beads in a fluid of known viscosity and subjecting them to a known, small oscillating magnetic field (on the order of 1-10 mT, much like during the twisting phase in OMTC) for calibration[151,152]. Since the torque applied to the beads by this calibrating magnetic field is resisted by the fluid (with a

known viscosity), by measuring the angular velocity of the beads in the fluid, a useful quantity where a force per unit area ($N \cdot m^{-2}$) is given per unit of external magnetic field applied (mT)[149]. Known as the bead constant (c_{bead}), it takes on the unit Pa/mT and normalizes the torque applied to the bead based on bead size.

The torque we apply on cell-bound beads during OMTC may now be defined as a specific torque with the following equation:

$$T_s(t) = c_{bead} \cdot H_z(t) \cdot cos\ \theta(t)$$

where $T_s(t)$ is the specific torque (i.e. the torque per unit volume of the bead and is expressed in the unit stress, Pa)[153], $H_z(t)$ is the sinusoidally-oscillating vertical magnetic field we apply (of magnitude 3.390 mT/A, with a period of 2 seconds and a peak amplitude of 1.5A in our protocols), and θ is the angle between the beads' magnetic moment (*M*) and the horizontal plane[149,154]. Since the beads are bound to the cell surface, a torque causes the bead to pivot and is resisted by the cell's mechanical (e.g. cytoskeletal) elements. This pivoting motion causes an apparent change in bead position, which may be detected under an inverted microscope with a camera as lateral bead motion *Δx* (Figure 1.8.1). This displacement is typically small (approximately 50 – 200 nm) relative to the circumference of the bead, so that the angle θ is also small (a bead size of ~ 4.5 μm in diameter gives a circumference of ~ 14.1 μm; if lateral bead motion (*Δx*) is approximately the distance along the circumference that the bead rotates along, then $\frac{200\ nm}{14.1\ \mu m} \times 360°$ results in $\theta(t)$ being approximately $\pm 5°$ from horizontal, and therefore, $\cos\theta \approx 1$)[149].

We can now take the specific torque (T_s) and the displacement of the bead *Δx* and take the ratio of these (so that $\frac{T_s}{\Delta x}$) to obtain a modulus with units Pa/nm[155] (which arises because

stress is divided by a displacement, rather than a strain, since the 'resting state' of the cell is not measured). Since an oscillating specific torque is applied to the beads, we can further take the specific torque and the bead displacement along the frequency domain (applying a Fourier transformation to each), then dividing the transform of T_s by the transform of Δx to give the following complex modulus G^*:

$$G^*(f) = \frac{T_s(f)}{\Delta x(f)} = G'(f) + iG''(f)$$

which contains the real component G' and the imaginary component G''[149,156]. The real component G' is a storage modulus, which is in-phase with the applied torque on the beads and represents the elastic component of bead motion. The imaginary component G'', on the other hand, is a loss modulus representing the viscous component of bead motion and out-of-phase with the applied torque. In this work, we primarily consider the elastic modulus G'.

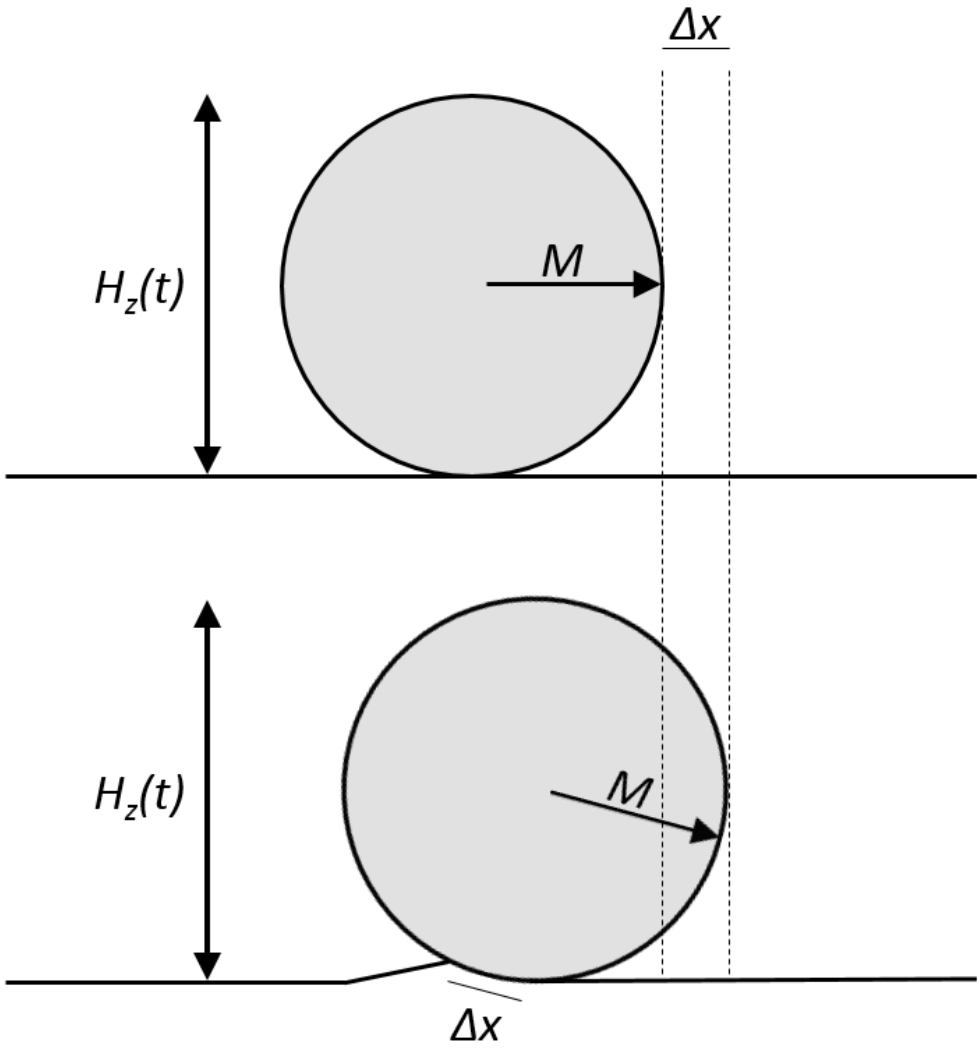

Figure 1.8.1: A sinusoidally oscillating magnetic field ($H_z(t)$) acts along the vertical axis to exert a torque on a bead with a horizontally-aligned magnetic moment vector (M). Lateral bead motion (Δx) is approximately the distance along the circumference of a bead that the bead rotates along.

1.9 General Hypothesis

There is evidence of interactions between the individual elements (TGF-β1, AE, and ASM) we plan to study. TGF-β1 can influence airway epithelium, disrupting normal AE function and inducing EMT-like changes to AE cells, such as loss of cell-cell contacts and loss of apical-basal polarity[86], which was further reviewed in Section 1.5. The growth factor can also influence

airway smooth muscle, leading to increased ASM proliferation and potential changes to ASM cell contractile function[72,74], covered in Section 1.3.2. These changes in response to TGF-β1 are similar to some of the changes observed in asthmatic airways, so TGF-β1 is suspected in development of these traits in asthma[3,61,79,80]. We also know that the AE modulates the ASM, and in our laboratory, previous work has shown that AE can affect ASM cell stiffness and contractile function[157,158]. However, we do not know how the combination of AE and ASM might respond to TGF-β1.

Changes to ASM contractile function may play a significant role in exaggerated airway narrowing in asthma. *In vivo*, AE cells are topographically close to the ASM and can modulate ASM function, but this process is not well understood. It is believed that the AE may release a number of factors, reviewed in Section 1.5, that contribute to relaxed ASM in normal airways. This process may be dysregulated in asthma, where a number of cytokines and growth factors show increased expression in the airways, including TGF-β1, reviewed in Section 1.2.2. We hypothesize that the elevated TGF-β1, which can cause EMT-like phenotypic switching in AE cells, leads to dysregulation of the communication between AE and ASM, potentially leading to ASM hyperresponsiveness, a hallmark of asthmatic airways.

Broadly, our approach to testing this hypothesis was to use conditioned media or co-culture methods to allow separate populations of AE and ASM to communicate with one another, better mimicking the topology of the airways *in vivo*, and then we potentially alter this communication by introducing our growth factor of interest, TGF-β1. We begin with characterizing the effects of our growth factor on each of our cell types. We then examine the interaction between non-growth factor-influenced or growth factor-influenced cells, assessing changes to cell stiffness, response to induced contraction, and changes to protein expression.

1.10 Thesis Aims

The primary aim of my research was to modulate the biochemical signals received by ASM cells *in vitro* and assess the resulting changes in ASM cell mechanics and ASM phenotype. Among the specific aims, the first two aims were directed at development of the protocols to be used in the latter two aims.

1.10.1 Aim 1

Assess whether TGF-β1 has a transformative effect on airway epithelial (AE) cells, specifically, immortalized 16HBE14o- cells, resulting in cells in an 'activated state' with the potential to differentially affect airway smooth muscle contractility assessed in later aims.

1.10.2 Aim 2

Establish whether TGF-β1 alone has a dose-dependent effect on ASM contractility. Since TGF-β1 will be present in a co-culture (described in a later aim) where ASM will also necessarily be in contact with TGF-β1. Coupled with Aim 1, the objective here is to help establish whether an optimal dose of TGF-β1, which would influence the AE without effecting a change in ASM contractility, exists.

1.10.3 Aim 3

Establish a conditioned media (CM) system where ASM cells are exposed to CM derived from AE cells, and assess the influence of TGF-β1 on the system in terms of cell phenotype and cell mechanics.

1.10.4 Aim 4

Use a co-culture system to culture AE and ASM cells in close proximity, allowing continuous paracrine signaling between the two cell types. TGF-β1 will be introduced to the system, and phenotype and mechanics will both be assessed.

Chapter 2: Common Methods

2.1 Cell Culture

Two types of cells were used for all experiments: [1] normal human airway smooth muscle (ASM) cells from multiple donors and [2] the immortalized 16HBE14o- human bronchial epithelial cells (16HBE, 16HBE14o-) obtained as part of an ongoing collaboration with Dr. Elizabeth Cowley (Department of Physiology and Biophysics, Dalhousie University).

2.1.1 Normal Human Airway Smooth Muscle Cells

Normal human airway smooth muscle cells were collected from airway tissue sections obtained from multiple donors undergoing thoracic surgery. Patients had no history of prior airway disease. Informed consent was obtained and approved by the Capital Health District Authority Ethics Review Board. Tissue sections were maintained in Dulbecco's Modified Eagle's Medium and Ham's F12 (DMEM/F12, 1:1, Invitrogen 11330, Burlington, ON) media supplemented with 10% fetal bovine serum (Invitrogen 12483, Burlington, ON) and 1% penicillin-streptomycin (Invitrogen 15140, Burlington, ON), which will be noted subsequently as '10% media'. Blood and other debris were removed from the tissue, and the luminal surface was scraped to remove epithelial cells. The tissue was then sectioned into 3x3 mm squares, which were placed into 100 mm petri dishes, secured under glass coverslips with sterile silicone grease, submerged in 10% media, and incubated at 36°C and 5% CO_2, with a media change every two days. At approximately 2 weeks, adherent cells were trypsinized and transferred to a larger cell culture flasks to expand the population, then trypsinized once more and stored in liquid nitrogen until use.

Preparation of ASM cells for experiments began with expansion of cell number in 10% media. The cells were defrosted and cultured in T75 flasks with 10mL of media, which was again

refreshed every two days. Once the cells reached >90% confluence, they were maintained in DMEM/F12 media as above, but with a reduced fetal bovine serum concentration of 0.5% (0.5% media), also refreshed every two days until ready for subculture in 12-well or 24-well plates. Due to varying growth rates between different donors, cells were seeded in the 12- or 24-well plates at between 50 000 - 80 000 cells/mL. The 24-well plates (growth area: ≈1.9 cm^2, Corning) received 0.5 mL/well while the 12-well plates (growth area: ≈3.8 cm^2, Corning) received 1.0 mL/well. These cells were subsequently used for dose-response testing in Aim 2, conditioned media experiments in Aim 3, and co-culture experiments in Aim 4.

2.1.2 Immortalized Human Bronchial Epithelial Cells (16HBE14o-)

16HBE14o- cells are SV40-transformed bronchial epithelial cells, initially established for the study of chloride ion transport[159]. These cells were transfected to express the SV40 large T-antigen, which primarily acts by inhibiting certain tumor-suppressor proteins, such as p53, contributing to the tumorigenicity of these cells[159,160]. 16HBE14o- cells develop features that are convenient for the development of our co-culture system, where cell signaling between AE and ASM and the influence of TGF-β1 on mature cells are central to the study. 16HBE14o- cells are robust, continuing to grow up to 100 passages; they can form a contiguous layer with appropriate tight junctions and adherens junctions, retaining a degree of normal barrier function; in addition, 16HBE14o- cells can demonstrate other evidence of differentiation, including apical-basal polarity and the presence of cilia[159,161]. Interestingly, 16HBE14o- cells formed a well-developed epithelial layer best when in liquid-submerged conditions, while cells grown in an air-liquid interface failed to form normal cell contacts[161]. Because of this, in our experiments, 16HBE14o- cells will be grown in liquid-submerged culture to best replicate the *in vivo* environment.

The cell culture of 16HBE14o- cells varied depending on experiment objectives. Broadly, 16HBE14o- cells were thawed and expanded in T75 flasks containing 10% media (as described in Section 2.1.1). These cells were incubated at 36°C, 5% CO_2, and kept in high humidity conditions and media was refreshed every other day. Post-confluence, the cells remained in 10% media for maintenance until subculture into 12-well, 96-well, Transwell, T25, or T75 cell culture vessels. Specific detail on the culture of these cells is further described in subsequent chapters.

2.2 Antibody Staining

Immunofluorescent staining was used to quantify the relative abundance of certain proteins associated with the contractile phenotype in smooth muscle cells. ASM cells were fixed using 3% formaldehyde in cytoskeleton buffer (CB) at room temperature (RT) for 20 minutes. Formaldehyde solution was then aspirated and cells washed twice with 5 mM ammonium chloride in 1X phosphate buffered saline (PBS, Sigma P5493). Then cells were permeabilized with 0.3% Triton X-100 (Sigma 9002-93-1) in PBS at 4°C for 15 minutes. After the Triton X-100 solution was aspirated, blocking solution (PBS/BSA, 1X PBS and 1% (w/v) BSA) was added and allowed to incubate for a minimum of 20 minutes at RT. Then, primary antibodies corresponding to our proteins of interest were added (reviewed under Section 1.7 and summarized in Table 2.2.1).

Infrared fluorophore-conjugated secondary antibodies were used to label the primary antibodies for later quantification using In-cell™ Western analysis. After two 15-minute washes with PBS/BSA to remove unbound primary, the cells were incubated with IR 680RD (Anti-goat, LI-COR Biosciences, 926-68074) and IR 800CW (Anti-rabbit, LI-COR Biosciences, 926-32213), both at 1:800 dilution, for 1.5 hours in low-light conditions. Samples were washed with 1X PBS, then allowed to dry overnight before analysis.

Data was collected using the Odyssey CLx infrared imaging system and In-cell™ Western analysis software (v3.0, LI-COR Biosciences), which used dual infrared diode lasers at 685 nm and 785 nm to excite the corresponding fluorophores. The dual lasers raster across a preset field containing the samples to be measured and detect the resulting IR emission from the locally excited fluorophores, minimizing auto-fluorescence from typical sources in the visible spectra and excitation from secondary sources (e.g. adjacent wells). Emission maxima for IR 680RD and IR 800CW antibody-conjugated fluorophores are 694 nm and 794 nm, respectively. Since two excitation channels were available, two targets could be simultaneously measured; therefore, proteins and their corresponding antibodies were paired accordingly. A summary of antibodies and detection parameters is provided in Table 2.2.1.

In each experiment, wells in control and experimental groups were left naïve to primary antibody, receiving secondary antibody only. IR fluorescence from these wells were measured in order to provide 'background' values representing auto-fluorescence and non-specific binding of secondary antibody. Mean fluorescent intensity of these wells were subtracted from the corresponding non-'background' wells to provide a better measure of relative fluorescent intensity.

Protein Target	Primary Antibody	Primary Dilution	Secondary Antibody	Secondary Dilution	λ (nm)
Vimentin[A]	Rabbit Polyclonal (Sigma, SAB1305445)	1 : 50	IRDye 800 CW	1 : 800	794
E-Cadherin[A]	Goat Polyclonal (Santa Cruz Biotechnology, sc-1500)	1 : 50	IRDye 680 RD	1 : 800	694
Myocardin[B]	Goat Polyclonal (Santa Cruz Biotechnology, sc-34238)	1 : 200	IRDye 680 RD	1 : 800	694
Myosin Light Chain Kinase (MYLK, MLCK)[B]	Rabbit Polyclonal (Santa Cruz Biotechnology, sc-25428)	1 : 200	IRDye 800 CW	1 : 800	794
Smooth muscle Myosin Heavy Chain (Myosin II smMHC, MYH11)[C]	Goat Polyclonal (Santa Cruz Biotechnology, sc-79079)	1 : 200	IRDye 680 RD	1 : 800	694
Calponin[C]	Rabbit Polyclonal (Santa Cruz Biotechnology, sc-28545)	1 : 200	IRDye 800 CW	1 : 800	794
Myosin Phosphatase Rho Interacting Protein (M-RIP, MPRIP)[D]	Goat Polyclonal (Santa Cruz Biotechnology, sc-135495)	1 : 200	IRDye 680 RD	1 : 800	694
Calmodulin[D]	Rabbit Polyclonal (Santa Cruz Biotechnology, sc-5537)	1 : 200	IRDye 800 CW	1 : 800	794

Table 2.2.1: Primary and corresponding secondary antibodies used in immunostaining for protein detection. Antibodies were paired according to noted superscripts ([A], [B], [C], and [D]).

2.3 Cell Counting

Cell counts were used to normalize fluorescent intensity to cell number, analogous to using housekeeping proteins in standard Western blots, in order to allow relative comparison of protein expression between different groups. After In-cell™ Western analysis, cells were

rehydrated in 1X PBS and DAPI nuclear stain (0.5 µg/mL, Sigma, D9542) was added at RT for 15 min, followed by two washes with 1X PBS. Cells were imaged using fluorescence microscopy to capture the number of nuclei in 1280 x 1024 pixel fields at 20X magnification (approximately 640 x 512 µm). The number of nuclei corresponded to the number of smooth muscle cells and were used as an indicator of proliferativity. Because of uneven growth of HASM cells from some donors (see Figure 2.3.1), leading to a higher density of cells towards the center of the wells and a lower density of cells towards the edges, a systematic approach to sampling for fields to count was used.

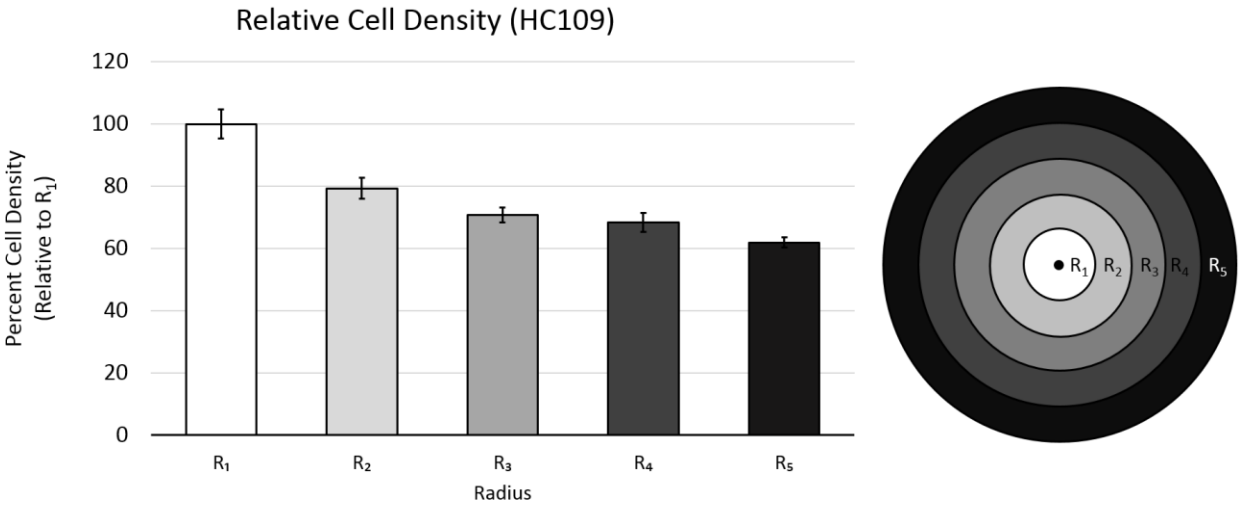

Figure 2.3.1: In certain donors, cells clustered more densely towards the center of each well. Representative images for cell counts were sampled in the areas bounded by two adjacent radii. Mean cell density for the entire well used a weighted average corresponding to the location the image was sampled from.

Each well was divided into a central circle with a radius of 1 AU (arbitrary units), with successively larger concentric rings with external radii of 2, 3, 4, and 5 AU. This meant that the area occupied by each ring were 3, 5, 7, and 9 times larger, respectively, than the area of the central circle (see Table 2.3.1). In 12-well plates, 1 AU corresponds to 2.1 mm; in 24-well plates,

1 AU corresponds to 1.4 mm. 5 AU corresponded with the radius of a well given the respective plate. A sample image was taken at each 'ring' for a total of five images per well, and cell counts determined from each image were given a weighting factor depending on which 'ring' they represented, then averaged to give the weighted mean cell count of a well.

$$A_n = \pi r_n^2 - \pi r_{n-1}^2$$

$$A_{\bar{X}} = \frac{A_1 + 3A_2 + 5A_3 + 7A_4 + 9A_5}{25}$$

Radius	Area (Total)	Area (Annulus)
1	1π	1π*
2	4π	3π
3	9π	5π
4	16π	7π
5	25π	9π

Table 2.3.1: A well can be divided into 5 concentric, evenly-spaced circles with radii r_n, where the area of each circle minus the next smallest circle equals $\pi(2r_n-1)$.

The weighted mean was again averaged over all the wells within an exposure group (i.e. TGF-β1 or AEC-exposed), and this was the mean cell count value that was used to normalize the fluorescence intensity measured (which is used as an index of relative protein expression) to cell density.

Cell density was determined using DAPI-stained nuclear cell counts, which were obtained using a semi-automated process involving ImageJ software (U.S. NIH, Bethesda, MD, USA). Image contrast was inverted and manually taken to threshold so that nuclei effectively appeared as black objects on a white background, then converted from greyscale to binary. The "Watershed" segmentation function ImageJ plugin was used to separate nuclei that appeared to be adjacent to one another (Figure 2.3.2). In brief, this function assigns a value to each black

Figure 2.3.2: Resolving overlapping nuclei with a "Watershed" segmentation function in ImageJ. Image intensity is inverted and converted to binary (B&W) between panels 1 and 2. Segmentation occurs between panels 2 and 3. This allows each dark region (corresponding to nuclei) to be considered a separate object.

pixel which indicates its distance to the nearest background/white pixel (described as the Euclidean Distance Map (EDM)). Segmentation occurs by starting from local maxima in the EDM, around which a 'bubble' expands outwards until it encounters the 'bubble' of another local maxima. The border at which this occurs is where the object is segmented. Successful segmentation with this method relies largely on the shape of the objects, and in cases where nuclei could not be properly resolved (Figure 2.3.3A) or where nuclei were inappropriately segmented (Figure 2.3.3B), manual counts were used to supplement automatic counts for a more accurate estimate of cell number.

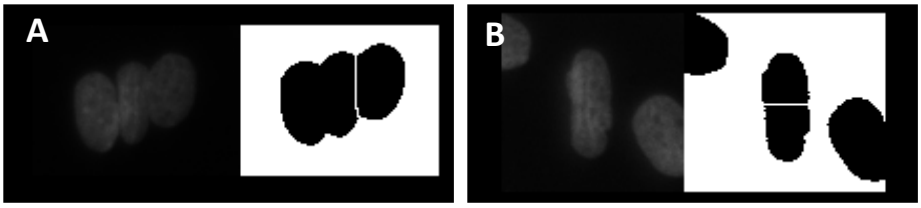

Figure 2.3.3: Two examples where objects are improperly segmented by ImageJ. In panel A, two distinct nuclei were unable to be resolved. In panel B, a single nucleus was erroneously segmented into two objects.

After segmentation, nuclei within the entire image field were then automatically counted using the "Analyze Particles" function. Settings were specified so that the function looked for objects larger than 400 pixels in area (nuclei were approximately 400-1000 pixels) with a 'circularity' value of 0.5 to 1.0, where 'circularity' is defined as $\frac{4\pi(Area)}{(Perimeter)^2}$ so that a perfect circle has a value of 1.0 (the 'size' filter helps eliminate debris and artifacts, while the

'circularity' filter eliminates excessively elongated objects that are distinctly not nuclei, i.e. debris or lighting artifacts). Nuclei that 'touched' the edges of the image field were also eliminated for image consistency.

2.4 Optical Magnetic Twisting Cytometry (OMTC)

Airway smooth muscle cell stiffness and contractility was determined using optical magnetic twisting cytometry (OMTC). ASM intended for OTMC were grown on 18mm glass coverslips in 12-well plates, as described in Section 2.1.1. Prior to OMTC, cells were serum deprived overnight in IT media (DMEM/F12 1:1 media supplemented with insulin (Sigma-Aldrich, I1882, Oakville, ON) and transferrin (Sigma-Aldrich, T4382, Oakville, ON); AE cells were removed from co-culture at this time as well. Coverslips with ASM were transferred and affixed into 35mm cell culture dishes using sterile silicone vacuum grease in order to allow mounting onto a custom microscope stage for OMTC, and cells were kept in 1.5 mL IT media. In OMTC, ≈4.5 μm diameter spherical ferrimagnetic beads (kindly provided by Dr. J.J. Fredberg, Harvard School of Public Health, Boston, MA) are coated with a synthetic RGD-containing peptide (Peptides International, PCS-37614-PI, Louisville, Kentucky, USA), which allows the beads to bind to integrins on the ASM cellular surface[148]. Beads were added 40 minutes prior to measurement and unbound beads were gently washed off the cells with fresh IT media 20 minutes prior to measurement. During bead binding and subsequent to the washing, cells were maintained at 37°C with 5% CO_2.

As covered in Section 1.8 , immediately prior to the OMTC measurement protocol, the beads were magnetized with a brief, high magnitude magnetic pulse in the horizontal plane using a pair of Helmholtz coils which generate a 1.61 mT/A field (for our experiments, a 560 μs current at 180 A generates a 290 mT field for magnetization)[149,156,162]. They were then subjected

to a lower magnitude (coil strength at 3.390 mT/A, with a peak current of 1.5 A, for maximum of 5 mT), vertically-aligned magnetic field that varies sinusoidally at 0.5 Hz. This vertical field applies a torque to the magnetized beads. Since the beads are bound to the cell surface, this results in a pivoting motion which can be observed and measured as a displacement, typically along the axis in which the beads are magnetized.

An estimate of cytoskeletal stiffness is calculated from the ratio of the specific torque applied (with a bead constant of 20.5 Pa/mT giving peak magnitude ≈100 Pa) and the displacement observed, computed in the frequency domain. The real part of this complex modulus, which is the in-phase component of the torque to displacement, describes a storage modulus G' (with the unit Pa/nm), and is the elastic component of the complex modulus G[153,163]. For all cells in a well, a set of baseline OMTC measurements were taken, after which a contractile agonist (here, an isotonic 80 mM KCl solution, designed to avoid osmotic effects across the cell membranes) was added to induce contraction. A second set of measurements is taken 3 minutes following the introduction of the contractile agonist. The change in the stiffness of each bead in response to the agonist provides an indication of the force generated by the corresponding cell. When this change in stiffness is normalized to the baseline stiffness, it gives an index of contractility in percent for the corresponding cell.

2.5 Bead Matching and Filter (Post-OMTC)

This section details the method I developed to match the coordinates of a bead in an image field taken at baseline (before KCl is added) with the coordinates of that same bead in a second separate image field taken post-KCl (after KCl is added). Due to a number of summative factors, including stage drift and disturbances during the addition of the contractile agonist, the pre- and post-agonist image fields do not ordinarily line up; thus, the coordinates of the beads are often

displaced by some amount between the two image fields. This can potentially lead to some error in the contractility assessed, since contractility is a function of bead stiffness in the context of OMTC. This is discussed later in detail below, in Section 2.5.1. Fortunately, bead coordinates, along with their motions, are tracked by the OMTC software during the measurement of stiffness before and after KCl addition. Therefore, it may be feasible, and useful, to pair matching beads. To accomplish this, custom code was written and executed using the Python(x,y) (2.7.9.0) distribution.

Two assumptions about the paired images were made in the development of the code used to match the beads across images. First, since our samples were firmly affixed onto the stage, and the stage was restricted, mechanically, to translate in the x or y directions (outside of focusing, i.e. up and down along a z-axis), we assumed that the sampled region (ROI) may be displaced along the x or y directions on a horizontal plane, but are not in any way rotated around any point in the plane. This assumption made it possible to use a fairly simple set of operations to align the ROIs. Second, because we were matching bead patterns, we assumed the beads were distributed randomly in a given ROI, with no regular pattern that could be a shifted, but identical pattern to the first or second image. If no regular pattern within a pair of ROIs exists, it is most probable that the program will find a single (and likely correct) solution.

The OMTC analysis software provides a list of recognized beads with their xy-coordinates within the 1280 by 1024 pixel image to sub-pixel accuracy. Bead locations are determined by an intensity weighted 'center of mass' algorithm[149,152]. The bead matching process first takes the x-coordinate of any bead in the pre-agonist (base) file and iteratively subtracts the x-coordinates of all the beads in the post-agonist (post) file; the *differences* between the 'base' bead and the multiple 'post' beads are each appended to a list and rounded to the nearest even pixel (the rounding effectively bins the differences). With approximately 50-

100 beads per sample pair, list lengths are typically on the order of 10^5 elements and are easily handled by Python.

If the beads of the 'base' and 'post' files are completely unrelated (i.e. the locations of all beads in the two files are random with respect to each other), we would expect the distribution of the differences between x-coordinates to also be random, although since we define 1280 x 1024 regions on the sample and exclude beads outside the region, the distribution of differences becomes triangular (Figure 2.5.1). However, if the beads of the 'base' and 'post' files can be overlaid with an approximately common within-pixel displacement, then there exists a particular difference in x-coordinates between the 'base' and 'post' beads that recurs more often than the random 'background' of other differences (Figure 2.5.2). The bead-matching program then selects this solution. The same process for the y-coordinates gives the xy-shift between the 'base' and 'post' images. It is then a simple matter of adding shifts in the x and y coordinates to the coordinates of the 'post' files to line them up, approximately, with the 'base' files.

The process used to match the beads works well for small misalignments between 'base' and 'post' files, as in Figure 2.5.3, illustrating a strong high peak above the noise with a misalignment of 92 pixels (corresponding to approximately 46 μm). There is a slight spreading in the peak to neighboring bins, indicating some noise in the shift, possibly due to variation in bead position from the KCl-induced contractions. I explored what would happen with larger misalignments using a sham OMTC run with beads fixed in epoxy. This produced >640 pixel shifts along the x-coordinate, causing a displacement of larger than half the image. In this case, peaks are less well resolved from the 'noise' (Figure 2.5.4) as more 'matching' beads are lost. Such large motions between 'base' and 'post' images do not typically occur during normal OMTC use. Finally, to match the beads, the program looks at a bead coordinate in the 'base' file and

determines whether a corresponding bead exists in the ‘post’ file, with some margin of error permitted; for our purposes, ±6 pixels was used. Only these beads are used to compute stiffness data and the change in stiffness between pre- and post-agonist addition.

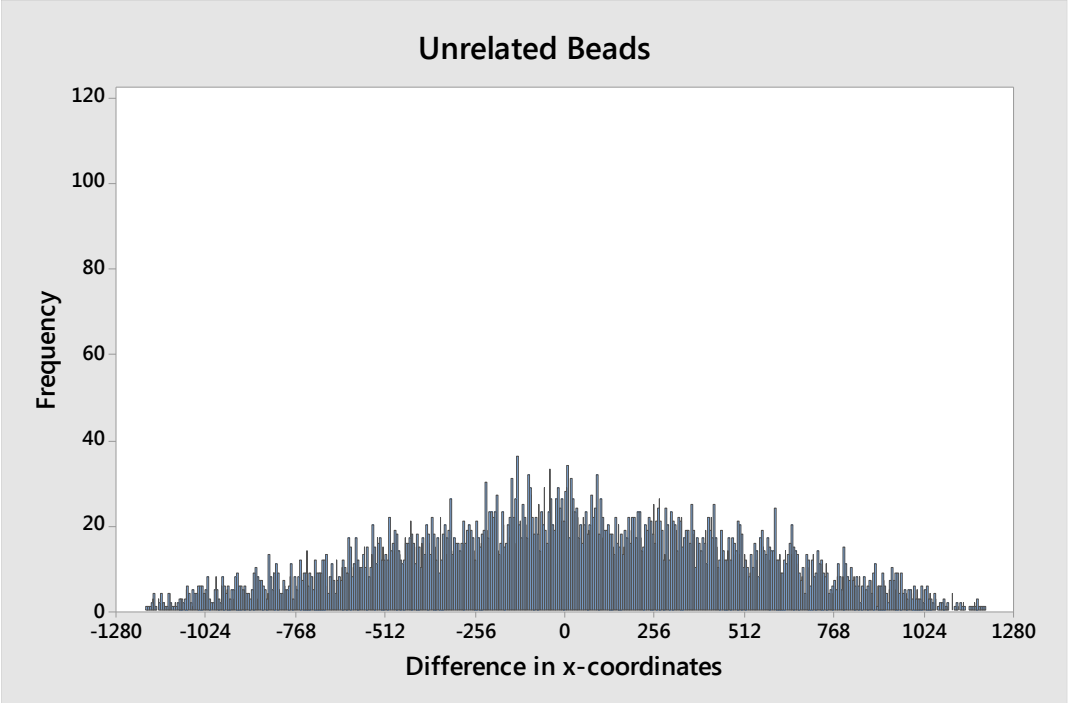

Figure 2.5.1: Histogram of the differences in x-coordinates of two sets of unrelated beads. Since the sets contain no regular overlap, no 'difference value' occurs significantly more than any other. Differences calculated between two sets containing 73 and 98 beads, respectively, resulting in 7,154 pairs.

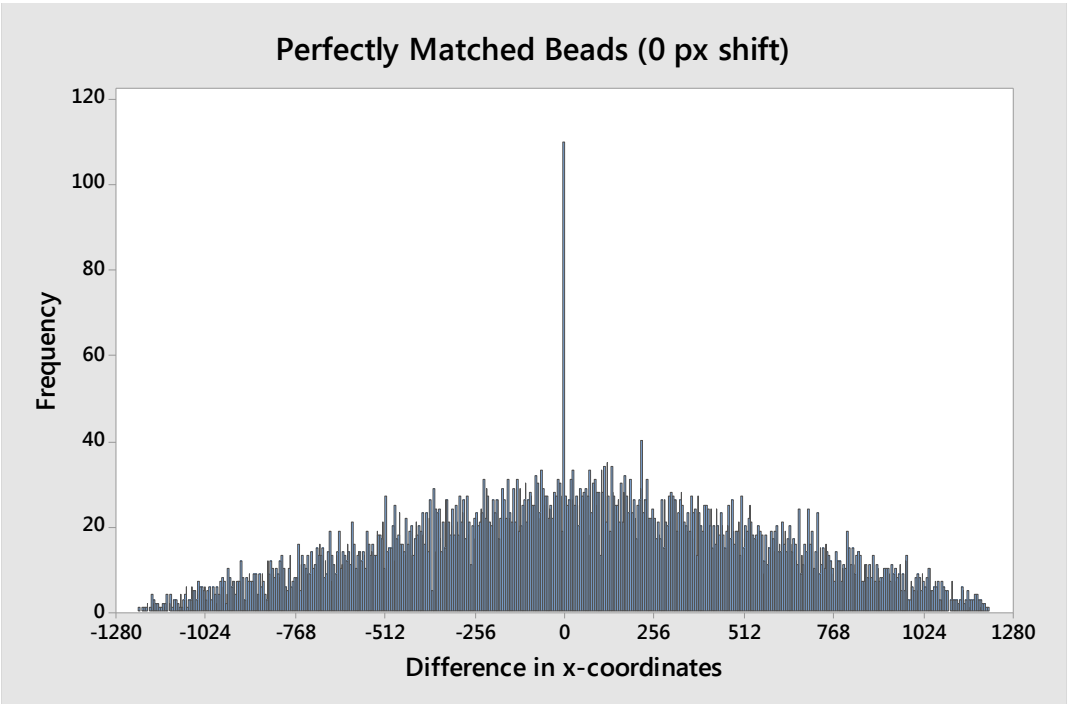

Figure 2.5.2: Perfect overlap of two sets of beads from two images. A clear and distinct peak is seen at 0 px, indicating no shift has occurred in the horizontal direction between the two images. Data from 9,180 pairs of beads. Note that bin widths are set to 4 px for visual clarity (in the bead-matching program, bin widths are at 2 px).

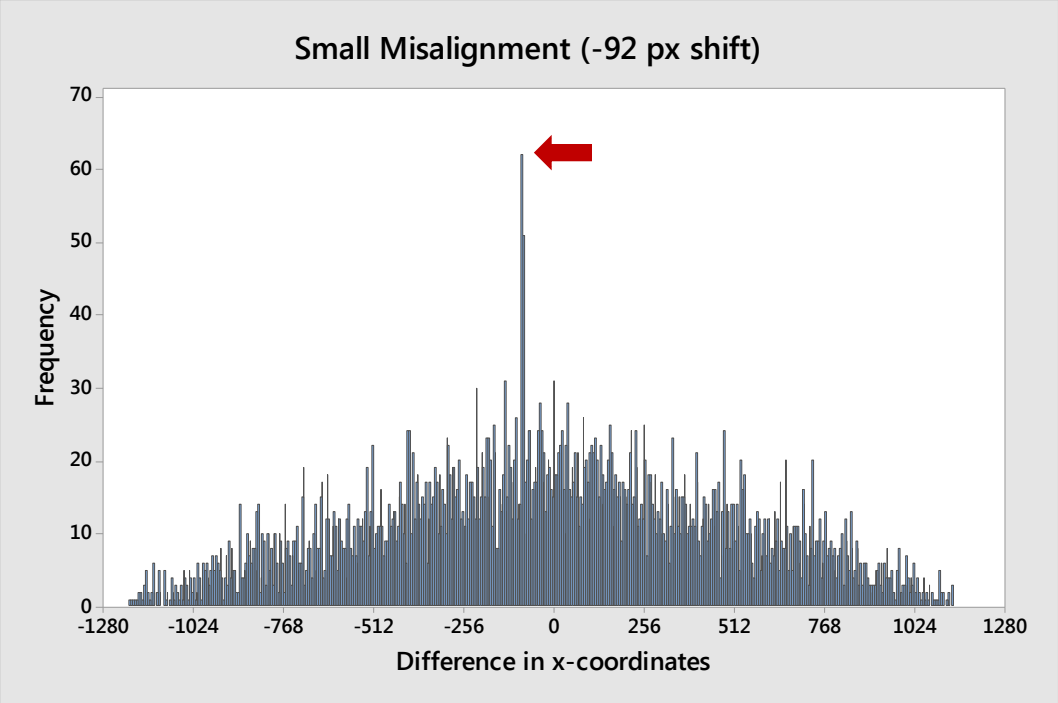

Figure 2.5.4: Distribution of differences in bead x-coordinates where the second image is displaced along the horizontal axis by approximately -92 pixels relative to the first image. Images were taken from beads bound to ASM cells pre- and post- contraction with KCl. A distinct peak is seen at -92 px, with a slightly lesser peak at -90 px (red arrow). Data from 6,162 pairs of beads.

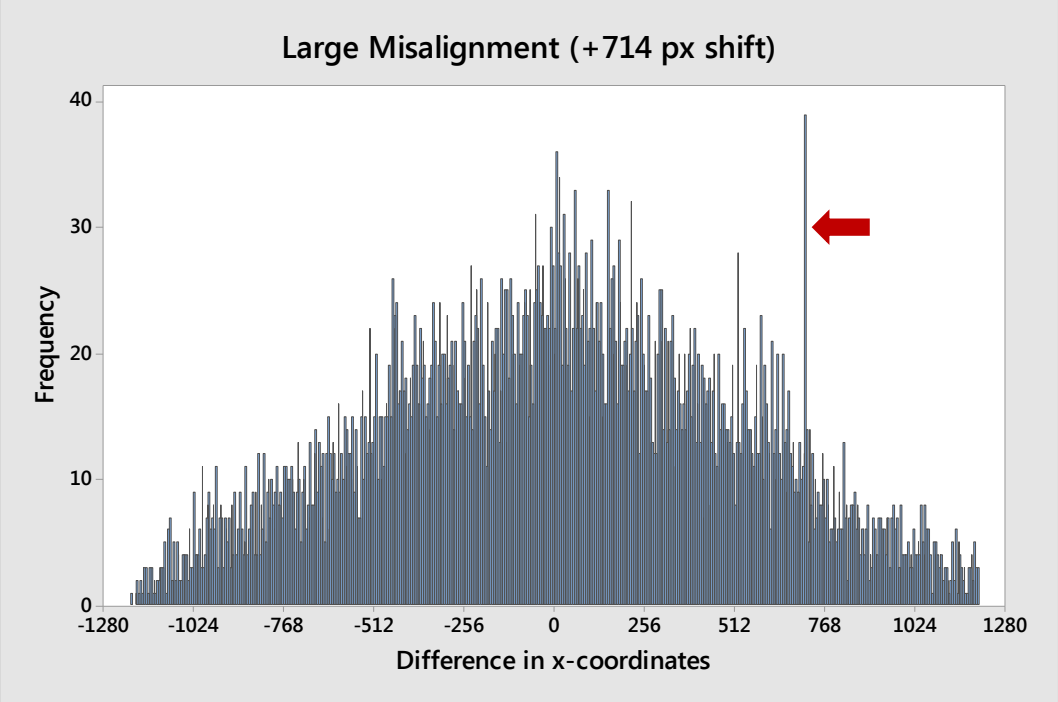

Figure 2.5.3: Distribution of differences in bead x-coordinates where the second image is taken after deliberately displacing the stage more than halfway across the image field. A peak is observed at +714 px, but is only marginally greater than the noise at 0 px. Data from 7,623 possible bead pairs.

2.5.1 Rationale for Bead Matching

Cell stiffness values measured using OMTC are approximately log-normally distributed, with significant heterogeneity in the measured cell stiffness values of individual cells due to factors intrinsic to the OMTC methodology, including cell height and the degree to which an individual bead is bound to a cell[149,152]. Because of this, the median was used instead of the arithmetic mean as the measure of central tendency for cell stiffness, since the arithmetic mean may be susceptible to bias by high stiffness values at the tail end of the distribution. Median baseline stiffness for all our control beads (i.e. beads bound to untreated cells, n = 2378) was 0.57 (95% CI (95% confidence interval) [0.54, 0.60]) Pa/nm, while mean baseline stiffness was calculated at 1.70 (95% CI [1.51, 1.89], SD 4.65) Pa/nm.

Cell contractility can be determined by comparing the cell stiffness after exposure to a contractile agonist (G'_{post}) to the cell stiffness before the agonist is added ($G'_{baseline}$), so that:

$$Percent\ Contractility = 100\% \times \frac{G'_{post} - G'_{baseline}}{G'_{baseline}} \qquad \text{Eq. 2.5.1}$$

where the change in stiffness is normalized to baseline cell stiffness. Without bead matching, it is not possible to obtain the percent contractility measured by any particular bead. Instead, to calculate percent contractility, the median G' values across all beads in a treatment group are used as a substitute in Equation 2.5.1 above to give an estimate. However, the contractility values appraised in this manner deviate from the median percent contractility calculated with

	Baseline (G')	Post-KCl (G')	Cell Contractility (%)
Bead 1	1	2	100
Bead 2	1	4	300
Bead 3	5	6	20
Well Median	1	4	Median contractility from matched beads: 100 Contractility from well medians: 300

Table 2.5.1: Simplified, simulated data illustrates how the contractility obtained from well median stiffness values can deviate from the median contractility obtained from matched beads.

bead matching. For instance, with bead matching of all our control beads, the median percent contractility was 62.12 (95% CI [59.78, 65.41]) %, while without bead matching the percent contractility calculated using median stiffness values comes out to 76.52% (with no useful estimates of variance available).

To obtain an estimate of variance without bead matching, percent contractility may be calculated on a 'per well' basis. That is, for each well from the tracked beads in a well, the median $G'_{baseline}$ is obtained, contractile agonist is added, and then a median G'_{post} is obtained. With these, Equation 2.5.1 above is applied for each well, resulting in a set of percent contractility values for wells in a treatment group. From here, a mean and standard deviation can be computed. This is effectively the "mean contractility of well medians". Again, the results of this method are slightly different compared to the median of all matched beads. Simple, simulated data analyzed in these two different ways illustrates the potential for differences in the results in Table 2.5.1. Looking at the contractility from each bead gives us the actual 'median contractility from matched beads', for this simplified sample, of 100%; meanwhile, the 'contractility from well medians' overestimates this to 300%. In our real (i.e. actual, collected OMTC) data, the 'contractility from well medians' also appears to have the tendency to

	Median contractility from matched beads (%)	Contractility from well medians (%)
Group 1	56.72	65.85
Group 2	33.22	40.68
Group 3	54.29	71.98
Group 4	55.56	76.56
Group 5	38.90	65.07
Group 6	27.63	44.78

Table 2.5.2: Contractility of multiple groups of beads from actual data sets, calculated with and without bead matching. Contractility calculated from well median stiffness values consistently appear greater than the median contractility from matched beads.

overestimate the actual median of contractility by approximately 10% to 70% depending on treatment group (Table 2.5.2).

If we look at contractility values in a 'per bead' manner, we can pool beads from the same treatment groups, across multiple wells to provide a larger pool of samples to draw our statistics from. Looking at bead-wise contractility also provides us with some additional information, such as the distribution of contractility (shown below as being approximately log-normally distributed, Figure 2.5.5), which we will use to decide appropriate methods for statistical testing in our eventual data sets.

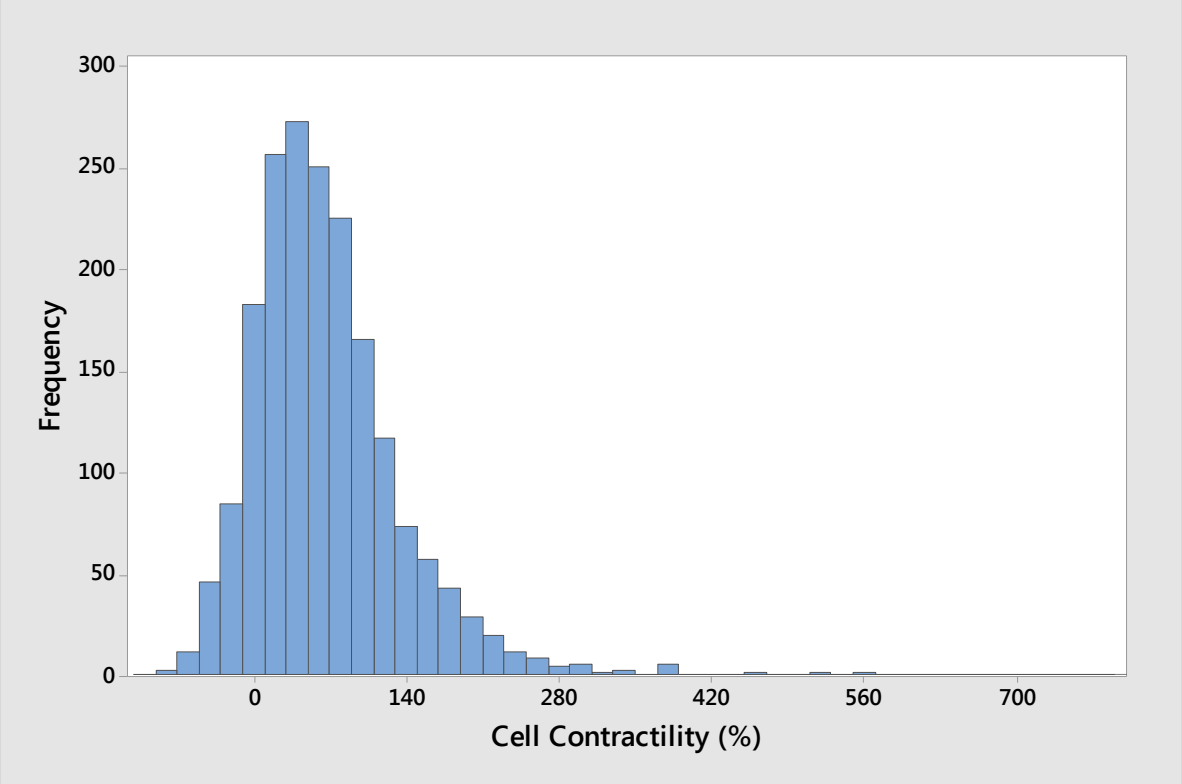

Figure 2.5.5: Histogram of cell contractility values of each bead, pooled across 12 untreated (control) wells, showing a log-normal distribution of changes in cell stiffness in response to KCl-induced contraction. Most beads show an increase in cell stiffness due to the addition of KCl, with a few dramatic increases in cell stiffness accounting for a long right-side tail, but a number of beads also show little change in stiffness, with some indicating a degree of relaxation (i.e. negative contractility) on the left side of the distribution.

Chapter 3: Airway Epithelial Cell Response to TGF-β1

3.1 Rationale

As reviewed in Chapter 1, changes to the airway epithelium may contribute to the airway remodeling observed in asthma. In asthmatic airways AE cells have impaired barrier function, demonstrated by the loss of normal cell-cell contacts and downregulation of tight junction and adhesion proteins[86,164,165]. Indeed, functionally, AE cell cultures from asthmatic airways demonstrated decreased TEER values and increased permeability to large molecules[165]. How this change in the epithelium arises and how it may influence the other cells of the airways and lead to remodeling is not well-understood. It has been suggested that the growth factor TGF-β1 may induce EMT-like changes to the airway epithelium, leading to decreased expression intercellular junction proteins, possibly diminishing normal barrier function[81,166]. In addition, TGF-β1 may sensitize the epithelium, allowing allergens such as HDM (house dust mite) to induce a more acute EMT-like change in AE cell phenotype[166]. Asthmatic airway epithelium may be more susceptible to the effects of TGF-β1, resulting in EMT. Taken together, this motivated us to examine the role of TGF-β1 through a cell culture model utilizing 16HBE14o- cells (Section 2.1.2).

Previous work in our laboratory with AE cells involved the use of immortalized human bronchial epithelial (of the cell line, 16HBE14o-) cells, as well as normal human bronchial epithelial cells (NHBE). 16HBE14o- cells are robust in monoculture and have been successfully co-cultured with ASM cells in our laboratory[157]. Additionally, other laboratories have demonstrated that 16HBE14o- cells form an intact epithelial layer that express tight junction proteins, whose function can be assessed using TEER[161]. NHBE cells, on the other hand, have the intrinsic advantage of being primary cells, which may be regarded as being more physiologically relevant and have the ability to be differentiate into a more distinct epithelial cell phenotype in

air-liquid interface culture conditions. However, previous work in our laboratory indicated that culturing NHBE cells in our co-culture system faced a number of technical challenges; NHBE cells require different, specialized cell culture media and growth conditions, and they may fail to form an intact layer[158]. In addition, for physiological relevance to be fully realized, NHBE cells would need to be differentiated to form the typical pseudostratified layer (described in Section 1.6), which requires culture on a semipermeable membrane at an air-liquid interface (ALI), which is more challenging, time-consuming, and requires a ready source of normal cells. Both 16HBE14o- and NHBE cells appeared to respond in an EMT-like fashion (in terms of protein expression) in several published works (see Table 3.1.1) after exposure to TGF-β1. Due to these confluence of factors, we determined that using 16HBE14o- cells would initially provide better feasibility, while the use of NHBE cells would be a secondary objective.

In this aim, we sought to confirm that TGF-β1 has a transformative effect on our AE cells, specifically, our 16HBE14o- cell line. This was a component of our hypothesis regarding the potential influence of AE cells on ASM cell function and phenotype (to be examined in later aims). To detect a change in the AE cell state due to TGF-β1, we selected one marker that is typically downregulated in EMT—the adhesion protein E-cadherin, and one marker that is upregulated in EMT—the intermediate filament vimentin. Published literature indicates that TGF-β1 is implicated in EMT, and leads to detectable changes in the expression of E-cadherin and vimentin in both NHBE and 16HBE14o- cells (Table 3.1.1). We will describe the methods used for our 16HBE14o- cells here, as our completed work uses this cell line.

In addition to the confirmation that TGF-β1 would affect our AE cells, we sought to determine two additional parameters. First, we wanted to determine the appropriate media to use for our AE cells, which would also carry over to our conditioned media and co-culture experiments. Preliminary tests indicated that 16HBE14o- cells failed to thrive when cultured

without serum after several days, but survived in both low (0.5%) and high (10%) serum-supplemented media (data not shown). We suspected a low serum media would allow for normal growth and survival of our 16HBE14o- cells without significant interference from the unknown factors typically present in serum. In addition, it is known that 10% FBS-supplemented media can contain 1-2 ng/mL of latent TGF-β[167]; therefore, we characterized our 16HBE14o- cells in our low serum (0.5%) media, which may be expected to contain 0.05-0.1 ng/mL of latent TGF-β (which are concentrations that are at least an order of magnitude smaller than our lowest planned dose of 1 ng/mL). Second, we needed to find an appropriate dose of TGF-β1 for our AE cells. Since TGF-β1 can influence both AE and ASM cells, it would be useful to establish whether an optimal dose (which would influence the AE without effecting a change in the ASM) exists.

Author	Cell Type	TGF-β1 Dose	Exposure Duration	Detection Method	Response
Zhang 2009[168]	16HBE14o-	10 ng/mL	72 hr	Immunofluorescence	↓ E-cadherin ↑ α-SMA F-actin reorganization
Hackett 2009[81]	NHBE	10 ng/mL 50 ng/mL	48 hr (24 hr x2) 72 hr (24 hr x3)	Immunofluorescence Western Blot	↓ E-cadherin ↑ α-SMA ↑ EDA-fibronectin ↑ Vimentin
Câmara 2010[169]	NHBE	5 ng/mL	72 hr	Western Blot	↓ E-cadherin ↑ α-SMA ↑ N-cadherin ↑ Vimentin ↑ MMP-2
Heijink 2010[166]	16HBE14o-	5 ng/mL	1-72 hr	Immunofluorescence Western Blot	↓ E-cadherin ↑ Vimentin ↑ Fibronectin
Johnson 2011[87]	16HBE14o-	10 ng/mL (+50 ng/mL EGF)	72 hr	Immunofluorescence	↓ E-cadherin ↓ CAR ↓ Occludin ↑ Vimentin

Table 3.1.1: Literature in which AE cells were treated with TGF-β1. Our treatment and detection protocols considered the methods used in each of these papers.

3.2 Approach

In the literature, cells are often serum-starved immediately prior to the addition of TGF-β1, then cultured for up to 72 hours[87,166,168]. Since, in our preliminary testing, the 16HBE14o-

cells appeared to do poorly without serum, and because we intended to use these cells in conditioned media and co-culture models lasting up to 7 days, we opted to use serum. However, the presence of unknown factors may interfere with normal cell behavior and the response to our experimental conditions; hence, we decided to characterize the influence of serum on our 16HBE14o- cells in the presence of TGF-β1.

16HBE14o- cells were cultured in T75 flasks with 1:1 DMEM/F12 media supplemented with 10% FBS (10% media) until >90% confluence. Cells were then trypsinized, subcultured into 96-well plates, and again allowed to grow until >90% confluence in 10% media at 200 µL. The cells were then switched to a lower serum 1:1 DMEM/F12 media supplemented with 0.5% FBS (0.5% media) or remained in 10% media (which was refreshed). These were supplemented with 10 ng/mL TGF-β1 (240-B, R&D Systems, Minneapolis, MN, USA) or with a corresponding volume of vehicle (the diluent for the TGF-β1, i.e. 4mM HCl with 0.1% BSA in ddH_2O) and allowed to incubate over 48 hours. After the 48 hours, cells were fixed and immunostained using the procedure (outlined in Section 2.2) with a polyclonal anti-vimentin antibody (Sigma, SAB1305445) and a polyclonal anti-E-cadherin antibody (Santa Cruz Biotechnology, sc-1500), both at a 1:50 dilution.

The concentration of TGF-β1 that AE cells may be subjected to locally *in vivo* is difficult to determine; however, *in vitro* studies typically utilize concentrations between 5-50 ng/mL (Table 3.1.1). In the first part of our approach, described in the paragraph above, a moderate 10 ng/mL appeared to be sufficient to cause a measurable change in E-cadherin and vimentin expression. Here, we examined whether a lower 5 ng/mL dose of TGF-β1 would also be sufficient to cause a change in protein expression. Again, 16HBE14o- cells were cultured in T75 flasks as above, then subcultured into 96-well plates and grown in 10% media until >90% confluence, after which, the cells were switched to 0.5% media. TGF-β1 at 5 ng/mL, 10 ng/mL, or an equivalent volume of

vehicle was added and allowed to incubate over 48 hours. After the 48 hours, cells were fixed and immunostained with anti-E-cadherin and anti-vimentin at a 1:50 dilution (described in Section 2.2).

In analysis of data for both of the above experiments, as described in detail in Sections 2.2 and 2.3, the mean background fluorescence intensity was subtracted (wells stained with 2° Ab only to asses non-specific binding) from the sample data; then all values were normalized to the mean vehicle fluorescence intensity. The mean vehicle fluorescence intensity was set to 1.0 to allow the comparison of data from different experimental runs across different days, to account for day-to-day variability. The collected data is reported below as mean ± SEM of percent change, and statistics were performed using the Minitab® 17.3.1 software package. Statistical tests involved a one-way ANOVA with Tukey post-hoc tests for pairwise comparisons; significance was taken at the $p < 0.05$ level.

3.3 Results

In our comparison of high and low serum media, merely switching to reduced serum media (10% to 0.5% serum) led to an increase in the expression of E-cadherin by 14.6 ± 2.7% ($p < 0.05$) (Figure 3.3.1A). Unexpectedly, the addition of TGF-β1 at 10 ng/mL led to a 36.4 ± 3.0% increase in E-cadherin expression ($p < 0.001$) in cells that had remained in 10% serum media. However, cells that had been switched to 0.5% serum media, TGF-β1 did not have a significant effect on E-cadherin expression at 48 hours. Unlike E-cadherin, the expression of vimentin was not altered by reducing the serum concentration used. As expected, vimentin expression did increase with exposure to TGF-β1; a 56.3 ± 4.3% increase was observed in cells that had remained in 10% serum media, while a 24.5 ± 3.6% increase was observed in cells in 0.5% serum media ($p < 0.001$) (Figure 3.3.1B).

In the second experiment, where we maintain a low serum (0.5% media) environment, we examined whether a reduced concentration of TGF-β1 would still lead to a detectable change in protein expression in our system. Whereas we noted an increase in vimentin expression at 10 ng/mL of TGF-β1 by 18.16 ± 0.03% ($p < 0.001$), this was not the case when TGF-β1 concentration was lower, at 5 ng/mL (Figure 3.3.2B). 16HBE E-cadherin expression was, again, unaffected by TGF-β1 at 48 hours in 0.5% media.

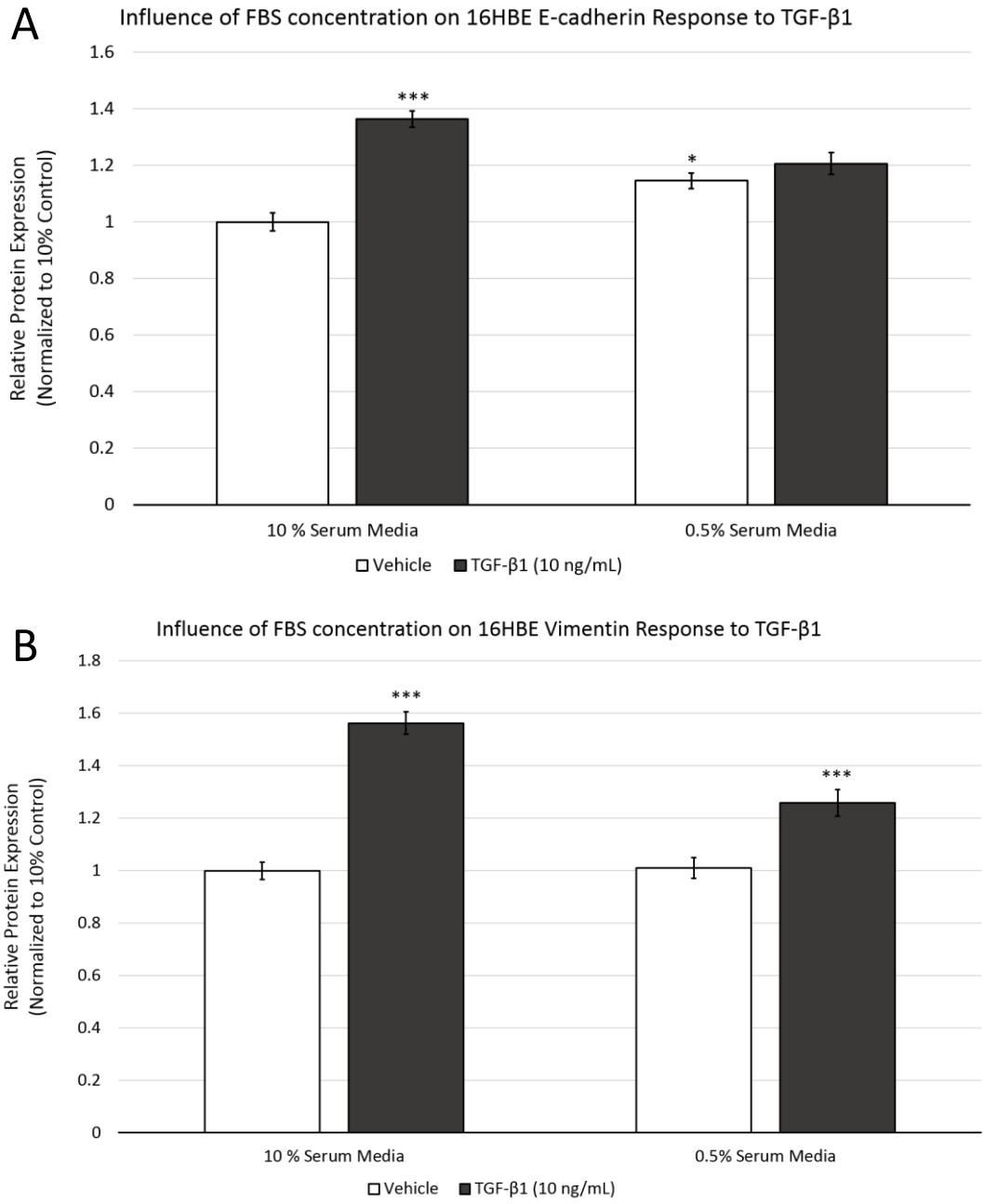

Figure 3.3.1: (A) When FBS concentration was reduced from 10% to 0.5%, 16HBE14o- cells increased E-cadherin expression 14.6 ± 2.7% compared to cells that remained in 10% media ($p < 0.05$). TGF-β1 at 10 ng/mL led to a 36.4 ± 3.0% increase in E-cadherin expression ($p < 0.001$) in 16HBE14o- cells in media with 10% FBS, but not in cells in media with 0.5% FBS. (B) Vimentin expression did not change in response to reduced FBS concentration. TGF-β1 exposure increased vimentin expression by 56.3 ± 4.3% in cells in media with 10% FBS, and increased by 24.5 ± 3.6% in cells in 0.5% serum media compared to vehicle in 0.5% serum media ($p < 0.001$). Statistics for each marker done using ANOVA followed by Tukey post-hoc tests for multiple comparisons (n = 24 per group).

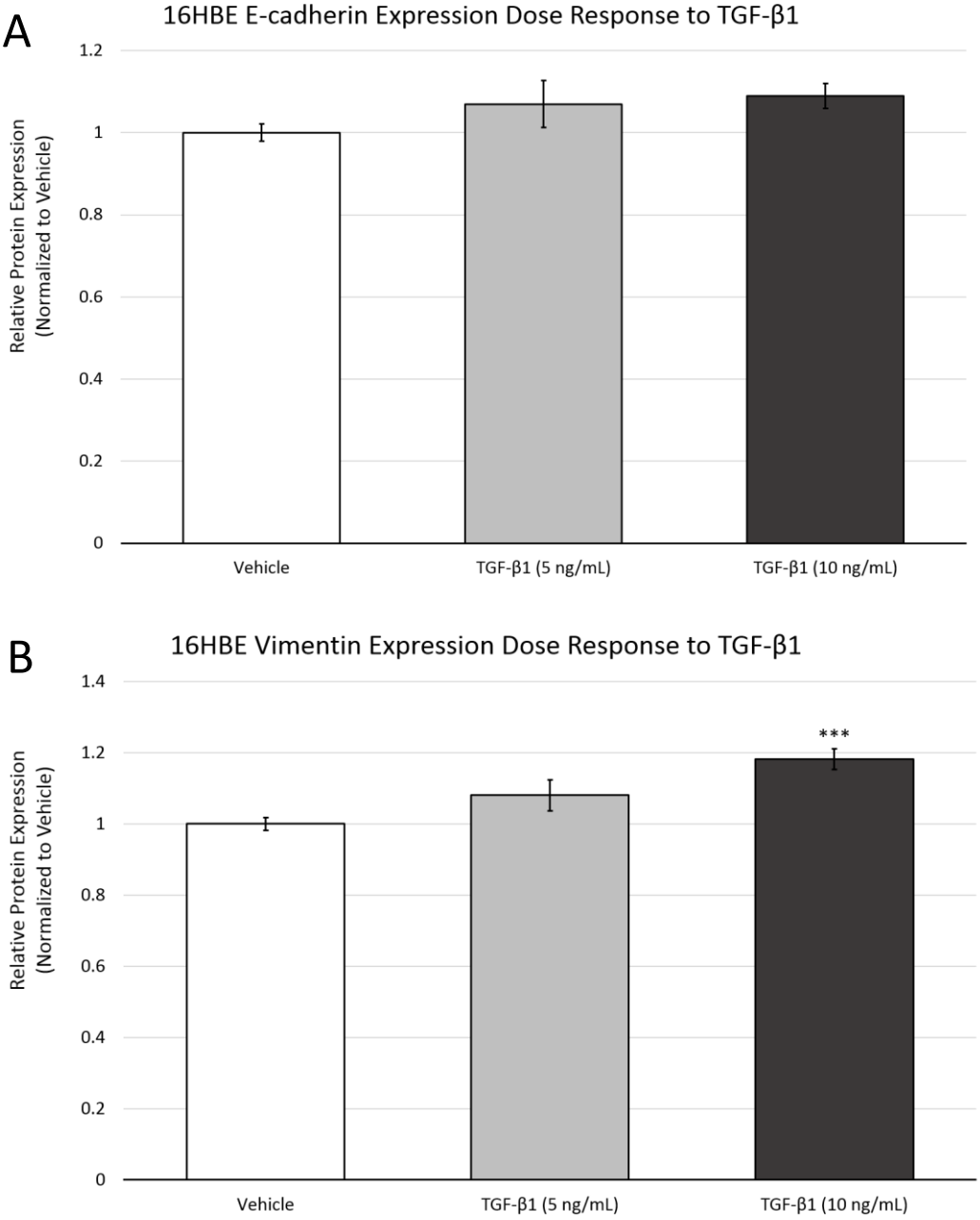

Figure 3.3.2: (A) E-cadherin expression did not change with a lower 5 ng/mL dose of TGF-β1. (B) The lower dose of TGF-β1 also saw a diminished the vimentin response in 16HBE14o- cells. Statistics for each marker done using ANOVA followed by Tukey post-hoc tests for multiple comparisons ($n_{vehicle}$ = 64, $n_{5\ ng}$ = 20, $n_{10\ ng}$ = 44).

3.4 Discussion

The primary objective of this aim was to demonstrate that TGF-β1 could adequately augment 16HBE14o- cells in culture, which would be detected by changes in protein expression. The increase in vimentin expression in 16HBE14o- cells that were exposed to TGF-β1 (Figure 3.3.1B) are consistent with the changes typically observed in EMT, as a relative increase in the expression of vimentin is characteristic of epithelial cells transitioning into mesenchymal cells[87,166].

If we consider the hypothesis that the asthmatic airway epithelium is in a state of chronic injury, one might initially expect an increase in TGF-β1 and vimentin to be beneficial (i.e. promote repair) to the epithelium given both proteins' ability to improve wound healing rates (Section 1.7.7). However, a more likely scenario is that asthmatic airway epithelium are in a chronic "wounded" state, and the increase in growth factors like TGF-β1 seen in patients, are a component of the signaling involved in an attempt to repair the epithelium (which resists normal repair due to other more fundamental defects)[5]. Therefore, we believe that vimentin serves as a good indicator that our cells could similarly be responding to TGF-β1, potentially in an EMT-like fashion.

Interestingly, E-cadherin expression did not decrease with the addition of TGF-β1 in any condition. The reduction or loss in E-cadherin expression can typically be considered a fundamental characteristic of EMT (Section 1.5 and 1.7.8). Indeed, several aforementioned studies that demonstrated a decrease in E-cadherin with TGF-β1 exposure used a 72-hour end point (Table 3.1.1). It is possible that our 48-hour incubation period was an insufficient timescale in which a decrease in E-cadherin occurred or could be observed; had exposure continued into 72 hours, a decrease in detectable E-cadherin may have been more readily observable.

Alternatively, E-cadherin at the cell junctions may indeed have decreased; however, since our protocol called for the detection of both E-cadherin and vimentin, the cells were permeabilized to allow antibody access to the IF vimentin. Since surface E-cadherin is regulated through regular recycling by endocytosis, there is an internal pool of E-cadherin[146]. A comparison of (untreated) permeabilized and unpermeabilized 16HBE14o- cells immunostained for E-cadherin shows better localization of E-cadherin at the cell borders in the unpermeabilized cells (Appendix A). If downregulation of E-cadherin begins with this internalization step, our immunostaining protocol may have additionally measured this internal pool of E-cadherin.

The purpose of immunostaining for E-cadherin, in our context, was to show a decrease (in response to TGF-β1) in the presence of a cell-cell junction protein, which itself was an indicator of a loss of barrier function, a defining characteristic of EMT. To capture this feature of EMT, it is possible to measure the change in barrier function more directly, using techniques such as trans-epithelial electrical resistance measurement (TEER), where the electrical resistance between two chambers separated by a layer of epithelial cells is measured[161]. In our later co-culture experiments, epithelial cells will be cultured in this configuration on a semi-permeable membrane (Section 6.2); this will allow measurement of barrier function during the culture in lieu of measuring E-cadherin protein expression at the end of culture.

In all, although the E-cadherin protein expression data may show an increase in some conditions at 48 hours, the aforementioned changes to vimentin expression in response to TGF-β1 exposure are sufficient to suggest that 16HBE14o- cells are already altered to a degree by 48 hours, potentially in an EMT-like fashion. Nonetheless, we would still like to demonstrate a change in AE barrier function in response to TGF-β1. Other published works already demonstrate that 16HBE14o- cells do have decreased E-cadherin expression in response to TGF-

β1 (Table 3.1.1). It may be more useful, therefore, to show functional changes to the AE barrier, which will be covered later, in parallel with our co-culture experiments (Chapter 6).

A slight increase in the expression E-cadherin in 16HBE cells switched to a lower serum media (open bars in Figure 3.3.1A) suggests that reduced serum is better for promoting the formation of a more typical epithelium with barrier function, even in our immortalized cell line. A high concentration of serum (i.e. 10% FBS) in media is normally used to drive cell growth and expansion in culture, while serum deprivation is used to render cells quiescent. Though it was not feasible to completely remove serum from our culture media, dropping serum concentration to 0.5% may be sufficient to restore some normal epithelial function to our 16HBE14o- cells.

Paradoxically, E-cadherin expression increased significantly with the addition of TGF-β1 while in media supplemented with 10% FBS (Figure 3.3.1A). While the reason for this is unknown, this may be the result of undetermined interactions with unknown mediators present in the serum since, as described in Section 1.2.1, a cell's response to TGF-β1 is highly context dependent. An increase was not observed in TGF-β1-exposed cells in the 0.5% (low) serum media compared to the 0.5% serum media control. Together, these data suggested that, going forwards, low serum media would be a more appropriate medium when dosing our cells in subsequent experiments.

Despite the mixed results in E-cadherin protein expression analysis, the increase in vimentin expression in 16HBE14o- cells exposed to TGF-β1 was sufficient to determine that a change in AE cell behavior had occurred in response to the growth factor, so it would be appropriate to include TGF-β1 supplemented and naïve AE cells in our subsequent AE-ASM interaction studies. While a reduced concentration of TGF-β1 at 5 ng/mL did not affect the

expression of vimentin significantly at 48 hours, a concentration of 10 ng/mL did lead to an increase in vimentin expression (Figure 3.3.2B). Thus, 10 ng/mL is the minimum concentration of TGF-β1 needed to see a confirmed change in our 16HBE14o- cells, and this would be the concentration of TGF-β1 that would be used in subsequent conditioned media and co-culture experiments.

Chapter 4: Airway Smooth Muscle Response to TGF-β1

4.1 Rationale

In either a conditioned media or co-culture system, where ASM cells are subjected to the TGF-β1-exposed AE cell secretome, ASM cells will also be exposed, in some degree, to TGF-β1. From a physiological standpoint, with respect to the airways, some exposure is normal as latent TGF-β1 is typically localized in the ECM, which includes the subepithelial layer; this is in close proximity to the ASM cells (specifically, between the AE cells and ASM cells)[24,170]. Upon *in vivo* activation of this latent TGF-β1, it is reasonable to expect the exposure of ASM cells to active TGF-β1. While it has been shown that TGF-β1 increases ASM cell proliferation and expression of some contractile proteins, how these changes simultaneously affect ASM cell contractility is less understood. In Goldsmith et al. 2006, free-floating TGF-β-exposed ASM cells could decrease their cell body length to a greater extent in response to acetylcholine (ACh), compared to untreated cells, implying enhanced contractility. While it is unclear whether unloaded cells, untethered to any substrate (in contrast to the case *in vivo*, where cells are loaded and tethered to the surrounding ECM) behave typically without a restoring force, it does make the case that TGF-β1 influences contractile function. In comparison, our OMTC system requires cells that are necessarily adherent on a flat, 2-D surface. These differences mean that it will be important to establish the effect of TGF-β1 in our system and characterize the OMTC response to TGF-β1-treated ASM cells.

We looked at the OMTC-measured response of ASM cells exposed to TGF-β1 in order to establish whether TGF-β1 had a dose-dependent effect on airway smooth muscle (ASM) contractility, as it would be present with both AE and ASM in the co-culture (Aim 4). The goal was establish whether there was an optimal dose within our testing range in which TGF-β1

would influence the airway epithelium without effecting a change in ASM contractility. However, if TGF-β1 effects a change in ASM contractility at concentrations less than the doses that would be used to influence the AE (so that no 'optimal' dose exists), then our hypothesis is slightly altered in subsequent aims, but is still useful as we will properly be investigating the co-effects of TGF-β1 directly on the ASM together with the AE cell-mediated signaling to the ASM. This would reflect the *in vivo* situation, where the two cell types are both likely exposed to elevated TGF-β1 in asthmatic airways.

4.2 Approach

Since later assessment of the interactions between AE and ASM will utilize optical magnetic twisting cytometry (OMTC) to measure changes in ASM cell stiffness and determine contractility, we first used OMTC to similarly determine changes in ASM cell stiffness and contractility after exposure to TGF-β1 at varying concentrations. Primary ASM cells were grown in DMEM/F12 with 10% serum on round glass coverslips in 12-well plates to >90% confluence, then transferred to reduced serum DMEM/F12 (with 0.5% serum). ASM cells were either given a single dose of 1, 5, or 10 ng/mL of TGF-β1 or vehicle (0.1% BSA w/v + 4 mM HCl) at the beginning of a 72-hour period. Alternatively, cells were also treated with TGF-β1 at 1, 5, and 10 ng/mL or vehicle and re-dosed every other day for a total of 6 days of continuous exposure to TGF-β1 to examine the effect of TGF-β1 at a longer time point. After treatment, the cells were switched to serum-free media supplemented with insulin and transferrin (IT media) for 24 hours in preparation for measurement of contractility. OMTC was used to measure cell stiffness before and after exposure to 80mM isotonic potassium chloride solution (KCl, to induce cell contraction), and the change in cell stiffness was used as an index of contractility (Section 2.4).

Beads across three wells in each treatment condition (e.g. all wells treated with TGF-β1 at 5 ng/mL) were aggregated across three donors (e.g. three wells from donors 1, 2, and 3 with TGF-β1 at 5 ng/mL, for a total of 9 wells per treatment condition) into a single group per condition. To compare the groups, statistical tests were performed using the Minitab® 17.3.1 software package. Since contractility and stiffness values were non-normally distributed, I used a non-parametric Kruskal-Wallis test (one-way ANOVA on ranks) with multiple Mann-Whitney U tests for pairwise comparisons; significance was taken at the $p < 0.05$ level. Bonferroni correction was used to avoid a Type I error (and since four groups were compared, $m = 6$ so that $\alpha = \frac{0.05}{6} = 0.008\bar{3}$). The data are presented below as the median percent contractility, the median difference in cell stiffness between baseline and post-KCl addition, or the median cell stiffness of all beads in a treatment condition. Error bars denote the 95% confidence intervals around each median.

4.3 Results

Repeated exposure to TGF-β1 at 1, 5, and 10 ng/mL over 6 days led to an increase in median baseline ASM cell stiffness by 41.2%, 34.4%, and 32.0% ($p < 0.001$ for all comparisons), respectively, compared to vehicle (Table 4.3.1, Figure 4.3.1A). However, there were no significant differences between groups receiving the different concentrations of TGF-β1. Median ASM cell contractility decreased with the addition of TGF-β1 at 1, 5, and 10 ng/mL by -24.4%, -21.0%, and -21.6% ($p < 0.01$, $p < 0.05$, $p < 0.05$), respectively (Figure 4.3.1B), although again, with no significant differences in contractility found between groups that received different concentrations of TGF-β1. Whereas the contractility is the percent change in cell stiffness with respect to baseline stiffness, in Figure 4.3.2C, we show the magnitude of the change in stiffness before and after KCl-induced contraction. This is simply the absolute difference between post-

KCl and baseline stiffness and is reported as the change in G' (Pa/nm). Between vehicle-treated and TGF-β1-treated ASM, we found no change in the absolute difference in G' (Figure 4.3.1C).

	Baseline Stiffness (G') (Pa/nm) with 95% CI	Post-KCl Stiffness (G') (Pa/nm) with 95% CI	Percent Contractility with 95% CI
Vehicle	1.10 [1.02, 1.25]	1.74 [1.62, 1.93]	47.57 [40.48, 54.44]
1 ng/mL	1.55 [1.39, 1.67]	2.15 [2.00, 2.34]	35.94 [32.31, 40.66]
5 ng/mL	1.48 [1.38, 1.64]	2.15 [1.95, 2.29]	37.59 [32.74, 42.83]
10 ng/mL	1.45 [1.34, 1.62]	2.02 [1.79, 2.23]	37.30 [32.04, 42.37]

Table 4.3.1 ASM cell stiffness and contractility following 6 days of continuous exposure to TGF-β1.

Exposure to a single bolus of TGF-β1 at the start of a 72-hour period also led to an increase in median baseline ASM cell stiffness. Compared to the vehicle group, cell stiffness at baseline increased by 74.2%, 46.0%, and 45.8% ($p < 0.001$ for all comparisons) with exposure to concentrations at 1, 5 and 10 ng/mL, respectively (Table 4.3.2, Figure 4.3.2A). A significant decrease in contractility compared to vehicle was observed in cells treated with 5 or 10 ng/mL TGF-β1 (-42.3% and -36.5%, respectively; $p < 0.01$), but not at 1 ng/mL (Figure 4.3.2B). Between vehicle-treated and TGF-β1-treated ASM, similar to our results from the 6-day TGF-β1 exposure, we again found no change in the absolute difference in G' (Figure 4.3.2C).

	Baseline Stiffness (G') (Pa/nm) with 95% CI	Post-KCl Stiffness (G') (Pa/nm) with 95% CI	Percent Contractility with 95% CI
Vehicle	0.75 [0.66, 0.88]	1.29 [1.15, 1.44]	63.23 [52.23, 71.49]
1 ng/mL	1.31 [1.10, 1.47]	2.16 [1.76, 2.43]	49.52 [41.89, 60.36]
5 ng/mL	1.10 [0.91, 1.26]	1.62 [1.38, 1.99]	36.46 [26.68, 45.39]
10 ng/mL	1.10 [0.93, 1.33]	1.56 [1.32, 1.86]	40.15 [32.77, 49.63]

Table 4.3.2: ASM cell stiffness and contractility after a single bolus of TGF-β1 introduced at the start of a 72-hour exposure period.

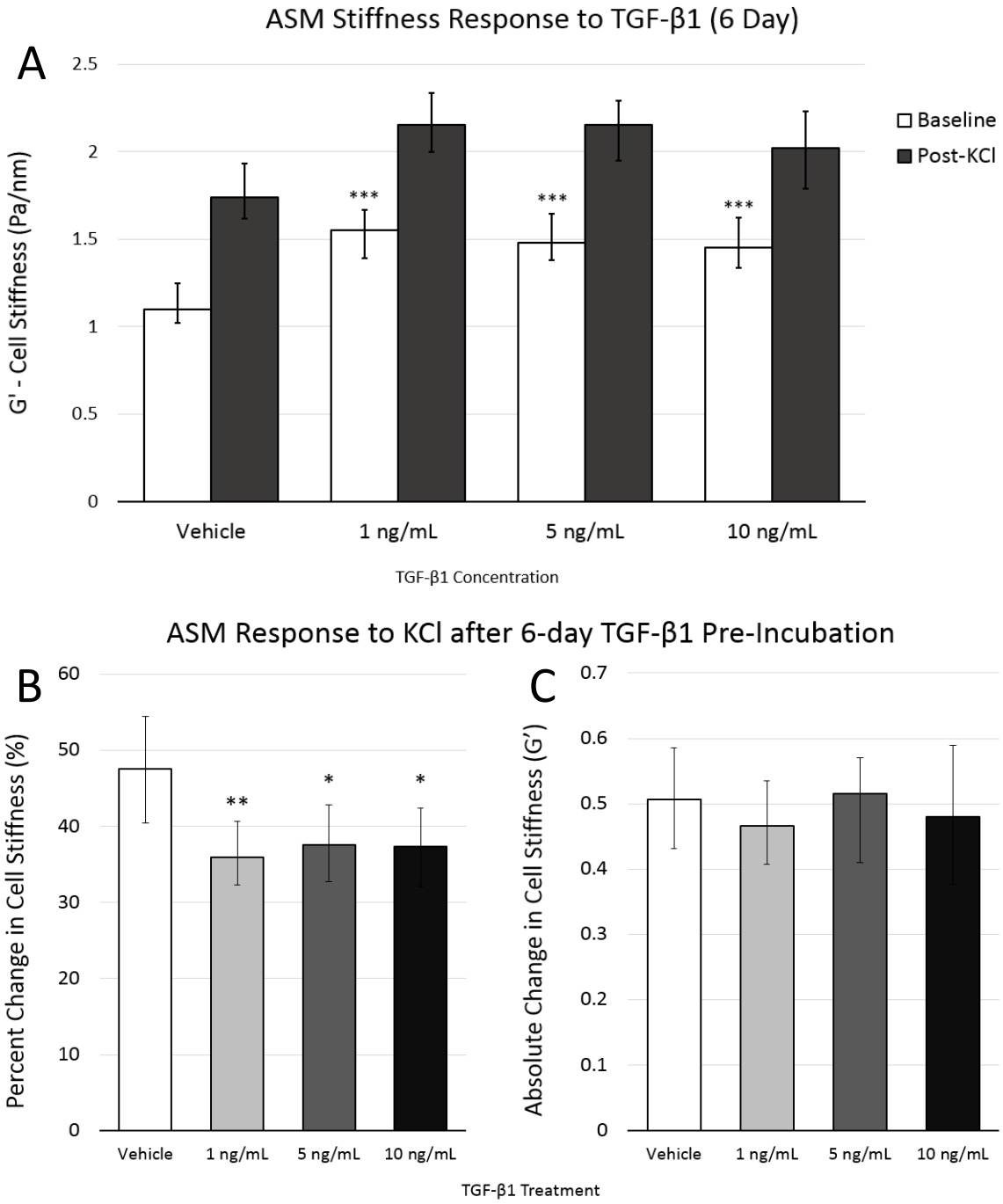

Figure 4.3.1: (A) TGF-β1 at 1, 5, and 10 ng/mL increased ASM median cell stiffness ($p < 0.001$). However, amongst the different concentrations of TGF-β1, no difference in cell stiffness was observed. Cells responded typically to isotonic 80 mM KCl solution by acutely increasing cell stiffness (filled bars) over the 3 minutes of KCl exposure. (B) Contractility, reported as the percent change in cell stiffness relative to baseline stiffness, correspondingly decreased with TGF-β1 exposure at any concentration ($p < 0.01$). (C) However, between all groups, the absolute change in cell stiffness (Post-KCl minus Baseline) did not change. Data are presented as medians and 95% confidence intervals of cells across 3 donors (n = [466, 649]). Statistical significance was obtained using a Kruskal-Wallis test across the 4 treatment groups, and using multiple Mann-Whitney U tests for pairwise comparisons between groups with Bonferroni correction.

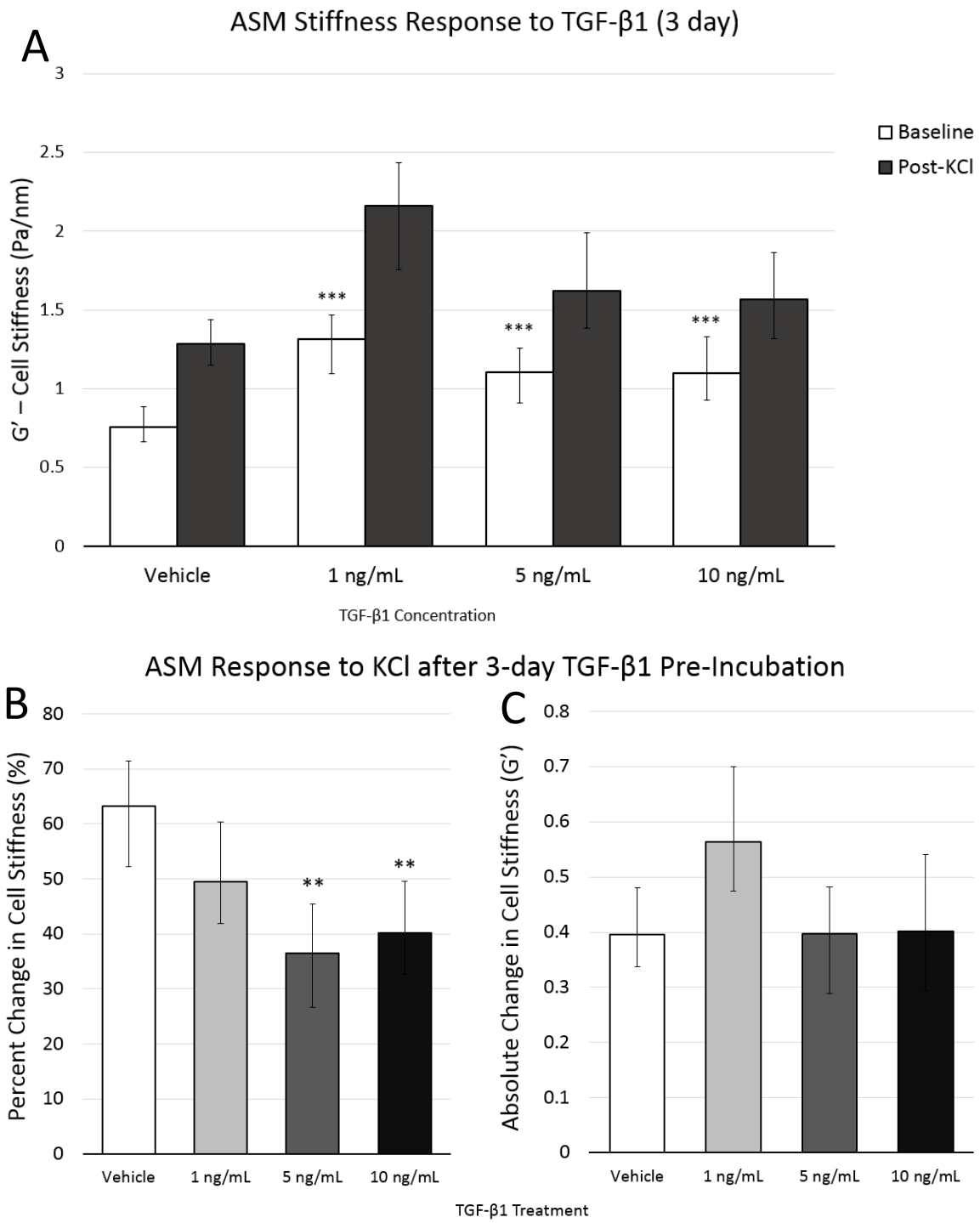

Figure 4.3.2: (A) TGF-β1 at 1, 5, and 10 ng/mL increased median ASM cell stiffness ($p < 0.001$). All groups responded typically to an isotonic KCl solution and increased cell stiffness (filled bars) after 3 minutes of exposure. (B) Percent contractility decreased with 5 and 10 ng/mL TGF-β1 exposure, but not with 1 ng/mL ($p < 0.01$). (C) Absolute change in cell stiffness in response to KCl was not significantly different between groups. Data presented as medians with 95% confidence intervals of cells across 3 donors (n = [323, 467]). Significance determined using Kruskal-Wallis test across the 4 treatment groups with multiple Mann-Whitney U tests for pairwise comparisons between groups and Bonferroni correction applied.

4.4 Discussion

In this section, we examined the effects of different concentrations of TGF-β1 on ASM cell stiffness and the corresponding change in cell stiffness in response to the contractile agonist KCl. Continuous exposure to TGF-β1 at concentrations as low as 1 ng/mL (i.e. at any of the tested concentrations) over 6 days saw an increase in baseline cell stiffness (G') and a decrease in ASM cell percent contractility in response to KCl. It is unclear at what concentration below 1 ng/mL cell stiffness and contractility may become dose-dependent to TGF-β1. However, concentrations below 1 ng/mL may not useful for subsequent experiments, since our epithelial cells required higher doses in order to elicit a measurable response.

4.4.1 Presence of TGF-β1 altered cell stiffness and contractility, but did not produce a dose-dependent response

There were no significant differences in baseline cell stiffness percent contractility between the ASM cells that were continuously exposed to 1, 5, and 10 ng/mL concentrations of TGF-β1 over 6 days. This could mean that our ASM cells were already saturated with TGF-β1 at 1 ng/mL. However, others have reported dose-dependent effects, although contractile function with respect to dose has not been previously measured. For example, Xie et al. 2007 found that ASM cell proliferation in response to TGF-β1 increases gradually with increasing doses between 0.1 and 10 ng/mL (notably, between 1, 3, and 10 ng/mL). Typically, cell contractility is often thought to be inversely related to proliferation in terms of being opposite phenotypes for smooth muscle; however, it is possible that with respect to TGF-β1 stimulation, contractile function and cell proliferation are the result of separate activated pathways. We can infer that TGF-β1 can activate multiple separate pathways in ASM cells, as TGF-β1-stimulated ASM cell proliferation is unaffected by inhibition of the Smad pathways, which are known to be activated

by TGF-β1 (though we do not known whether ASM contractile function is linked to a Smad pathway)[72].

The primary mechanism of TGF-β1 elimination occurs through cellular uptake of the ligand after it has bound to a TGF-β RII receptor, after which it is internalized and transported to lysosomes via vesicles for degradation[171,172]. As a result, TGF-β1 is eliminated at a constant rate proportional to the number of cells (more specifically, TGF-β RII receptors) so that a large enough dose of TGF-β1 corresponds to a constant "active" signal[171]. With respect to our 6-day experiment, our lowest dose of TGF-β1 (1 ng/mL) appears to already have been a saturation dose for our ASM, and the elimination of TGF-β1 was insufficient to deplete the ligand as we continued to refresh TGF-β1 every other day in our system throughout a 6-day exposure period. In contrast, our single-dose, 3-day experiments show that a single bolus of 1 ng/mL TGF-β1 significantly increases cell stiffness but maintains percent contractility to KCl, unlike the corresponding 5 ng/mL and 10 ng/mL groups (Figure 4.3.2B). This suggests that while lower doses might have elicited a dose-dependent response in stiffness, although again, these lower doses would not have been useful for our purposes, since they would be unlikely to elicit a response from our 16HBE14o- cells.

4.4.2 Magnitude of ASM cell stiffness response to KCl was unaffected by continued TGF-β1 exposure

In our TGF-β1 exposed ASM cells, although we observed a decrease in contractility expressed as a percent response to KCl (Figure 4.4.1B), this could be explained by the increase in baseline stiffness (observed in Figure 4.4.1A), as the absolute changes in stiffness were in fact unchanged (Figure 4.4.1C). This may indicate that contractile function was potentially preserved, and there may instead have been an increase in passive activation of the smooth muscle (i.e.

tone) induced by TGF-β1. Overall, therefore, TGF-β1 led to higher absolute stiffness values and thus would agree with the observations of Goldsmith et al. 2006, where increased cell shortening of non-adherent cells was observed with TGF-β1 exposure[74]. If this mechanism were present in the asthmatic airway, it may contribute to the hallmark exaggerated airway narrowing observed in asthma.

However, the primary aim of these experiments was to determine whether a dose-dependent effect on ASM cell stiffness or contractility could be measured using OMTC after exposure to TGF-β1 at working concentrations between 1 and 10 ng/mL. This was to find a dose that was low enough so that it did not stimulate contraction in our ASM cells, while still being sufficient to cause EMT-like changes in our 16HBE14o- cells as previously reported in Section 3. Since the strongest evidence for EMT in our 16HBE14o- cells from Section 3 did not occur until a concentration of 10 ng/mL TGF-β1 was used, this was the dose selected as the concentration necessary for our subsequent conditioned media and co-culture protocols. This meant we would need to design our AE-ASM interactions with TGF-β1 around this fact.

One possibility was to separate AE cell exposure to TGF-β1 temporally from ASM cell exposure to the AE. This would involve first exposing AE cells to TGF-β1 until the AE cells demonstrated changes indicating EMT, then introducing those AE cells to ASM cells. However, there is a possibility that a reverse process, mesenchymal to epithelial transition (MET) occurring once the TGF-β1 signal is removed. Another potential design is to separate AE-TGF-β1 exposure and ASM-AE exposure spatially. This could be achieved by exposing AE to a constant TGF-β1 signal in a vessel separate from the ASM, then obtaining the AE secretome and transferring it to the ASM (which is the basis for our conditioned media experiments). A third potential design is to simply allow both the AE and ASM to be exposed to TGF-β1. With this method, we reasoned that since TGF-β1 is ubiquitous and both cell types have the capacity (i.e.

receptors) to respond to TGF-β1 signaling, it is likely that they are both exposed to elevated TGF-β1 in asthmatic airways *in vivo*. Therefore, we could potentially combine all three elements, the AE, ASM, and TGF-β1 in a single environment. This third design informed our subsequent co-culture experiments.

Chapter 5: ASM Response to Airway Epithelium-Conditioned Media

5.1 Rationale

A conditioned media (CM) system was one of the methods we used to examine the effects of AE-released mediators on ASM cells considered. Previous work in our laboratory (Chen 2009) indicated that AE-conditioned media (AE-CM) on ASM cells decreased ASM response to the contractile agonist histamine measured by OMTC[157]. This suggested that AE cells may release an unknown relaxing factor that helps maintain a low contractile state in the ASM, akin to the interaction between vascular endothelial and smooth muscle cells (with possible intermediaries reviewed in Section 1.6). This inhibition of ASM contractile response to histamine occurred shortly after (approx. 5 minutes) the introduction of AE-CM and persisted up to 24 hours; however, the addition of AE-CM alone did not decrease cell stiffness, which suggested that AE-CM did not contain an active relaxing factor (such as NO) but rather, a contraction-inhibiting factor[157]. The action of such a 'contraction-inhibiting factor' may involve causing a contractile agonist to be less effective (e.g. by blocking GPCRs or disrupting the pathway leading up to smooth muscle contraction). Another proposed possibility was that the AE-CM contained elements that caused more intrinsic (potentially phenotypic) changes to the ASM that led to decreased ASM contractile response to an agonist[157].

Our aim was to further investigate the influence of AE cells on ASM phenotype over a long-term period of six days. This, we believe, would provide ample time for the ASM cells to alter their gene and protein expression profiles in response to the AE-CM. In addition to measuring cell stiffness with OMTC, we also looked at changes in the levels of protein expression in our ASM cells in order to probe the potential antecedents for the changes in

contractility we expected. We also incorporated TGF-β1 into this, due to TGF-β1's known ability to induce EMT-like changes in AE cells, with both TGF-β1 elevation present in asthma and EMT being implicated in asthma. The objective here is to alter AE cells in order to modulate the factors present in the AE-conditioned media. Since we know TGF-β1 can cause EMT-like changes in AE cells, including our 16HBE14o- cells, we hypothesized that the mediators released by AE cells also change and may consequently influence ASM cells differently from TGF-β1-naïve AE cells. It might be that AE cells typically release a contraction-inhibiting factor that maintains a quiescent, non-contractile phenotype in ASM that normally operates in healthy airways. In asthma however, an elevated presence of TGF-β1 act to may diminish the effects of these factors on ASM (such as through decreased expression), resulting in increased response to contractile agonists and may indicate a potential contribution to the hyperresponsiveness observed in asthma. We explored the effects of AE-CM taken from 16HBE14o- cells that were exposed to TGF-β1 to see if it effected a change in ASM cells that was different from normal AE-CM from naïve 16HBE14o- cells.

5.2 Approach

In these experiments, we used media conditioned by our 16HBE14o- cells and introduced this to primary ASM cells from multiple donors. In preliminary experiments, we noted that the immortalized 16HBE14o- cells depleted and acidified their culture media rapidly, which could affect our ASM cells negatively when this CM is directly introduced. The use of 100% CM on our ASM resulted in an exceedingly "spindly" morphology in the ASM, with several thin and elongated processes reminiscent of neuronal dendrites. We suspected that depletion of vital components in the CM or a significant change in pH in the CM (which could drop from a pH of ~ 7.20 down to ~ 6.45 following a 24-hour incubation with our 16HBE14o- cells, data not shown) to be contributory factors resulting in these effects. In order to mitigate these effects, we

limited the time our AE cells were allowed to condition our CM to 4 hours. Even with the 4-hour limit, however, the media phenol red indicator showed there was likely significant metabolic activity in 16HBE14o- containing wells (approximately pH 6.8 while the flasks were in the 5% CO_2 environment of the incubator). While it may have been possible to precisely adjust the pH, we opted for a simpler method of diluting the CM with fresh media 0.5% media (0.5% serum in a 1:1 DMEM/F12 media) at ratios of 1:1 and 1:4 (CM : fresh media, respectively). The additional media (containing HEPES buffer) could help stabilize pH (to approximately 7.1 – 7.2), and the addition of fresh media would provide additional vital components to support the ASM over the following 48-hour incubation period[173,174]. The lower concentration 1:4 CM served as a backup group in our experiments case the ASM did poorly in 1:1 CM.

To produce our conditioned media in each iteration of the experiment, 16HBE14o- cells were cultured in a single T75 flask to confluence and subsequently subcultured into multiple T25 flasks, which were again grown to confluence in 10% media (DMEM/F12 media supplemented

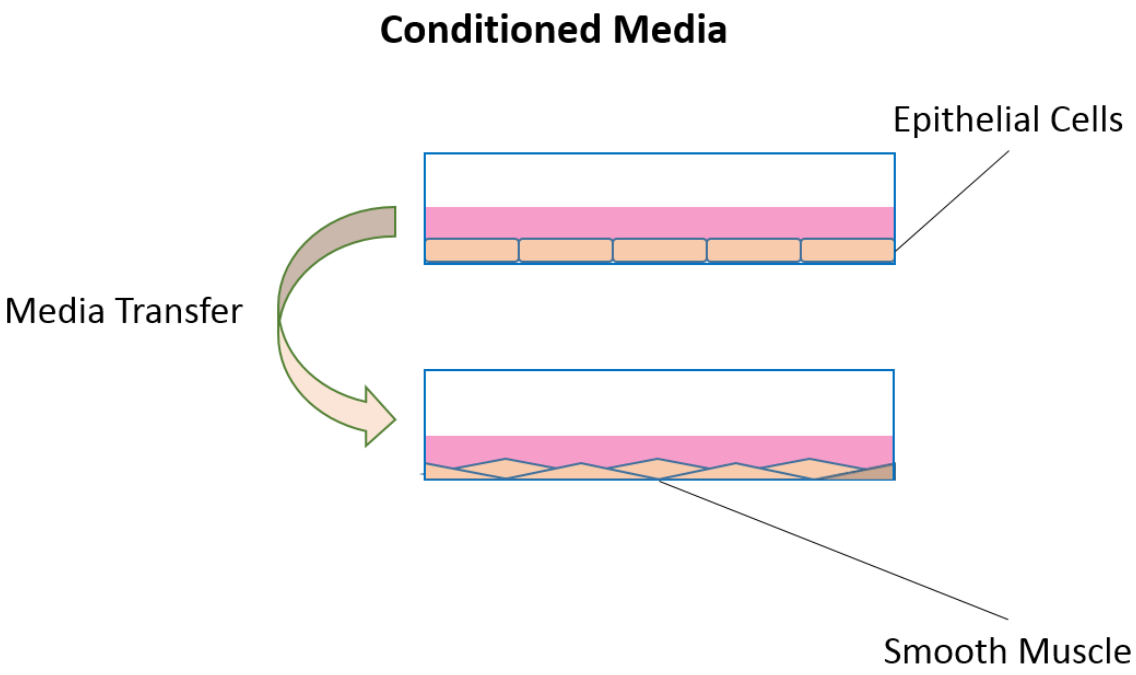

Figure 5.2.1 Basic schematic of conditioned media procedure. Media that is conditioned by AE cells are periodically transferred to ASM cells. The effect on the ASM is subsequently assessed.

with 10% serum). Once at confluence, the cells were exposed to TGF-β1 at 10 ng/mL or a corresponding volume of vehicle for 48 hours. CM was produced by washing the cells once with 0.5% serum media, then adding 5 mL 0.5% serum media in each T25 for 4 hours in order to obtain the cell secretome. This media (now CM) was collected at the end of the 4 hours and syringe-filtered through 0.45 µm filters to remove cells and other debris. The 16HBE14o- cells were returned to 10% serum media for maintenance. This process was repeated every 48 hours for a total of three CM samples per flask.

Primary ASM cells were grown on collagen-coated glass coverslips (for OMTC) in 12-well plates or on the collagen-coated surface of the 12-well plate (for LI-COR) to confluence in 10% serum media, after which they were maintained in 0.5% serum media. The ASM cells were exposed to diluted CM (to ensure cell survival, both 1:1 or 1:4 CM to fresh media, were used) for three 48-hour periods over 6 days. Following the 6 day CM exposure, cells were either prepared for OMTC by switching to serum-free IT media for 24 hours. For our OMTC data, statistical significance was determined using Kruskal-Wallis tests followed by multiple Mann-Whitney U tests for pairwise comparisons, with Bonferroni correction applied to account for multiple comparisons. As we later observed that the ASM cells in 1:1 CM survived and developed a normal smooth muscle cell morphology, we proceeded to examine protein expression in the 1:1 CM-exposed ASM. These cells were fixed with formaldehyde (outlined in detail in Section 2.2) and immunostained for myocardin, smooth muscle myosin heavy chain (smMHC), calmodulin (CaM), myosin light-chain kinase (MLCK), myosin light-chain phosphatase (MLCP), and calponin. LI-COR data was normalized to the relative mean cell density of each treatment group (i.e. cell counts). Statistical analyses for relative protein expression were done independently for each protein of interest. This involved one-way ANOVAs followed by Tukey post-hoc tests for pairwise comparisons (Figure 5.3.4). Cell density was determined with ImageJ-aided nuclear counts

across 16 wells per donor over 3 donors, for a total of 48 wells per group. Counts were normalized to counts of the vehicle-treated wells of each donor before the mean relative cell density was calculated. Statistical analysis of cell density was done using a one-way ANOVA with Tukey post-hoc test for pairwise comparisons (Figure 5.3.5). All immortalized cells were under passage 25 and all primary cells were less than passage 5.

5.3 Results

Long-term exposure of ASM cells to the 16HBE14o- cell secretome via CM led to a significant decrease in the baseline cell stiffness to 68.2% and 77.9% (at 1:4 and 1:1 dilutions, respectively) of vehicle-treated cells. Cell stiffness was also decrease in response to CM from TGF-β1-treated 16HBE14o- cells by a similar degree, to 73.0% and 80.5% of vehicle baseline at 1:4 and 1:1 dilutions, respectively (open bars, Figure 5.3.1). ASM cell stiffness following KCl-induced contraction (i.e. post-KCl stiffness) was also diminished, to 71.0% and 82.9% of vehicle when the ASM cells were exposed to CM at 1:4 and 1:1 dilutions, respectively. Again, with the addition of CM from TGF-β1-treated 16HBE14o- cells, smooth muscle post-KCl stiffness was again decreased, to 66.7% and 83.5% of vehicle post-KCl stiffness (filled bars, Figure 5.3.1). Cell stiffness values (G') with 95% CI are also reported in Table 5.3.1.

The magnitude change in cell stiffness before and after KCl addition was smaller in most CM-exposed ASM (Figure 5.3.2) compared to ASM not exposed to CM (vehicle). Interestingly, this was most pronounced in ASM that were given the lower 1:4 dilution of CM and much less so in the higher 1:1 CM. When the magnitude change in cell stiffness was normalized to the baseline stiffness of each cell, only ASM cells exposed to a 1:4 dilution of CM from AE cells with prior exposure to TGF-β1 show a significant change in percent contractility from control (fourth bar, Figure 5.3.3).

	Baseline Stiffness (G') (Pa/nm) with 95% CI	Post-KCl Stiffness (G') (Pa/nm) with 95% CI	Percent Contractility with 95% CI
Vehicle	0.57 [0.53, 0.62]	0.94 [0.89, 1.01]	56.72 [54.00, 61.96]
1:4 CM	0.39 [0.36, 0.44]	0.67 [0.62, 0.73]	54.61 [50.29, 63.50]
1:1 CM	0.44 [0.41, 0.49]	0.78 [0.72, 0.88]	55.56 [52.38, 61.46]
1:4 CM (TGF-β1)	0.41 [0.37, 0.47]	0.63 [0.57, 0.72]	43.82 [40.31, 49.40]
1:1 CM (TGF-β1)	0.46 [0.43, 0.51]	0.78 [0.71, 0.89]	54.29 [49.56, 62.36]

Table 5.3.1: ASM cell stiffness and contractility following 6 days of continuous exposure to CM.

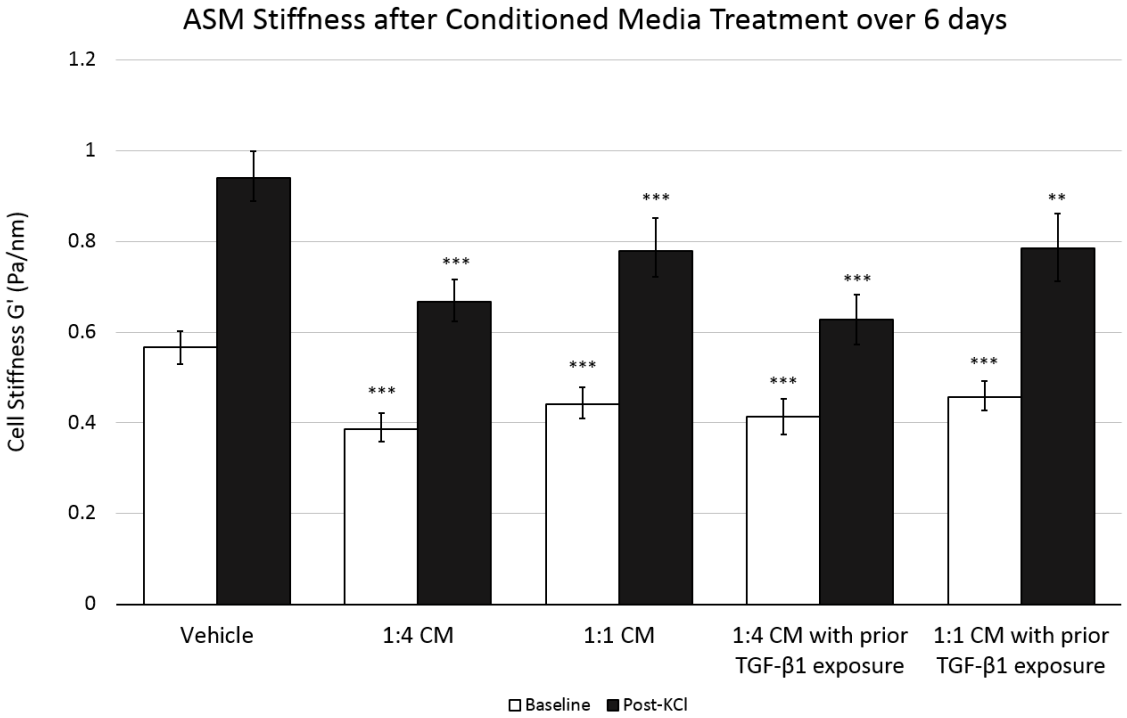

Figure 5.3.1: Continued exposure to CM over 6 days led to a general decrease in ASM baseline cell stiffness (open bars, $p < 0.001$). Cells responded typically to an isotonic 80 mM KCl solution with an acute increase in cell stiffness (filled bars) following a 3-minute KCl exposure. Post-KCl cell stiffness was also significantly diminished with a 6-day exposure to CM ($p < 0.001$). CM derived from cells with prior exposure to TGF-β1 did not lead to a significant departure in ASM cell stiffness compared to CM derived from TGF-β1-naïve cells. Data here are presented as the median cell stiffness of cells across 3 donors, with error bars representing 95% confidence intervals ($n_{Vehicle} = 1897$, $n_{Conditioned\ Media} = [1002, 1064]$).

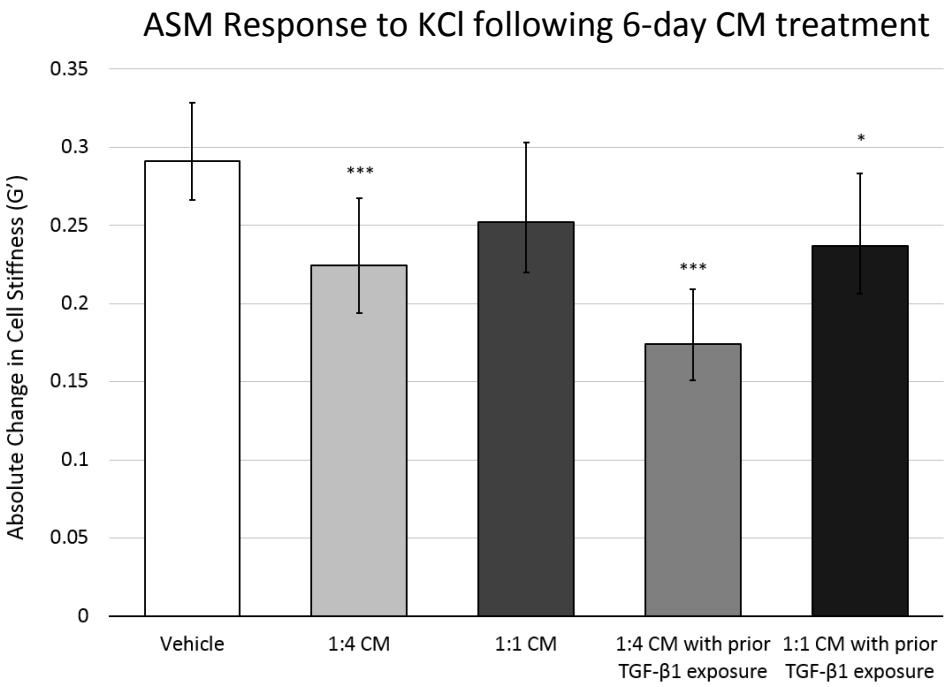

Figure 5.3.2: The difference in baseline and post-KCl stiffness values from Figure 5.3.1 is shown here for clarity. However, it should be noted that the data here shows the median absolute change in cell stiffness on a per cell basis, with error bars indicating the 95% CI. The change in ASM cell stiffness in response to KCl is smaller in the more dilute 1:4 CM, while the 1:1 CM does not have as much of an effect with respect to vehicle. The prior exposure of 16HBE cells to TGF-β1 does not further diminish the ASM contractile response to the contractile agonist KCl.

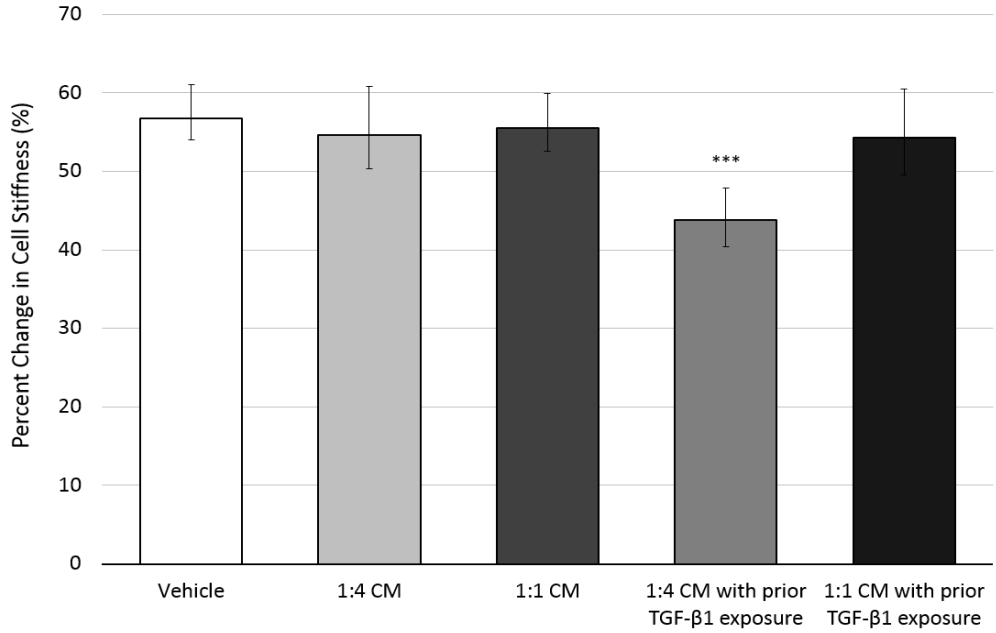

Figure 5.3.3: Change in ASM cell stiffness due to KCl (on a per cell basis) is normalized to the baseline stiffness of each cell, so that the median of the change in stiffness relative to the baseline stiffness of each cell are illustrated. Error bars indicate the 95% CI. Only CM at a 1:4 dilution from 16HBE cells with prior TGF-β1 exposure demonstrated a diminished contractile response relative to baseline stiffness.

Protein expression was examined in ASM cells that had received the higher 1:1 dilution of CM (instead of the 1:4 dilution), as that is where we believed we would see more pronounced changes in ASM protein expression. All relative protein expression values were normalized to relative cell density. With exposure to 1:1 CM, there was a marked increase in mean ASM myocardin expression to 563±34% of control (relative protein expression ± SE). Additionally, smMHC expression decreased slightly to 85.9±2.5% of control, and calponin expression decreased moderately to 72.6±1.7% of control. No significant changes in the expression of CaM, MLCK, or M-RIP were observed (shaded bars, Figure 5.3.4).

ASM cells exposed to CM from AE with prior TGF-β1 exposure had comparable responses in protein expression compared to the TGF-β1-naïve CM. Calponin expression in ASM treated

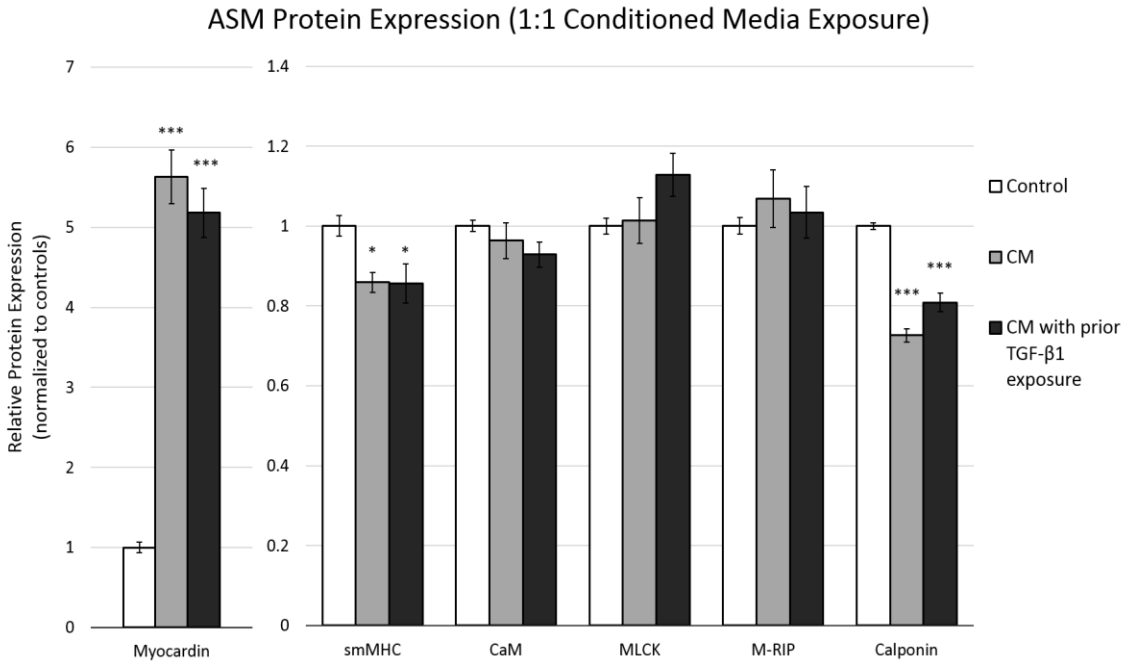

Figure 5.3.4: ASM relative protein expression following treatment with 1:1 CM over 6 days. The relative protein expression of cells treated with vehicle, 16HBE CM, or TGF-β1-treated 16HBE CM were compared for six contraction-associated proteins (myocardin, smMHC, CaM, MLCK, M-RIP, and calponin). Data shows the mean relative expression of each protein across 4 wells per donor with 3 donors, for a total of 12 wells per bar. Expression for each protein was normalized to relative cell density and to the vehicle-treated group (control) of each donor before wells between donors were pooled. Expression of vehicle-treated groups were set to a standard value of 1.Error bars denote the SEM.

with the TGF-β1-exposed CM was slightly higher than in ASM with normal CM (80.8±2.3% vs 72.6±1.7% of control).

Nuclear counts of fixed, adherent ASM cells indicated that CM from 16HBE14o- cells over 6 days increased relative ASM cell density by 12.0±2.4%. CM from TGF-β1-exposed 16HBE14o- cells over 6 days increased ASM cell density by 9.7±2.2% of control (Figure 5.3.5).

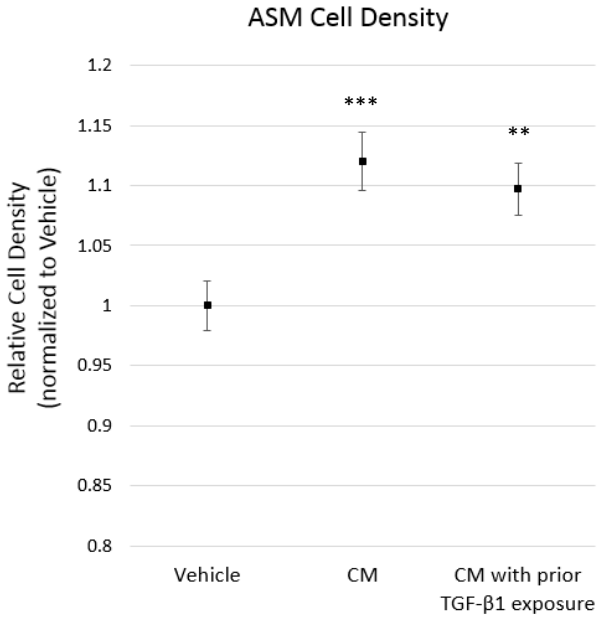

Figure 5.3.5: Relative mean cell density of ASM cells modestly increased with long-term (6-day) exposure to CM. Error bars show the SEM. ASM relative cell density was significantly higher when AE-CM was added to wells. Addition of CM from TGF-β1-treated 16HBE14o- cells did not result in significantly different ASM cell density compared to naïve 16HBE14o- CM.

5.4 Discussion

Our working hypothesis was that, while AE-conditioned media could influence ASM cell contractility in the short term[157], over a longer period of time, if AE contributes to 'normal' (i.e. less contractile) ASM function, we would also see a more persistent decrease in ASM

contractility. We also expected changes in the expression of a range of contraction-associated proteins, which may be indicative of more long-term changes which may reflect a change in ASM cell phenotype. Our secondary hypothesis was that TGF-β1-influenced 16HBE cells produced an altered secretome, so that the CM derived from these cells could remove any beneficial effect on ASM protein expression and function—that is, TGF-β1 might enhance the contractile function and the expression of contraction-associated proteins in ASM cells compared to naïve 16HBE14o- CM.

5.4.1 AE-Conditioned Media Decreases ASM Cell Stiffness and Diminishes ASM Contractile Function

We found that ASM cell stiffness decreased after long-term (6 day) exposure to AE-conditioned media, which confirmed our initial hypothesis and suggested that AE may indeed produce factors that alter ASM cell phenotype (open bars, Figure 5.3.1). The decrease in the stiffness of the cytoskeleton may indicate a decrease in the internal pre-stress of a cell[175]. This can be typically attributed to reduced actin-myosin contraction. Other factors, such as reduced adhesion of the bead to the cytoskeleton, or changes in the cytoskeleton such as reduced cross-linking or reduced F-actin, can also explain our decreased stiffness measurements. However, we did not see any change in the magnitude of the contractile response, which likely means adhesion was similar so that reduced stiffness of the cytoskeleton is the more likely explanation. Indeed, the decreases in smMHC expression in CM-exposed ASM supports the interpretation of a decrease in tension or tone (Figure 5.3.4), since actin-myosin interactions form the basis of the force-generating component of smooth muscle cells.

What factors could be responsible for this decrease in baseline stiffness? While it is possible that the CM-exposed ASM cells may be switching to a less contractile phenotype, it is

also possible that a number of proposed AE-derived relaxing factors may be actively contributing to ASM relaxation[89,90,176]. However, with respect to the timeline in of our experimental design, ASM cells bound for OMTC were given the final dose of CM 3 days prior to measurement. Additionally, these cells were given fresh IT media 24 hours before OMTC (whereas the LI-COR bound cells were fixed immediately following the 6-day exposure). It is therefore highly unlikely that active relaxing factors (such as NO) played a part in the decrease in baseline stiffness in CM-exposed ASM in the OMTC-analyzed cells, as any such agents would likely have been depleted or washed out. In this context, it is likely that more permanent, potentially phenotypic changes to the ASM are responsible for the change in baseline stiffness. Moreover, post-KCl ASM cell stiffness was also diminished with CM exposure (filled bars, Figure 5.3.1). If the decrease in ASM cell stiffness were due to transient relaxing factors, it would be expected that once these factors were washed out, the ASM would retain the ability to achieve post-KCl cell stiffness values comparable to that of vehicle-treated cells. In all, the cell stiffness data suggests that AE-CM contain factors that can lead to phenotypic changes in ASM cells.

While AE-CM definitively decreased ASM cell stiffness, its influence on the active contractile component of the ASM (i.e. the change in cell stiffness in response to KCl or percent contractility) in our study was more mixed. Like the reduced baseline stiffness, the KCl-induced absolute change in cell stiffness was smaller in ASM exposed to CM; this effect was more salient in the 1:4 dilution of CM, whereas the 1:1 dilution of CM did not show a significant reduction in the absolute change in cell stiffness in ASM with KCl-induced contraction (Figure 5.3.2). Moreover, in terms of percent change in ASM cell stiffness in response to KCl, only the TGF-β1-influenced CM at a 1:4 dilution showed a decrease (Figure 5.3.3). The use of CM can be a “black-box” since it is difficult to determine all the factors present in the media. Unknown mediators in the CM may ultimately influence the ASM response to these same mediators (e.g. by

modulating receptor expression). Nevertheless, for all ASM cells exposed to AE-CM, inducing ASM contraction with KCl resulted in a final post-KCl stiffness that was lower than unexposed ASM (Figure 5.3.1), ultimately implying that the exposure of ASM to some factor or factors in the AE-CM may be protective against excessive contractility and could inhibit the generation of maximum force.

The absence of AE cells has been associated with increased contractile response in ASM, but the mechanism through which this occurs is still unclear. In muscle strip studies from humans, as well as several animal models, tissue samples denuded of AE demonstrated increased contractile responses[177–179]. However, caution should be used in associating these studies, since the ASM was examined shortly following the removal of AE, so that the changes in contractility observed could likely be the result of constitutive factors released by AE that actively diminish ASM contractile response. Therefore, we cannot attribute the reduced contractility in intact tissue strips with the more chronic changes in contractile phenotype we investigated here. Additionally, in our control (vehicle-treated) groups, cultured ASM was grown removed from the presence of AE for several cell passages (passage 2 through passage 4). In fact, it could be said that our CM-treated cells that are more akin to the denuded tissue strips: both have been previously exposed to the AE secretome, the denuded tissue strip when it was previously intact *in vivo*, and our CM-treated ASM during the incubation with AE-CM; furthermore, tissue strip contractile function was measured following epithelial denudation, and OMTC measurement of CM-treated ASM contractility necessarily takes place after AE-CM is removed and replaced with IT media (as described in the protocol). This distinction is important to keep in mind when we consider potential changes in phenotype; cultured ASM with no prior exposure to the AE secretome may not completely reflect the state of AE-denuded ASM in

asthmatic airways. Nevertheless, our data still suggest that AE can influence ASM contractility by influencing phenotype.

5.4.2 16HBE CM Altered ASM Protein Expression

Due to experimental limitations and the expectation that the larger dose at 1:1, which was still well-tolerated by the ASM cells, would be more informative, analysis of protein expression was solely done on 1:1 rather than 1:4 diluted CM. Associated with the observed decline in stiffness in the ASM, we also found decreases in the expressions of smMHC and calponin. The functional protein smMHC is the motor protein that confers to smooth muscle the ability to contract, and thus, the decrease in smMHC expression may have directly contributed to the decreased baseline stiffness. The loss in stiffness coupled with the decrease in smMHC therefore appear to indicate a loss in basal tone. This might have also occurred in the 1:4 diluted CM groups, but was not measured. Both calponin and smMHC are associated with the contractile phenotype in smooth muscle, where calponin acts as a regulatory element[56,131,180]. Therefore, the modest decrease in calponin expression in CM-treated ASM further supports the notion that the AE secretome contained factors that led to a less contractile and more synthetic/proliferative phenotype in ASM. Further evidence for this potential shift comes from the greater relative cell density in CM-treated groups following the 6-day treatment period (Figure 5.3.5).

However, the most striking and contradictory change in CM-exposed ASM was the dramatic increase in the expression of the transcription co-factor myocardin. As reviewed in Section 1.7.1, the expression of myocardin indicates the maturation of synthetic/proliferative smooth muscle cells into more contractile smooth muscle since it regulates many smooth muscle genes. With a more than four-fold increase in myocardin expression in 1:1 CM-exposed

ASM, we should have reasonably expected corresponding increases in the expression of proteins that myocardin regulates, including smMHC, MLCK, and calponin. However, in our CM-exposed ASM, no other contractile markers have increased expression; in fact, smMHC and calponin expression decrease instead. This contrasts with other reports that indicate that simply overexpressing myocardin was sufficient to induce the expression of contraction-associated proteins, even in cell lines that are not typically contractile, such as BC3H1[104,111,181].

It is unclear why the dramatic rise in myocardin was not associated with increased stiffness and an increase in the expression of other protein markers associated with the contractile phenotype in our ASM cells. In some less differentiated cells (i.e. more progenitor-like cells), the presence of myocardin alone has been suggested to be possibly insufficient to develop a contractile smooth muscle phenotype[182]. However, our cells were prepared as originally described in Panettieri et al., where normal primary human ASM cells are obtained and used at a very early passage[183]. These cells can take on a synthetic/proliferative or a contractile phenotype, and they are commonly used as contractile cells, meaning they readily differentiate into the contractile phenotype[124,184,185]. Since myocardin is a transcriptional co-factor, the associated transcription factor SRF is necessary for myocardin action on contraction-associated genes. It may be possible that SRF expression was unchanged or diminished, or the interaction between myocardin and SRF was inhibited. However, myocardin by itself may elevate the level of SRF transcription factor when overexpressed, so decreased SRF may not be sufficient explanation for the ineffectiveness of myocardin in our CM-exposed ASM[111]. In subsequent co-culture experiments (to be described in the following chapter), where the ASM is directly exposed to the AE, ASM does not show the same increase in the expression of myocardin with exposure to the AE secretome; the increased myocardin measured in the CM-

treated ASM may be a consequence or artifact of the one-way nature of AE to ASM communication in a conditioned media system.

5.4.3 Prior Exposure to TGF-β1 did not Modulate AE Influence on ASM

The CM produced following the addition of TGF-β1 to 16HBE14o- cells did not alter ASM cell stiffness or contractility in a manner that was significantly different from ASM that was given CM from TGF-β1-naïve 16HBE14o- (naïve CM). Both ASM baseline and post-KCl cell stiffness decreased after having been exposed to TGF-β1 CM over the 6-day period, but the effect of TGF-β1 CM on ASM cell stiffness was not significantly different from naïve CM (Figure 5.3.1). Similarly, the ASM contractile response to KCl was also largely the same between groups treated with TGF-β1 CM and naïve CM (with the exception of the percent change in cell stiffness measure in 1:4 diluted CM, which was a statistically significant but functionally small decrease, Figures 5.3.2 and 5.3.3). It is perhaps unsurprising then, that there was no difference in the ASM response, in terms of the expression of each of the contraction-associated proteins that we examined, between TGF-β1 CM and naïve CM groups (Figure 5.3.4).

Overall, we had hypothesized that AE cells that could be induced to undergo EMT-like changes by TGF-β1 (which may occur in asthmatic airways); these altered AE cells might then modulate ASM function differently from normal AE, possibly through paracrine signaling. Using our conditioned media method, we found that CM from normal and altered AE did not affect ASM cells differently when we examined ASM stiffness, contractility, or the expression of contraction associated proteins in the ASM. This could suggest that the AE secretome was not altered by TGF-β1, at least as far as the effects we examined on ASM; however, given the major changes to epithelial cell morphology and function that accompanies EMT (Section 1.5) and the development of EMT-like changes in our 16HBE14o- cells (Section 3.4) it seems unlikely that AE

paracrine signaling is entirely unaffected. It is possible that changes to the AE lead to signaling changes to other cell types, such as fibroblasts in the subepithelial layer, which may alternately be the source of factors that in turn affect the ASM[89]. However, we already show that AE can directly influence ASM stiffness, protein expression, and proliferation via CM (i.e. the AE secretome), so the possibility of such an indirect pathway between TGF-β1-treated AE and the ASM that is altered is not as attractive. Another possibility is that differences between the ASM treated TGF-β1 ASM and naïve ASM were present, but were not related to contractility with respect to our measures of stiffness, KCl-induced contraction, and protein markers; it is not known what these changes would be, however. Lastly, we might consider that the conditioned media protocol was not the ideal method for testing our hypothesis, in that the effect of the CM was not sustained, but instead introduced to the ASM as a bolus every other day, so that there may have been spikes in the concentration of AE secretome during the protocol. Additionally, *in vivo*, both the AE and the ASM would be in direct communication, and both may also be continuously affected by any elevated TGF-β1. If our aim is to determine whether AE-ASM communication is dysregulated, then our conditioned media method was likely insufficient, as the ASM were isolated from exogenous TGF-β1 by design. We know ASM cells are altered by TGF-β1, as we demonstrated earlier in Section 4 as well by other authors[71,72,74], and we also know that TGF-β1 is elevated in the submucosa of asthmatic airways, located between the AE and the ASM[186]. ASM exposure to TGF-β1 may be an important part of the story, which we address with our co-culture model in the following chapter.

Chapter 6: AE and ASM Co-culture

6.1 Rationale

We used a co-culture system to culture AE and ASM cells in close proximity, allowing continuous communication between the two cell types. This contrasts with the one-way, periodic AE-to-ASM communication inherent to the design of our CM model in Chapter 5. In the topology of a normal airway *in vivo*, AE cells line the luminal surface of the airway, supported by a basement membrane[77]. The AE and basement membrane overlie a mesenchymal layer with ECM and fibroblasts, below which lies the ASM. The co-culture system attempts a more faithful reproduction of this topology by having AE cells cultured in a layer on a semi-permeable membrane, which is suspended over ASM cells and share a common media between them. In this configuration, the ASM cells are exposed to products secreted by the AE, and vice versa, as would occur *in vivo*.

When ASM cells were exposed to CM from AE cells in Chapter 5, ASM cell stiffness (both at baseline and after contraction was induced) was generally diminished compared to CM-naïve ASM cells. We expected a similar response in the ASM to co-culture with AE cells, where baseline stiffness is diminished following long-term exposure (and likely, communication) with AE cells. Indeed, in Chen 2009, a similar co-culture protocol saw a decrease in baseline stiffness in ASM cells that had been co-cultured with AE cells, but this difference in G' was not apparent at 6 hours, but was present at day 4 of the co-culture[157]. My hypothesis was that AE cells release factor(s) that result in a quiescent, non-contractile phenotype in ASM cells, indicative of long-term, persistent changes to the cultured ASM. While it is possible in cell culture to characterize a single type of cell and grow it in isolation, avoiding potential confounding factors introduced by other cell types, such conditions are atypical *in vivo*, so our proposed co-culture system helps to

recreate an environment more akin to that of an intact airway. It is in this environment that we can then examine the effects of other external influences. In our case, this was the presence or absence of the TGF-β1 growth factor, which, as covered in Section 1.2.2, is upregulated in asthma and may dysregulate normal communication between the AE and ASM in co-culture.

6.2 Approach

Broadly, immortalized 16HBE14o- were co-cultured with primary human ASM cells from 3 different donors over 6 days, with or without the addition of exogenous TGF-β1. ASM cell stiffness and contractility was assessed with OMTC, and ASM relative protein expression was measured using immunofluorescent staining followed by LI-COR for quantification. Both measures were assessed from 3 independent experiments (one for each donor) with 3 individual wells assigned to each treatment group (so that overall, n_{wells}=9 for each measure). DAPI staining was used for obtaining cell counts, which were also used to normalize the LI-COR intensity data. OMTC and bead matching was used to analyze cell stiffness, as described in Sections 2.4 and 2.5. Finally, TEER was used measure electrical resistance across the 16HBE14o- cell layer in isolated culture or co-culture, with and without the addition of TGF-β1. For OMTC data, statistical significance was determined using Kruskal-Wallis tests, followed by multiple Mann-Whitney U tests for pairwise comparisons between appropriate groups, and Bonferroni correction was applied.

6.2.1 AE-ASM Co-culture

We used 16HBE14o- cells to form an intact, continuous layer of AE cells for our co-culture. 16HBE14o- cells were first grown to confluence in T75 flasks in 1:1 DMEM/F12 media supplemented with 10% FBS (10% media). They were then trypsinized and transferred into Corning Transwell (Corning Inc., Kennebunk, ME, USA) permeable supports (at 40,000 – 60,000

cells/well), so that the epithelial cells grew on the apical surface of the Transwell, a semipermeable membrane containing 0.4 μm pores to allow exchange of mediators with the basal chamber. These cells were fed with 10% media until confluent, forming an intact layer of cells within the Transwell insert (which took approximately 5-7 days). At confluence, cells were maintained with 10% media until co-culture.

Primary human ASM cells were prepared as described in Section 2.1.1. The cells were grown on either collagen-coated round glass coverslips which were seated in 12-well tissue culture plates, or on the collagen-coated surface of a 12-well tissue culture plate. Cells were initially fed with 10% media to expand the cell population until confluence, after which they were switched to 0.5% media (1:1 DMEM/F12 with 0.5% FBS) for maintenance prior to co-culture.

To initiate the co-culture, confluent layers of 16HBE14o- cells in Transwells™ were placed in the wells containing confluent ASM cells. In this configuration (Figure 6.2.1), the basal chamber would contain 1.5 mL of 0.5% media, while the apical chamber contains 0.5 mL of 0.5% media. The AE and ASM cell layers are approximately 1.2 mm apart in this configuration. For comparison, a typical airway can have a distance of 0.3 - 0.5 mm between the AE and ASM layers, although this could vary depending on local airway tissue morphology[157,187]. The surface area of the Transwell™ membrane insert containing our AE was 1.12 cm^2, while the surface area of each tissue culture well containing our ASM was 3.8 cm^2. It should be noted that when filling the chambers, only 1.0 mL of media is added to the basal chamber at first, followed by 0.5 mL of media in the apical chamber; finally, an additional 0.5 mL of media is added to the basal chamber. This sequence avoids any upwards hydrostatic pressure which risks dislodging the AE layer in the Transwell. For groups to be treated with TGF-β1, 10 ng/mL of TGF-β1 was added to

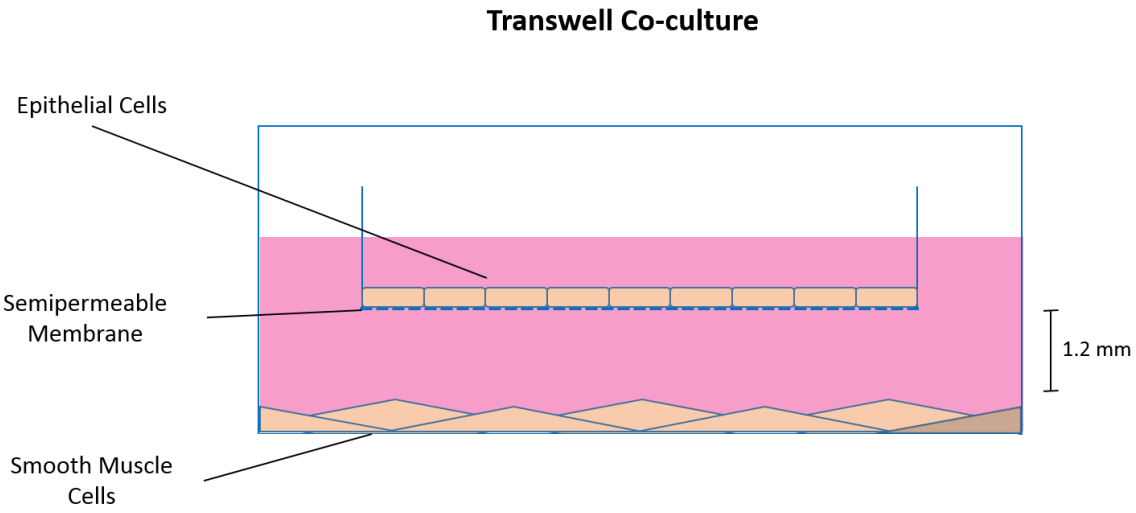

Figure 6.2.1: Diagram of Transwell™ co-culture system, with epithelial cells growing in a chamber suspended over smooth muscle cells. The cells are kept separate using a semipermeable membrane with pores approximately 0.4 µm in diameter to allow most ligands to pass through. The two cell layers are approximately 1.2 mm in distance apart, greater than what might be seen with in vivo airways; however, there is also little, if any, ECM between the AE and SMC layers so that bulk fluid movement is possible between the two layers.

the 0.5% media prior to feeding the cells, so that the apical chamber received 5 ng of TGF-β1, and the basal chamber received 15 ng of TGF-β1.

The cells were co-cultured for a total of 6 days. In the course of the 6-day co-culture, TGF-β1 was added (in the appropriate groups) only at the start of co-culture, so that the cells only receive a single bolus of TGF-β1 (or vehicle, i.e. 4mM HCl with 0.1% BSA in ddH_2O) at the beginning of the 6 day culture/co-culture period. The 0.5% media was changed at 48 and 96 hours (every two days, which essentially means the period of cell exposure to TGF-β1 was limited to the first 48 hours). At the end of the 6 days, the Transwells containing the AE were removed from the ASM; the ASM cells on glass coverslips were switched to IT media for 24 hours in preparation for OMTC (Section 2.4), while cells grown on the plate surface (w/o coverslips) were fixed and stained in preparation for LI-COR (Section 2.2) and then DAPI stained for counting after LI-COR analysis (Section 2.3).

6.2.2 Transepithelial Electrical Resistance

To demonstrate that the addition of TGF-β1 indeed induced changes in the 16HBE14o- cells that were potentially EMT-like (Section 3.4), we measured the transepithelial electrical resistance across the AE cell layer to indirectly assess how well-formed the tight junctions between the cells were. The AE cell layer in the Transwells that were removed at the end of the 6-day co-culture, described in the previous section, were transferred to empty 12-well plates and the 0.5% media was refreshed. The cells were allowed to rest after the media change for 15 minutes prior to TEER assessment.

A Millicell®-ERS (Millipore Corporation, Billerica, MA, USA) voltohmmeter was used to measure the resistance across the Transwell membrane. The device generates a 12.5Hz AC current with a square waveform (±2 μA) across a pair of two silver/silver chloride electrodes (MERS STX 01, Millipore Corporation, Billerica, MA, USA)[188]. The ends of the electrodes are placed in the apical or basal chambers so that the Transwell membrane and epithelial cell layer lie between the two electrodes. With the current applied, the device measures potential, then calculates and outputs the resistance value in ohms. Fluid (0.5% media) and electrode resistance is zeroed prior to measurement, so that the raw resistance measured is the AE cell layer and the Transwell membrane in series. Thus, the resistance of the Transwell membrane (taken from an average of blank wells, typically 136.7 ± 4.8Ω) may be subtracted from the raw resistance value to give the AE cell layer resistance[189]. Although all the Transwells for the AE were identical, resistance here is reported as resistance times the area of the growth surface/membrane (with a value of 1.12 cm^2) to allow for comparison with other cells grown in differently-sized Transwells. Data will be reported in the units $\Omega \cdot cm^2$. This value was used as an index of the integrity of intercellular AE cell junctions, which assumes that the path that current takes flows

primarily between the AE cells. It is possible that current may also flow through the cells (via ions and ion channels) so that there are two parallel paths, described as follows:

$$\frac{1}{R_{total}} = \frac{1}{R_{paracellular}} + \frac{1}{R_{transcellular}}$$

Therefore, the value of $R_{transcellular}$ may influence how well R_{total} reflects the value of $R_{paracellular}$ (our desired measure of intercellular junction integrity). We assume that AE cells have a comparatively high resistance to current such that $R_{transcellular} >>> R_{paracellular}$ so that $1/R_{transcellular}$ approaches zero.

TEER was measured at the end of the 6-day co-culture described in Section 6.2.1, but not during the co-culture due to concern over incidentally contaminating the co-culture system by introducing the external electrodes. Thus, we have TEER measures of 16HBE14o- cells 6 and 8 days after the start of co-culture (which coincide with 0 and 2 days after the end of co-culture, respectively). A separate co-culture protocol was set up in order to measure TEER during the co-culture period. In this protocol, AE cells were cultured with or without ASM co-culture, and either TGF-β1 or vehicle was added once to the media at the initiation of co-culture. TEER was measured every 48 hours once co-culture began and continued over 8 days.

6.3 Results

6.3.1 Cell Stiffness and Contractility

Similar to the results in Section 4, the median baseline stiffness of TGF-β1-treated ASM cells 6 days after exposure was 42.6% greater, compared to the vehicle-treated ASM cells. However, the median cell stiffness after inducing contraction (with KCl) in the TGF-β1-exposed ASM was not different from the vehicle group (Figure 6.3.1). Meanwhile, ASM cells that were co-cultured with AE over 6 days had median baseline stiffness and post-KCl contraction stiffness

values that were less than the ASM cells that were not co-cultured (i.e. the "Vehicle" labeled group) by 31.0% and 46.9%, respectively (similar to the smaller cell stiffness values seen in CM-treated ASM cells in Section 5). When TGF-β1 was introduced to cells in co-culture, the ASM cells responded similarly, with stiffness values at baseline and post-KCl that were not significantly different from the co-cultured cells with vehicle only. Cell stiffness values with 95% CI are reported in Table 6.3.1.

	Baseline Stiffness (G') (Pa/nm) with 95% CI	Post-KCl Stiffness (G') (Pa/nm) with 95% CI	Percent Contractility (%) with 95% CI
Vehicle Only	0.57 [0.52, 0.62]	1.22 [1.10, 1.30]	83.79 [77.04, 90.48]
TGF-β1 Only	0.81 [0.72, 0.89]	1.14 [1.03, 1.27]	33.22 [28.30, 39.67]
Co-culture with Vehicle	0.39 [0.36, 0.43]	0.65 [0.58, 0.75]	38.90 [32.40, 46.31]
Co-culture with TGF-β1	0.43 [0.38, 0.48]	0.62 [0.51, 0.75]	27.63 [20.77, 33.38]

Table 6.3.1: ASM cell stiffness and cell contractility (change in stiffness normalized to baseline) following 6 days of culture, with or without AE co-culture, and with or without exposure to TGF-β1.

Unsurprisingly, the *absolute change in cell stiffness* in response to KCl-induced contraction was smaller (56.9% of 'vehicle only') in cells that had been treated with TGF-β1 (Figure 6.3.2), since baseline stiffness was elevated while post-KCl stiffness remained similar with those in the vehicle-treated group. In cells that were co-cultured, there is a clear difference in *absolute change in cell stiffness*, with a significantly smaller (33.2% of 'vehicle only') response in the AE-co-cultured ASM compared to ASM cells grown without AE exposure. When TGF-β1 is present in the co-culture, the KCl response of the ASM was even smaller (60.1% of 'co-culture with vehicle') compared to ASM in co-culture without TGF-β1 exposure. Normalization to the baseline stiffness of each bead gave the *percent change in cell stiffness* which demonstrated that with the changes in baseline stiffness and the reduction in absolute change in stiffness following KCl-induced contraction, the resulting KCl contractile responses in terms of percent were quite similar (Figure 6.3.3), which meant that co-culture resulted in both diminished cell

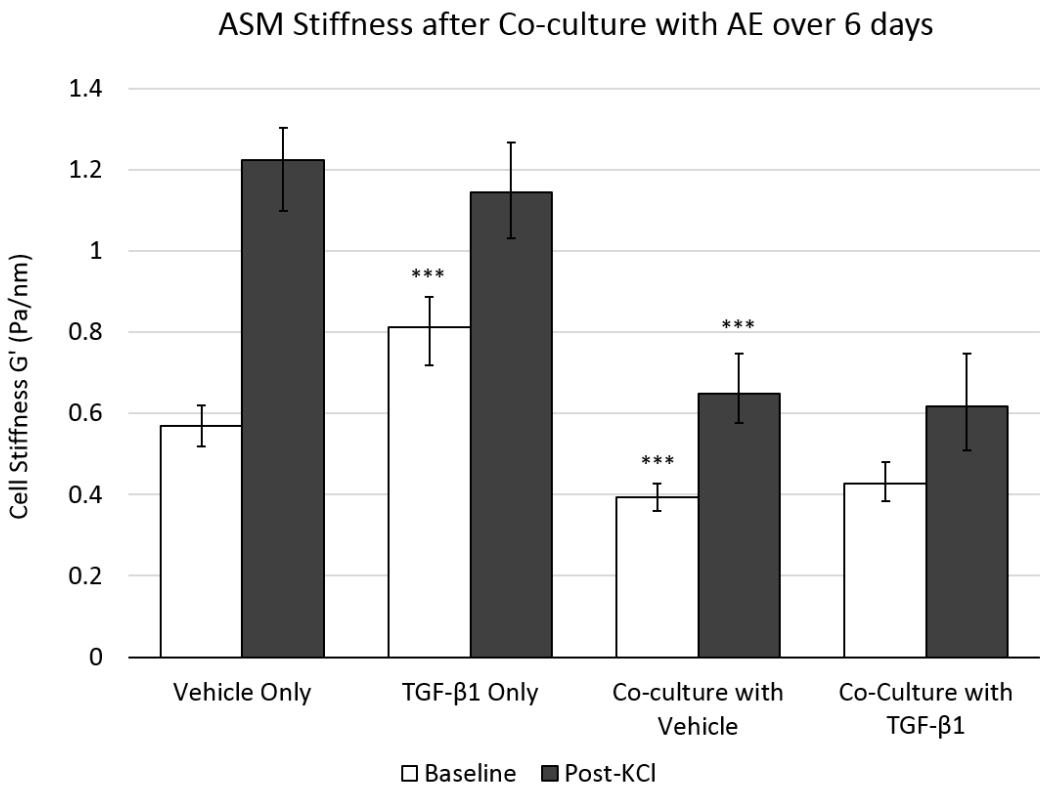

Figure 6.3.1: Exposure to TGF-β1 at 10 ng/mL led to a persistent elevation in baseline cell stiffness (open bars, $p < 0.001$). Conversely, exposure to AE cells via co-culture saw depressed baseline ASM cell stiffness following a 6-day co-culture ($p < 0.001$). However, co-cultured ASM cells did not have significantly different cell stiffness values (compared to co-culture only cells) when TGF-β1 at 10 ng/mL was present. Cells in all groups behaved typically, with an acute increase in cell stiffness, in response to KCl contractile agonist (filled bars). Data is presented as median cell stiffness of cells over 3 donors. Error bars denote 95% CI ($n_{vehicle} = 481$, $n_{TGF\text{-}\beta1} = 470$, $n_{co\text{-}culture} = 568$, $n_{co\text{-}culture+TGF\text{-}\beta1} = 419$).

stiffness at baseline, as well as final stiffness following KCl-induced contraction, independent of TGF-β1, as shown in Figure 6.3.1.

6.3.2 Protein Expression

Relative protein expression was measured using LI-COR (Section 2.2 and 2.3). The intensity of fluorescence for all cells in all treatment groups were significantly higher than background fluorescence, so that SNR for all wells were well within acceptable limits (data not shown). Mean background fluorescence was subtracted from all wells to give relative fluorescent intensity; these values were then normalized to a control group receiving vehicle

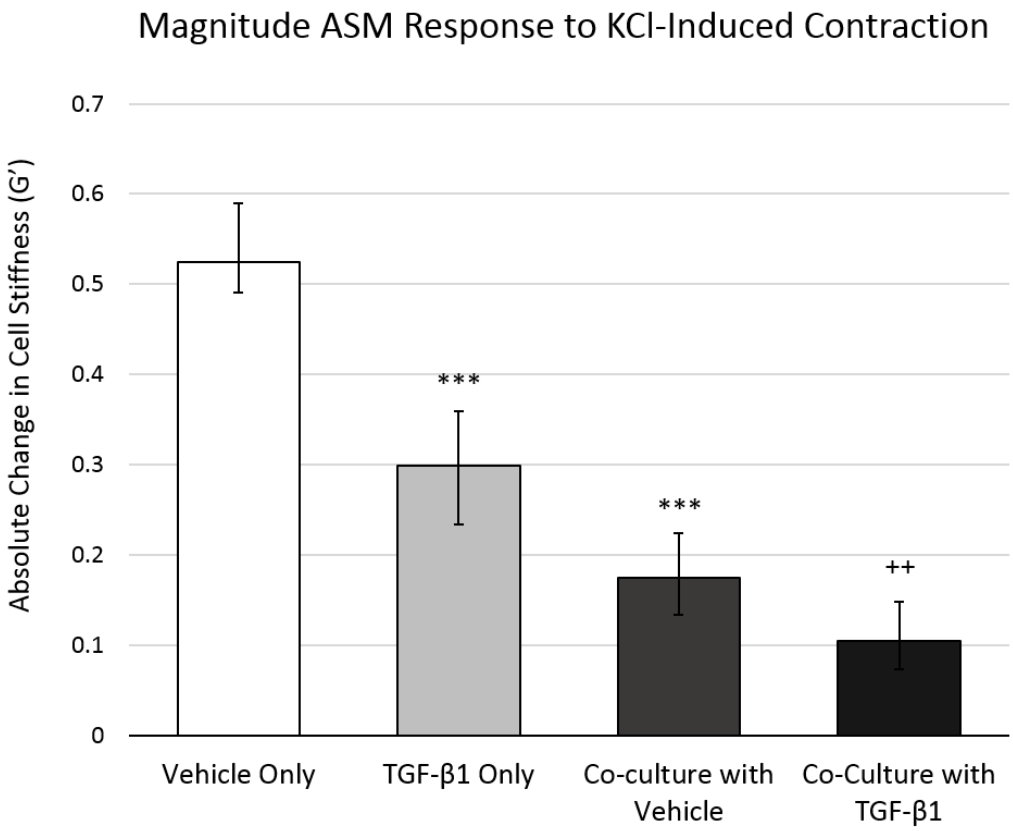

*Figure 6.3.2: The medians of the differences between baseline and post-KCl cell stiffness (from pair-matched beads) are presented here. Both exposure to TGF-β1 or co-culture with AE cells diminish the scope of ASM contraction, compared to ASM cultured exclusively (***p < 0.001). When co-cultured cells were also given a dose of TGF-β1 (10 ng/mL), the scope of ASM contraction was further diminished compared to co-cultured cells without TGF-β1 (++p < 0.01). Error bars show 95% CI.*

treatment to allow comparison between different independent experiments and donors (Figure 6.3.4, white bars). One-way ANOVAs were used to test for differences in protein expression for each of the proteins of interest with respect to TGF-β1-exposure and co-culture status. The following results are presented by treatment group, then by the immunostained protein, depicted from left to right in Figure 6.3.4.

We first examined the exposure of ASM cells growing in single culture to TGF-β1 at 10 ng/mL (+TGF-β1). Amongst our proteins of interest, myocardin, smMHC, CaM, MLCK, and M-RIP showed no significant change in protein expression. However, the addition of TGF-β1 did increase expression of the actin-binding protein calponin (Figure 6.3.4, blue bars). Here,

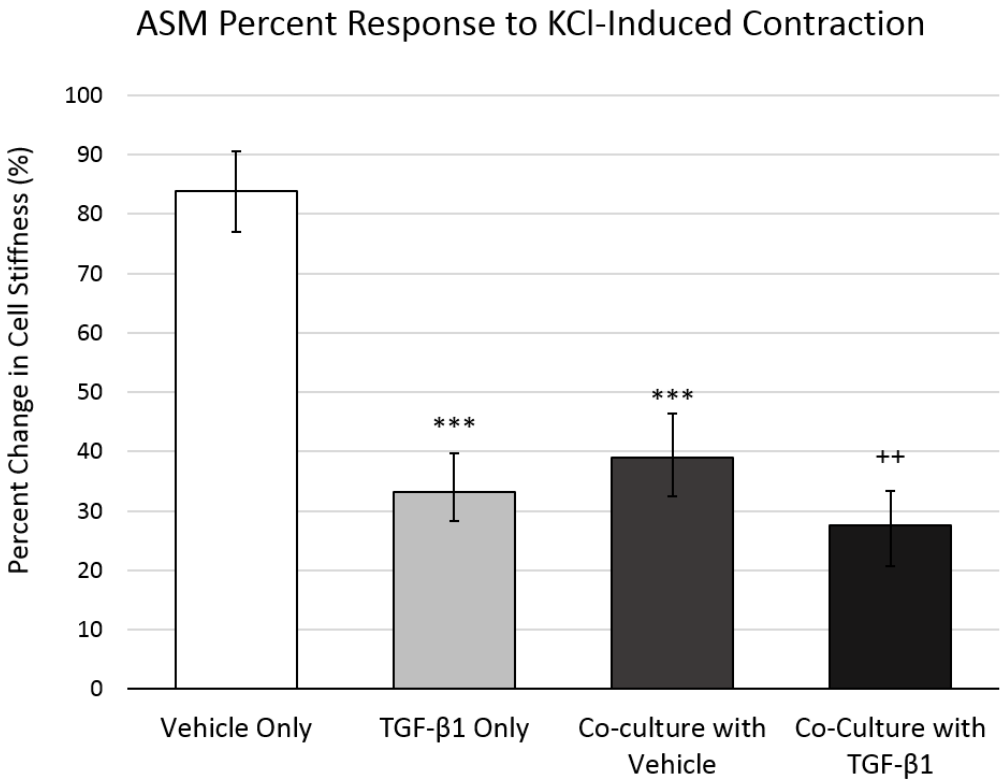

*Figure 6.3.3: The ASM cell stiffness responses to KCl contraction are normalized to the baseline stiffness of each cell and are presented here as the median value. Error bars indicate the 95% CI. As in Figure 6.3.2, either TGF-β1 (10 ng/mL) exposure or co-culture with AE cells reduce the ASM cell contractile response (***p < 0.001). Again, co-cultured cells given TGF-β1 result in ASM cells with reduced contractile response compared to co-cultured cells without TGF-β1 added (++p < 0.01). Statistical significance was obtained with a Kruskal-Wallis test, followed by multiple Mann-Whitney U tests with Bonferroni correction applied for multiple comparisons.*

calponin expression was significantly elevated, at 196.0 ± 9.7% compared to vehicle-treated ASM 6 days after exposure of the ASM to TGF-β1 (***p < 0.001).

Next, we compared ASM cells growing in co-culture with 16HBE14o- cells (+AE) against ASM cells growing alone in single culture (Figure 6.3.4, yellow bars). Both groups had been exposed to vehicle, but not to TGF-β1. The +AE group had markedly diminished expression of the smooth muscle motor protein smMHC and the MLCP/RhoA localization protein M-RIP, but modestly higher expression of MLCK, the kinase that phosphorylates myosin light chain. The amount of smMHC detected in co-cultured ASM was 60.9 ± 3.2% of that in the single-culture

ASM (***p < 0.001). M-RIP expression in co-cultured cells was 53.9 ± 7.0% of single-culture control (***p < 0.001). Conversely, MLCK expression was higher in co-cultured cells, at 132.4 ± 8.8% of the single-culture ASM vehicle group (*p < 0.05). No significant change in the expression of the other immunostained proteins was detected. Notably, unlike the dramatic increase in myocardin expression seen in Section 5 with AE-derived CM-treated ASM cells, co-culture with 16HBE14o- cells (and thus, exposure of the ASM to the AE secretome via co-culture) did not lead to any significant change in the expression of the transcription co-factor.

TGF-β1 was added to the co-culture of ASM and AE cells (+AE/+TGF, green) over the first 48 hours of the 6-day co-culture to examine whether AE cells altered by TGF-β1 exposure will influence the ASM cells differently from cells that are co-cultured with AE without TGF-β1 exposure (yellow) group. Therefore, the protein expression in co-cultured cells exposed to TGF-β1 were primarily compared to co-cultured ASM *without* TGF-β1 exposure (Figure 6.3.4, green bars versus yellow bars, respectively). Significant differences compared to vehicle (open bars) are denoted with asterisks (*) whereas significant differences compared to both the vehicle group and the co-cultured (without TGF-β1) group are denoted with plus signs (+). Again, unlike the CM-treated cells in Section 5, no dramatic change in myocardin expression was observed with co-culture, nor with co-culture plus TGF-β1 exposure. The expression of smMHC was smaller in ASM cells in co-culture compared to ASM without co-culture, whether or not TGF-β1 was added, as described in the previous paragraph (both yellow and green versus open bars), but there was no difference in smMHC expression between co-cultured ASM groups with and without the addition of TGF-β1 (green versus yellow). The expression of CaM, the calcium-binding protein that plays a role in MLCK activation, was higher in TGF-β1-treated co-culture, at 140.2 ± 4.5% of the +AE group (green versus yellow, +++p < 0.001).

While co-cultured ASM cells demonstrated a modest elevation in the expression of the MLC-phosphorylating protein MLCK (Figure 6.3.4, yellow), with the addition of TGF-β1 to the co-culture environment, MLCK expression was even greater in +AE/+TGF cells (green), at 154.9 ± 9.0% of +AE cells (+++$p < 0.001$). Also, while M-RIP expression in co-culture was diminished compared to the vehicle group (yellow vs open bars), the addition of TGF-β1 to co-culture (green versus yellow) did not lead to a significant difference from the +AE cells. Finally, similar to the +TGF group (blue), the expression of calponin in +AE/+TGF (green) cells was significantly greater compared to the corresponding vehicle-treated group, at 201.2 ± 13.5% of the +AE (yellow) group (+++$p < 0.001$).

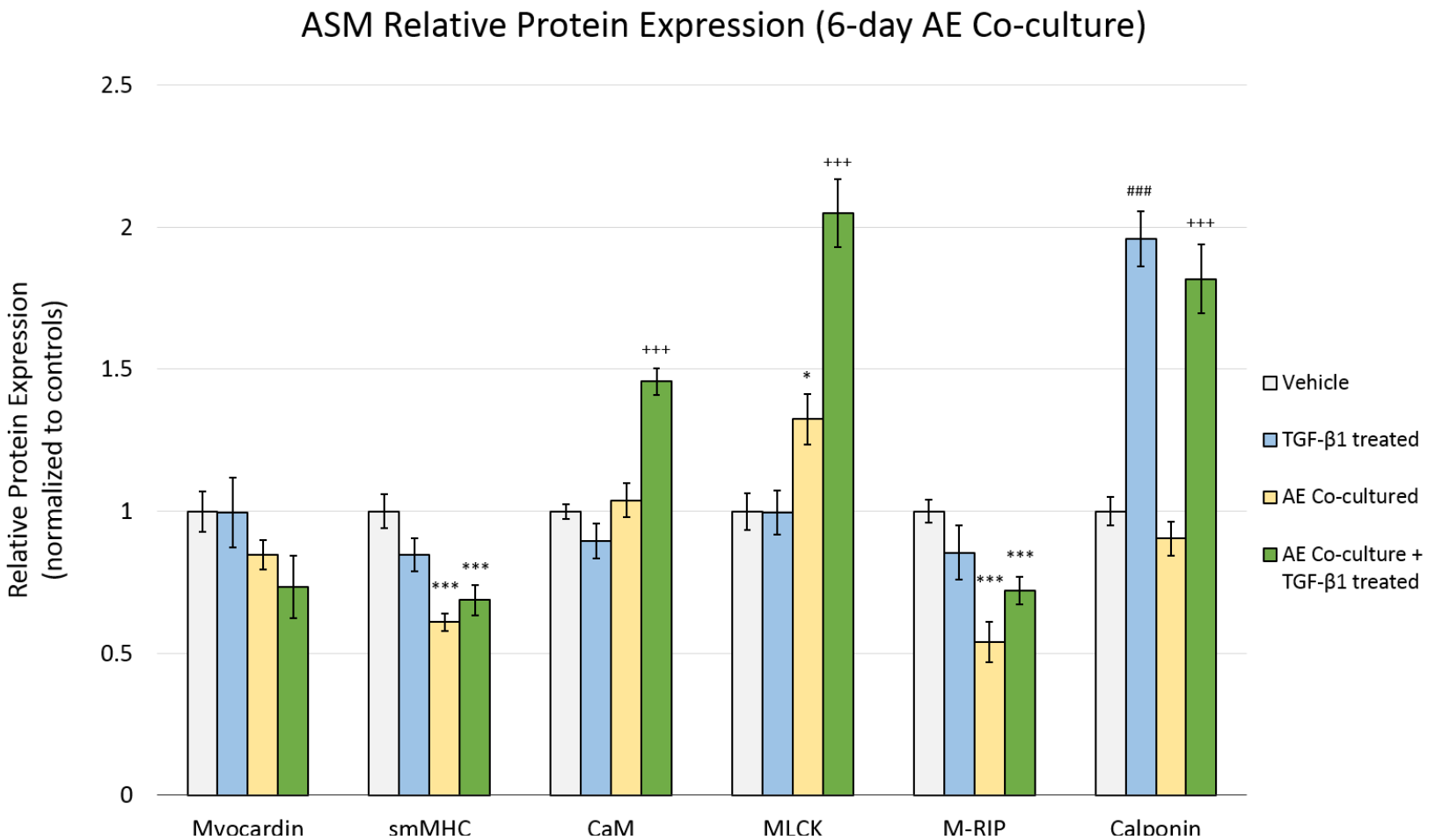

Figure 6.3.4: Relative protein expression of ASM, detected through immunofluorescent staining and LI-COR In-Cell Western™ quantification, following 6-day incubation periods in which the ASM cells were given TGF-β1 at 10 ng/mL for the first 48 hours (blue), co-cultured with 16HBE14o- cells (yellow), or both (green). For each protein examined, the amount of protein expression is normalized to the expression in vehicle-treated ASM, which is set to a value of 1. Data is presented as the mean relative protein expression of each protein, with error bars denoting the SEM. Means for each bar were calculated using expression data from ASM from three separate donors, with three wells per donor (n = 9). A one-way ANOVA with Tukey post-hoc test for pairwise comparison was used to determine statistical significance for each protein examined.

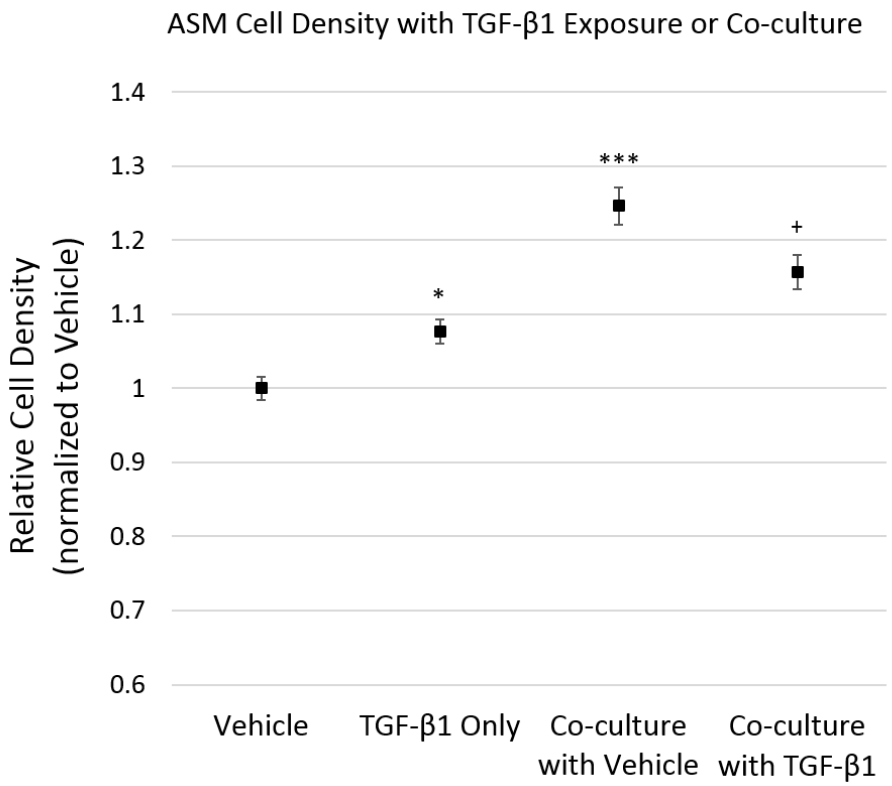

*Figure 6.3.5: Relative mean cell density of ASM cells modestly increased following TGF-β1 exposure (*p < 0.05). Cell density also increased, to a greater extent, with a long-term (6-day) co-culture with 16HBE14o- airway epithelial cells (***p < 0.001). Co-cultured cells that were also treated with TGF-β1 still showed a significant increase in cell density compared to single-culture, vehicle-treated ASM (+p < 0.001), but the cell density was also less than co-cultured ASM without TGF-β1 treatment (+p < 0.05).*

Finally, counts of DAPI-stained nuclei (detailed in Section 2.3) were used as an indicator of cell density. Interestingly, while exposure to the TGF-β1 growth factor led to a small, but statistically significant increase in cell density of 7.7 ± 1.6% (*p < 0.05), it was co-culture with 16HBE14o- cells that saw the most salient increase in cell density by 24.6 ± 2.5% (***p < 0.001). However, when TGF-β1 was introduced into the AE-ASM co-culture, cell density was slightly less than the TGF-β1-naïve co-culture, with a relative difference of -7.2 ± 2.3% (+p < 0.05).

6.3.3 Transepithelial Electrical Resistance

The electrical resistance across the 16HBE14o- cell layers in Transwells taken from the LI-COR protocol was measured at the end of co-culture, corresponding to Day 6, and two days after the end of co-culture, corresponding to Day 8 (Figure 6.3.6). Previous exposure to TGF-β1 (during the first 48 hours of co-culture) led to significantly lower mean TEER values on Day 6 and Day 8 (36.0 ± 7.0 Ω·cm^2 and 9.2 ± 7.3 Ω ·cm^2, respectively) compared to co-cultured AE cells that had not been exposed to TGF-β1 (122.1 ± 23.5 Ω·cm^2 and 60.9 ± 20.7 Ω ·cm^2, respectively).

In a second, independent experiment, we measured TEER over time, longer than our usual co-culture period for stiffness and protein expression, for 8 days of co-culture where 16HBE14o- cells are exposed to TGF-β1, co-cultured with ASM, or both. In the control group, where AE cells are cultured alone (Figure 6.3.7, black), TEER reached a peak of 605.0 ± 6.1 Ω·cm^2

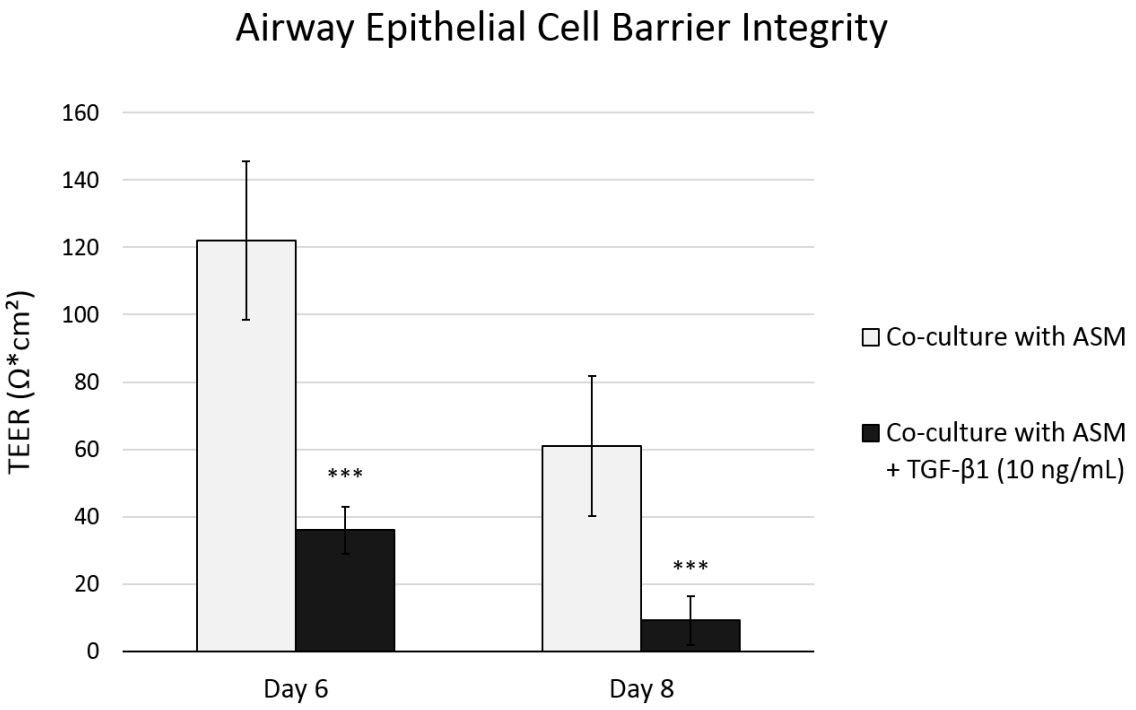

Figure 6.3.6: Transepithelial electrical resistance of 16HBE14o- cells after co-culture with primary ASM cells (n = 12). After 6 days of co-culture, wells that had been given TGF-β1 at the start of co-culture demonstrated significantly lower TEER values ($p < 0.001$). Two days after the end of co-culture (Day 8), TEER in the TGF-β1-exposed wells approached zero. Statistical analysis completed using two-sample t-tests for each day of measurement.

on Day 4. As expected, when TGF-β1 (10 ng/mL) was added at the beginning of co-culture, the cells did developed significantly less electrical resistance (blue), with TEER at only 247.9 ± 7.7 $\Omega \cdot cm^2$ (**p < 0.01) by Day 4, with a maximum value of 396.9 ± 37.4 $\Omega \cdot cm^2$ on Day 6. When the 16HBE14o- cells were co-cultured with primary human ASM (yellow), TEER reached a maximum of 675.2 ± 9.9 $\Omega \cdot cm^2$. Much like single-culture AE cells that were exposed to TGF-β1, AE cells in co-culture with ASM that were also given TGF-β1 (10 ng/mL) were limited to peak TEER of only 388.3 ± 16.0 $\Omega \cdot cm^2$ on Day 4 (++p < 0.01). Between Day 6 and Day 8, the vehicle-treated and co-cultured AE cells saw a considerable decrease in TEER; this coincided with the visual observation that a substantial number of 16HBE14o- cells had lifted off the Transwell surface by Day 8 in those groups. Interestingly, around the same time, single culture AE cells that were exposed to TGF-β1 (blue) were still intact, with a higher TEER of 370.4 ± 5.7 $\Omega \cdot cm^2$ than any other group on Day 8 (##p < 0.01).

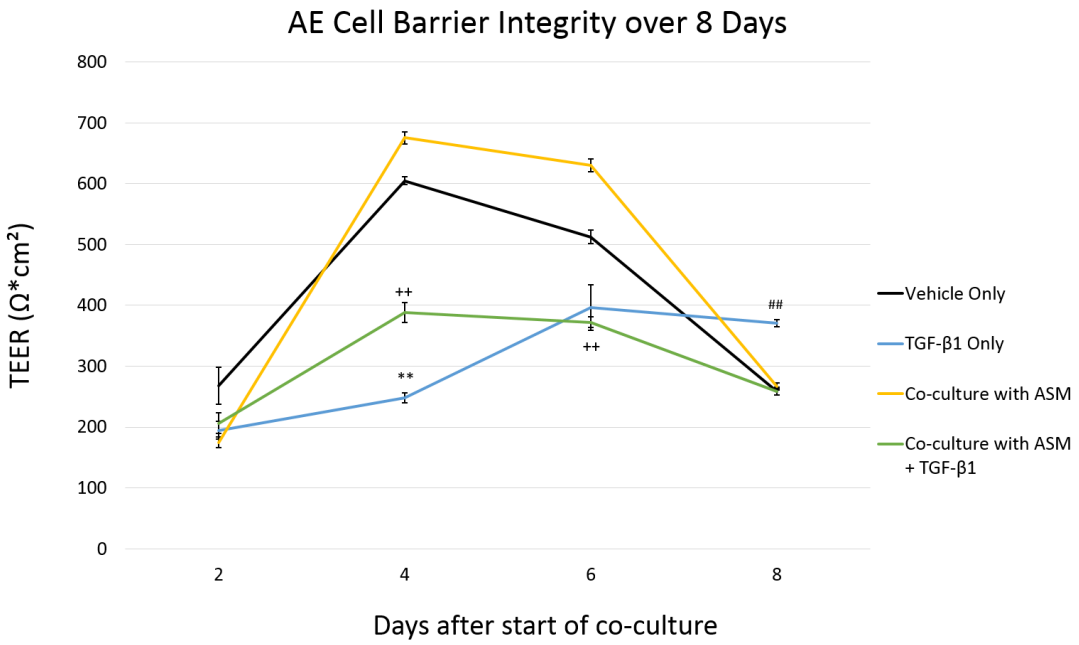

Figure 6.3.7: A second independent experiment measuring TEER of 16HBE14o- cells during co-culture with ASM cells and/or exposure to TGF-β1 at 10 ng/mL. Co-culture with ASM did not alter AE barrier integrity, but exposure to TGF-β1 at 10 ng/mL in both single culture and co-culture led to significantly lower TEER values, particularly on Day 4 and 6. By Day 8, the 16HBE14o- cell layer showed steep decreases in TEER values, likely due to significant cell lifting observed in most wells.

6.4 Discussion

In vivo, AE cells are located near the ASM and thus likely modulate ASM function, but this interaction is not well-understood. In this section, we examined the influence of co-culture on the contractile function and protein expression of ASM cells, as well as the additional influence of the growth factor TGF-β1 on this system, by recreating an environment (via co-culture) where AE and ASM could communicate, thereby allowing AE cells to potentially modulate ASM function. We found that co-culture with AE cells led to decreased ASM contractile function. Past TGF-β1 exposure also led to decreased ASM contractility, but may be attributed to a persisting increase in baseline stiffness. The expression of some contraction-associated proteins in ASM cells in co-culture with AE cells decreased (smMHC), while others increased (MLCK). Amongst the proteins we immunostained, only calponin showed any change in response to TGF-β1 exposure. ASM cell density was modestly greater in wells that had been given TGF-β1 (107.9 ± 1.6%) and was even greater in wells that were co-cultured with AE cells (124.6 ± 2.5%). Finally, we demonstrated a functional change in our AE cell layer in response to TGF-β1 and co-culture with ASM. These results are discussed in the sub-sections below.

6.4.1 TGF-β1 Exposure led to a Persisting Increase in ASM Baseline Stiffness

Our primary finding here was that the baseline stiffness of TGF-β1-exposed ASM remained elevated approximately one week after the addition of TGF-β1, despite no longer adding exogenous TGF-β1 after Day 2. It should be pointed out that our protocol in this section called for ASM cells to be exposed to TGF-β1 only during the first two days of a six-day incubation period, which contrasts with the constant re-exposure of ASM to TGF-β1 during the six-day incubation in Section 4. This was done to more closely match the TGF-β1 exposure periods used in Sections 3 and 5, where AE exposure to TGF-β1 was emphasized over ASM exposure to TGF-β1 (as our objective was to alter the AE with TGF-β1). This means that the

changes seen here as a result of TGF-β1 exposure are relatively long-lasting and persistent, at least up to four days following exposure. In the TGF-β1-treated ASM, baseline stiffness was elevated by approximately 0.2 Pa/nm (Figure 6.3.1). However, post-KCl cell stiffness was not any higher compared to vehicle. This corresponded to the smaller measured contractile responses in both absolute terms and relative to baseline cell stiffness (Figure 6.3.2 and 6.3.3) in TGF-β1-treated ASM.

It was mentioned previously in Section 4.4.2, that Goldsmith et al. 2006 showed that ASM cells continuously exposed to TGF-β1 had an increased shortening response to ACh compared to untreated cells[74].This agrees with the elevated post-KCl stiffness we observed in Section 4, which suggests that TGF-β1 led to an increased pre-stress from enhanced myosin activity at baseline, but with no change in contractile scope with KCl-induced contraction. Our results here however, show that while pre-stress may still be similarly elevated, the scope of contraction (i.e. the difference between baseline and post-KCl G') actually decreased. This may be due to the fact that that ASM cells were treated with TGF-β1 for only the first two days of a 6-day incubation period and contractility was measured at 6 days. The additional time after initial treatment may have led to reduced ASM contraction, although the mechanism is unknown.

Protein expression data from Goldsmith et al. 2006 shows that smMHC was slightly elevated in some TGF-β1-treated ASM cells after 72 hours, which contrasts with our protein expression data where smMHC expression was unchanged. However, our measurement of smMHC took place 4 days after the end of a 48-hour ASM exposure to TGF-β1, so that the ASM were not in contact with exogenous TGF-β1 for those last 4 days. This could suggest that smMHC expression was transiently increased in ASM in response to TGF-β1, with expression dropping back down to some baseline after the TGF-β1 signal is removed. As smMHC is the motor protein responsible for force generation, this may explain why we observed an increased

maximum (post-KCl) stiffness in TGF-β1-treated cells in Section 4 (when OMTC was conducted only 24 hours after TGF-β1 was removed from the cells) while the maximum stiffness in TGF-β1-treated cells in this section (where OMTC was conducted 4 days + 24 hours after the end of ASM exposure to TGF-β1) was not any greater than in the control group. However, we also observe that the increase in ASM baseline stiffness associated with TGF-β1 treatment is preserved up to Day 7, when we conducted OMTC. This may be due to upregulation of α-smooth muscle actin (α-SMA), reported by Goldsmith et al., in response to TGF-β1 addition[74]. An increase in α-SMA could help explain increased stiffness we observed, from the additional cytoskeletal elements that would be present if allowed to polymerize, potentially resulting in a cell that is more resistant to deformation. Alternatively, changes to the expression of other structural proteins that support the cytoskeleton could also occur. For instance, changes to the expression of smooth muscle titin (sm-titin), a long titin isoform that can bind to actinin in the smooth muscle dense body and may perform a similar function to its skeletal muscle counterparts by stabilizing the contractile apparatus, but whether this is altered with TGF-β1 is unknown[190]. Certainly, changes to the expression of other cytoskeletal, and even non-cytoskeletal elements (such as microtubules, which may be necessary as a compressive load-bearing element) may also ultimately influence the apparent stiffness of smooth muscle cells[191]. With the persisting, functional increase in ASM cell stiffness following TGF-β1 exposure, further examination of the expression and ubiquity of these cytoskeletal and other structural elements may be an interesting avenue for future work.

The primary change in protein expression that was associated with TGF-β1 exposure in our experiment was a nearly twofold increase in calponin detected (Figure 6.3.4). Calponin is the actin-binding protein that acts to regulate actin-myosin ATPase activity reviewed in Section 1.7.6. Since our anti-calponin antibody was polyclonal and could detect all three calponin

isoforms, it is difficult to discern whether calponin 1 or calponin 2 is elevated at Day 6 of this protocol[128,133,134,137]. Since calponin 1 co-localizes with actin and can regulate smooth muscle contractility, an increase in calponin 1 expression in ASM cells should indicate more contractile cells[128,133]. However, this is not the behavior we observe in our TGF-β1-treated ASM. Calponin 2 also binds to actin but is associated with proliferative cells, acting to regulate proliferation[128,137]. A slight increase in ASM cell density with TGF-β1 treatment was observed. However, we still cannot definitively determine which isoform was upregulated in our cells. Further tests with more specific antibodies are necessary (as the isoforms are similar in size and may not be sufficiently resolved in a gel). It is also unknown if the increase in calponin is linked to the increased baseline stiffness in TGF-β1-exposed ASM. However, in co-culture, TGF-β1 also led to an increase in calponin expression, but the ASM experienced a decrease in baseline stiffness with TGF-β1. This suggests that they may not be associated after all.

6.4.2 ASM Cells Co-cultured with 16HBE14o- Cells Have Diminished Stiffness and Contractile Function

The median baseline cell stiffness of ASM cells that were in co-culture with 16HBE14o- cells over a 6-day period was significantly less than the stiffness of non-co-cultured ASM (Figure 6.3.1). This agrees with our conditioned media results in Section 5.3, where we also saw a lower baseline stiffness in ASM cells that were exposed to the 16HBE14o- secretome via CM. The lower baseline stiffness, seen here in ASM co-cultured with AE, was again accompanied by a definitively lower level of smMHC expression in the smooth muscle compared to non-co-cultured ASM (Figure 6.3.4). As discussed in Section 1.7.2, smMHC is part of the motor protein complex that is integral to smooth muscle contraction. A baseline level of smooth muscle activation is responsible for the baseline stiffness (or tone) in the ASM, and smMHC contributes to this baseline level of activation. Therefore, a diminished level of smMHC expression, which

we observed in our AE-co-cultured ASM, may be partly responsible for the lower baseline stiffness compared to non-co-cultured ASM, with fewer force-generating elements adding stress to the cytoskeleton leading to the decreased cell stiffness[175]. Overall, this suggests that the airway epithelium released factors that lead to decreased ASM tone, which may be important in maintaining normal airway function.

ASM cells in co-culture with 16HBE14o- cells also experience a diminished contractile response to KCl-induced contraction. The change in G' in co-cultured ASM was significantly less in both absolute terms (Figure 6.3.2) and relative to the baseline stiffness (Figure 6.3.3) in co-cultured ASM. This again provides evidence that AE cells released factors that influenced ASM contractility. In addition to contributing to the smaller baseline stiffness, the decrease in smMHC expression (Figure 6.3.4) also likely played a part in why we observe a diminished contractile response in co-cultured ASM. Once more, we note that OMTC for measuring cell stiffness and contractility was conducted approximately 24 hours after the ASM was last in contact with the AE secretome (via co-culture), with several washes during this period. While this does not rule out the possibility of short-term agonists from the AE directly influencing the stiffness and contractility of the ASM, it does suggest that the differences in stiffness and contractility that we do measure are the result of more long-term, potentially phenotypic changes.

Increased protein expression of smMHC can be indicative of ASM cells taking on a more mature, pro-contractile phenotype, and this can be used as a marker for detecting such a change[123,124,192]; it may therefore be reasonable to posit that, in line with the decrease in smMHC expression, we were observing ASM cells adopting a less contractile, more synthetic-proliferative phenotype with the presence of AE cells. Indeed, wells containing ASM in co-culture with AE saw a significantly higher density of ASM cells, which supports the possibility of a phenotypic switch (Figure 6.3.5). However, the expression of other potential ASM phenotypic

markers did not appear to follow suit. No significant downregulation of myocardin, which controls smooth muscle differentiation into mature contractile cells, was observed, nor was there a change in total calponin expression (and while our polyclonal antibody used for the detection of calponin is more sensitive the calponin 1 isoform rather than the calponin 2 isoform[193], it is not possible to determine from the current data whether a switch from the 'contractile' calponin 1 to the 'quiescent' calponin 2 isoforms occurred).

Most notably, though, was the contradictory increase in the expression of MLCK, whose expression is typically indicative of a more contractile smooth muscle. There is the possibility that the increase in MLCK we detected was from increases in expression of the long-isoform MLCK or the telokin fragment[194]. Unfortunately, our methods did not allow for size discrimination of protein products, which can be achieved using Western blot. Another possibility is that the MLCK expression in ASM was simply being restored partially to a more "physiological" state with co-culture; as smooth muscle cells are passaged in culture, the expression of MLCK decreases substantially with the first passage and continues somewhat with increasing passage number, signaling a loss of normal physiological function in cell culture[122]. Thus, the increase might well be insufficient to be functional. If there is a pro-MLCK component from epithelial cells *in vivo*, this could mean that cells near the smooth muscle (e.g. endothelial or epithelial cells) may contribute to the maintenance of physiological levels of MLCK expression in smooth muscle, but this is speculative. Nonetheless, even if short-isoform (contractile) MLCK was upregulated, it is notable that neither cell stiffness nor contractility increased. Whether or not there is greater potential MLCK activity to phosphorylate MLC_{20}, if the mechanism for smooth muscle contraction (i.e. smMHC) is already downregulated with co-culture, then it should be expected that when function is measured, contractility is ultimately decreased, which

in this case would be regardless of changes in MLCK, possibly explaining the increase in MLCK while stiffness and contraction are decreased.

6.4.3 Further Changes to Contractile Function of ASM in Co-culture with Additional TGF-β1 Exposure

While the changes to ASM cell stiffness in co-cultured wells with TGF-β1 present appear similar to cell stiffness in co-cultured wells with only vehicle (Figure 6.3.1), closer examination of the pair-matched, absolute and percent change in stiffness in response to KCl-induced contraction (Figure 6.3.2 and Figure 6.3.3) revealed that the addition of TGF-β1 to the co-culture system further diminished contractile function. We looked once more to our protein expression data to better understand the changes taking place within these cells. The downregulation of smMHC, which we described above as potentially contributing to the diminished cells stiffness as well as contractile function, is also observed when TGF-β1 is introduced to co-culture, and is not significantly different from vehicle-exposed co-cultured ASM. Again, the decrease in smMHC may indicate that there were fewer actin-myosin motor units to generate baseline tension and generate force in response to KCl compared to non-co-cultured cells, but does not appear to account for the difference in contractile function between TGF-β1-exposed and naïve co-culture wells.

The upregulation of CaM and MLCK in TGF-β1-exposed ASM cells in co-culture (Figure 6.3.4, green bars) are unique to the intersection of these two treatments and make a case for more physiologically representative models of cell culture. A major objective in this work was to examine whether TGF-β1 could dysregulate the communication between AE and ASM. One way this may occur is if TGF-β1 alters the AE cells (potentially through an EMT-like process which we examined in Section 3), thereby altering the AE secretome. The altered AE secretome may go on

to modulate ASM function differently from a normal AE secretome. This is what we attempted to model with our conditioned media experiments in the previous chapter. Since we found no clear difference in the effect between TGF-β1 CM and naïve CM on ASM cells earlier, it was interesting to see a difference between TGF-β1-supplemented and TGF-β1 naïve co-culture wells. However, we need caution when interpreting our co-culture results. While we could attribute any differences in the ASM to differences in the AE secretome with our conditioned media experiments, in our co-culture, it is also possible that TGF-β1 may have instead altered the ASM response to an AE secretome. Therefore, we cannot definitively say that an altered AE secretome as a result of AE exposure to TGF-β1 is responsible for these differences we observe, although the physical result observed, the reduction in ASM stiffness and contractility, is nevertheless the same and potentially important if present *in vivo*.

6.4.4 ASM Relative Cell Density in Response to Co-culture and TGF-β1

Fully differentiated, normal AE cells typically do stimulate ASM proliferation through the secretion of several different mediators[195], and we showed that our 16HBE14o- cells have a similar effect on ASM. The relative cell densities of ASM in wells that had been in co-culture with 16HBE14o- cells were significantly higher than ASM wells in single culture (Figure 6.3.5), suggesting that our AE cells had a mitogenic effect on our ASM cells. However, when we added TGF-β1 to our AE-ASM co-culture, the cell density is smaller relative to co-cultured ASM without TGF-β1. This was unexpected, as TGF-β1 has been shown to have a mitogenic effect on ASM and is often implicated in ASM hyperplasia, a common feature of asthmatic airways[71,72,74,196]. Our results could mean that in the more physiologically relative context of co-culture, TGF-β1 does not enhance proliferation. Although our AE cells are immortalized, they are not model cells for asthma. If their influence on ASM cells is comparable to normal, healthy AE, this could mean they are protective against changes such as increases in TGF-β1. However, this does not explain

why cell density was smaller compared to TGF-β1-naïve co-culture. Certain signaling pathways may have opposite effects on ASM proliferation depending on whether ASM cells are in co-culture with AE or exposed to TGF-β1. For instance, AE co-culture appears to act through the p38 MAPK pathway in ASM to allow increased proliferation (as shown by Malavia et al., as inhibition of the p38 MAPK pathway while ASM is in co-culture with AE led to decreased proliferation[195]), while the TGF-β1-mediated increase in ASM proliferation is moderated (i.e. potentially inhibited) by the same p38 MAPK pathway (i.e. inhibition of the p38 MAPK pathway while ASM were exposed to TGF-β1 led to even greater increases in ASM proliferation, suggesting that the p38 pathway moderates/limits proliferation, instead, in this case)[72,195]. This means that while AE co-culture acts through (or alongside) the p38 MAPK pathway to promote proliferation, with the addition of TGF-β1, activation of the p38 MAPK pathway may inhibit proliferation instead, as activation of the p38 pathway can lead to downregulation of cyclin D1, a critical protein that allows progression of the cell cycle[197]. However, if this were the case, it is unclear why p38 in ASM in co-culture (without TGF-β1) promotes proliferation.

6.4.5 Airway Epithelium Barrier Integrity Remains Intact with ASM Co-culture but is Disrupted by TGF-β1

We measured the TEER across the AE following co-culture with ASM, with and without exposure to TGF-β1 in order to demonstrate that the addition of TGF-β1 to our co-culture system did indeed influence the 16HBE14o- cells (Figure 6.3.6). TEER is used as an indirect measure of the AE barrier integrity, which we expected to decline with TGF-β1 exposure if the AE cells began to undergo EMT-like changes. As expected, we found that in co-cultures where TGF-β1 had been added, TEER was significantly lower, implying lower barrier function as a result of TGF-β1. Interestingly, TEER continued to decline after co-culture, whether or not there was TGF-β1 exposure, so we conducted an experiment independent from our assessments of ASM

function and protein expression in order to track the changes in the TEER of AE during co-culture.

We again found that TGF-β1 exposure led to decreased TEER values, suggesting that EMT-like changes are occurring in the 16HBE14o- cells. However, major differences in TEER values between TGF-β1 and unexposed groups did not appear until four days after TGF-β1 was added or co-culture was started. This is notable as Day 0 corresponds to the day in which 16HBE14o- cells reached full confluence (i.e. cells covered the entirety of the plating surface), meaning our 16HBE14o- cells possibly did not fully develop features such as tight junctions at all cell boundaries until four days after the AE appeared confluent. Therefore, it may be more precise to say that the presence of TGF-β1 prevented the development of high TEER values. This may also explain why we did not observe a decrease in E-cadherin expression to TGF-β1 exposure back in Section 3. Our AE cells may not have fully expressed E-cadherin at the cell boundaries at the 48-hour time point used then (as dosing had begun once cells reached confluence). TEER declined dramatically after Day 6, which may be typical of 16HBE14o- cells in Transwells as decreases in TEER after extended culture have been reported elsewhere, which imply a limited time frame in which the 16HBE14o- cells form an intact layer[161,198]. Co-culture with ASM still allows for high TEER values to be achieved in the AE layer. However, with TGF-β1 added to the co-culture, barrier function is again impaired.

Chapter 7: Conclusions and Suggestions for Future Work

The primary objective of this thesis was to probe the effect that airway epithelial cells may have on airway smooth muscle contractility and phenotype and also to examine how TGF-β1 treatment of airway epithelial cells may alter these effects. We focused on describing changes to the mechanical properties (specifically, changes in cell stiffness) of ASM cells, as well as the changes in the ASM response to induced contraction via KCl. In addition to these changes in cell function, we examined phenotype via changes to protein expression. Because, in asthmatic airways, TGF-β1 expression is elevated and the effects of TGF-β1 on AE and ASM cells, separately, lead to changes that are reminiscent of the features observed in asthmatic airways, we assessed the effects of TGF-β1 on each of our cell types separately, and then we looked at the effects of AE on ASM using two different approaches. The first approach used conditioned media as a one-way route of exposure from AE cells to ASM cells, exposing the ASM to the AE secretome. The second approach established a co-culture in which a more topographically representative model of the *in vivo* airway was used, allowing two-way communication between the AE and ASM. In both approaches, we attempt to better understand the *in vivo* interactions between our two cell types, AE and ASM; however, some limitations emerge from the design of our two models. We used a mono-culture model, which certainly may not adequately provide a representative model of the *in vivo* airway; however, mono-cultures do allow isolation of potential mechanisms (e.g. TGF-β1 on ASM), making them easier to identify and characterize. The introduction of a second cell type to a cell culture system allowed us to explore potential mechanisms for cell-cell interaction, but also essentially introduced a “black box” where the particular mechanisms can become less clear. For instance, in our co-culture, we could not be certain whether TGF-β1 altered the 16HBE14o- cells (leading to a change in 16HBE to ASM communication), or whether TGF-β1 altered the ASM response to 16HBE14o- cells, or even

whether both could have occurred, but we were able to show that TGF-β1 had differing effects on some smooth muscle proteins depending on the presence of AE cells. In addition, although we examined both AE and ASM together in order to draw a better picture of an intact airway, even our co-culture model did not fully recapitulate the complex interactions that may be present *in vivo*, where other cell types, including cells in the ECM such as fibroblasts, as well as non-specific and, in particular, specific immune cells (given the atopic nature of allergic asthma) are not included in our model, nor are the many ECM proteins which can provide ASM cells with environmental cues and allow them to respond in context. In fact, in the particular case of TGF-β1, since TGF-β1 is typically present in a latent form, bound via LTBP to the ECM, *in vivo*, it is not unreasonable to postulate that *in vivo* TGF-β1 signaling is much more specific and localized in contrast to the generalized introduction of TGF-β1 we have used in our experiments. Nevertheless, as mentioned above, with the introduction of AE to ASM, we do demonstrate that the effects of other cell types can be significant, in our case by completely changing the ASM functional response to TGF-β1, suggesting that there is extensive and significant cross-talk between these cells, and that it is important to examine these interactions between different cell types.

The addition of TGF-β1 to AE alone led to increased vimentin expression and limited the development of normal barrier function, which is consistent with the changes expected during TGF-β1-induced EMT. Although E-cadherin expression did not decrease, this was potentially because our 16HBE14o- cells did not develop well-formed cell-cell contacts until several days after confluence, meaning that in our CM and co-culture, E-cadherin was not expressed until later (potentially Days 3 or 4). The increase in vimentin expression and the impaired barrier function, however, was sufficient to conclude that EMT-like changes were occurring in our 16HBE14o- AE cells and that a dose of 10 ng/mL TGF-β1 was sufficient to induce these changes.

We also found that ASM cell stiffness did increase in response to TGF-β1, but over concentrations of TGF-β1 from 1 ng/mL to 10 ng/mL, there was no dose-dependent response form ASM cells, at least in terms of cell stiffness and contractile function. Post-contractile (via KCl-induced contraction) stiffness also increased within 24 hours after the end of TGF-β1 exposure, but this effect did not appear after 96 hours, which suggested that some effects of TGF-β1 on ASM were transient.

We found that the exposure of ASM to the AE secretome via conditioned media led to diminished ASM stiffness, which was also decreased after KCl-induced contraction. Associated with this, we found an accompanying decrease in smMHC expression in CM-treated ASM. Since the stiffness of the ASM cells in in part due to actin-myosin activation, responsible for baseline tone, the diminished ASM stiffness and maximum stiffness after KCl-induced contraction may be a result of the decrease in smMHC expression. Exposure to AE-CM from 16HBE14o- cells that had prior exposure to TGF-β1 did not affect ASM differently from AE-CM from naïve 16HBE14o- cells, suggesting that TGF-β1 did not alter the AE secretome in a way that led to altered ASM cell stiffness. However, the use of conditioned media did lead to an unusual effect in ASM, a dramatic increase in myocardin expression that was unaccompanied by expected increases in other contraction-associated proteins that the myocardin transcription co-factor typically governs, or changes in contractile function. We are not aware if such a strong dissociation between myocardin and contractile phenotypic expression has been previously reported.

In our co-culture model, we saw a clear decrease in ASM cell stiffness, as well as smMHC expression when ASM were co-cultured with AE, but unlike the conditioned media experiments, we did not see an increase in myocardin expression. With co-culture, we also found that TGF-β1 in the AE-ASM environment further diminished ASM contractile response to KCl and led to a lesser relative cell density. This was an interesting result, as TGF-β1 has often been implicated in

increased ASM proliferation, resulting in the thickening of airway walls in asthma. Our results suggest that its activity, mediated by or through the AE, could play a role in moderating this effect. Interestingly, elevated TGF-β1 did not increase cell stiffness or contractile response to KCl when AE was present. Thus, it appears that despite simulating the epithelial cells into an EMT-like transition, this did not affect contractility differently than epithelial cells alone. Nevertheless, there were some changes in the ASM protein expression in co-culture with AE that were different with the presence of TGF-β1. The expression of the proteins CaM and MLCK were increased, but again, these changes, although associated with a shift to a more contractile phenotype, did not result in pro-contractile functional changes. Indeed, the co-cultured cells were mechanically less stiff and less contractile, with or without TGF-β1. This suggested that the expression of some canonical markers used to determine ASM phenotype, namely MLCK, might be expressed (or not expressed) independently from any ultimate effect on phenotype, at least in our model. This indicates that multiple factors and pathways ultimately contribute to altered phenotype and contractility, which might be present in some complex conditions such as in multi-cell culture with important modulating factors such as TGF-β1.

7.1 Statement of Contributions

(1) In this thesis, I developed an improved method for assessing changes in stiffness using OMTC. This added a bead-matching step to the analysis of OMTC data that improved the quality of bead-wise tracking of changes in cell stiffness measurements before and after a contractile agonist is added. This provided a better estimation of the median change in bead stiffness.

(2) I assessed the 16HBE14o- cell line response to TGF-β1. EMT-like changes did occur with TGF-β1 exposure, including increased vimentin and decreased barrier function via TEER,

but changes to the expression of E-cadherin in response to TGF-β1 may not be apparent at earlier time points in cell culture without AE cell differentiation.

(3) I showed that primary human ASM have increased cell stiffness values in response to TGF-β1, which was saturated even at a low dose of 1 ng/mL.

(4) I confirmed that AE exposure can lead to a long-term decrease in ASM cell stiffness via either conditioned media or co-culture, and it also leads to a decreased ASM contractility, but only via co-culture. Both of these functional changes were consistently accompanied by a decrease in the expression of the smMHC motor protein.

(5) I demonstrated that ASM in co-culture with AE responds differently to TGF-β1 exposure compared to ASM in single culture, both functionally and in terms of the expression of the proteins CaM and MLCK. This suggests that inter-cell communication is an important component to understanding the ASM response to stimuli and environmental changes that may occur in the airway.

7.2 Future Work

(1) In this thesis, immortalized 16HBE14o- cells were used as our airway epithelial cells, as they eventually formed a continuous, intact monolayer of cells, and they have been used by other researchers to demonstrate EMT-like changes in response to TGF-β1. However, to move forward and assess the susceptibility of AE cells to TGF-β1 in asthma, my data indicate that it is appropriate to assess how primary AE cells from normal and asthmatic airways respond to TGF-β1 in their potential effects on AE-ASM communication.

(2) Here, the AE cells I used do not differentiate fully as typical NHBE cells might, and were solely used in liquid-liquid interface. These cells were potentially in a state more akin to an inflammatory state. Where asthma is associated with a chronic inflammatory state in

the airways, it is hypothesized that the epithelium may be in a constant state of repair, such that a sizeable population of the cells *in vivo* do not fully differentiate. I suggest that comparisons between the effects of undifferentiated and differentiated primary AE cells on the ASM would an interesting avenue to explore. Nevertheless, since our immortalized 16HBE14o- cells can form tight junction cell-cell contacts (implying the potential for apical-basal polarity) and have also been shown to demonstrate some differentiated morphology under certain conditions similar to our protocols[159,198], this cell line may still be potentially considered for this purpose where primary cells are unavailable.

(3) We examined several contraction-associated proteins in the ASM, utilizing a 'wide' approach with In-cell™ Western analysis of LI-COR data to allow a high throughput of wells. Unfortunately, this meant we were unable to discriminate for protein size, meaning the results of our MLCK expression might be uncertain due to the potential presence of the telokin fragment, as well as the long/short isoforms. Thus, for MLCK it could be useful to repeat with a size discrimination technique (i.e. Western blots) where, if ASM become more synthetic/proliferative with co-culture we might find a shift to the less contractile long-isoform MLCK. Additionally, it could also be useful to use a more specific antibody (i.e. mAbs) for assessing the calponin isoforms, which may shift in expression from the calponin 1 to calponin 2 in response to co-culture.

(4) We noted long-term changes to ASM in response to TGF-β1 contrasted with some of the short-term changes observed by other authors (Sections 4.4.1, 4.4.2, and 6.4.1). It might be useful to look at changes in response over time, as TGF-β1 may not be chronically elevated in asthmatic airways, but can also be transiently overexpressed, and perhaps

protein changes in ASM follow, possibly reverting towards baseline following reduction in TGF-β1.

(5) Much of the cell culture work in this thesis was conducted using low-serum media. The use of FBS can be described as a 'black box' as it is difficult to determine what factors may be present. Development of a protocol which excludes FBS and uses more defined media may be useful in developing a more accurate understanding of the inter-cell signaling processes that might occur in the airway.

(6) Previous work in our laboratory examined the possibility of growing ASM cells in a 3D environment, where the cells may behave differently due to the altered arrangement of their environment[158]. OMTC analysis of ASM currently requires 2D culture, but alternate methods of examining ASM contractile function in 3D culture are possible. Thus, comparison of the responses of ASM to AE or TGF-β1 in 2D vs 3D culture may be helpful in validating the use of either method for testing ASM cell mechanics in culture.

(7) For our contraction studies, KCl was used as our contractile agonist, since it is not affected by changes in receptor expression. However, it does mean that these potential changes are missed, as KCl bypasses the upstream GPCR-associated contraction signaling pathway, which may be influenced by co-culture with AE or by TGF-β1. Using histamine to activate the H1 (or cholinergic drugs for the M3) receptor upstream may reveal changes to the contraction signaling pathway which may not be visible with KCl-induced contraction.

References

1. Anderson, G. P. Endotyping asthma: new insights into key pathogenic mechanisms in a complex, heterogeneous disease. *Lancet* **372,** 1107–19 (2008).

2. Siddiqui, S. *et al.* Emerging airway smooth muscle targets to treat asthma. *Pulm. Pharmacol. Ther.* **26,** 132–44 (2013).

3. Lambrecht, B. N. & Hammad, H. The airway epithelium in asthma. *Nat. Med.* **18,** 684–692 (2012).

4. Lin, T.-Y., Poon, A. H. & Hamid, Q. Asthma phenotypes and endotypes. *Curr. Opin. Pulm. Med.* **19,** 18–23 (2013).

5. Holgate, S. T. Pathogenesis of asthma. *Clin. Exp. Allergy* **38,** 872–97 (2008).

6. Woodruff, P. G. *et al.* T-helper type 2-driven inflammation defines major subphenotypes of asthma. *Am. J. Respir. Crit. Care Med.* **180,** 388–395 (2009).

7. Poon, A. H., Eidelman, D. H., Martin, J. G., Laprise, C. & Hamid, Q. Pathogenesis of severe asthma. *Clin. Exp. Allergy* **42,** 625–37 (2012).

8. Woolcock, A. J. & Peat, J. K. Epidemiology of Bronchial Hyperresponsiveness. *Clin. Rev. Allergy* **7,** 245–256 (1989).

9. Sterk, P. J. & Bel, E. H. Bronchial hyperresponsiveness: the need for a distinction between hypersensitivity and excessive airway narrowing. *Eur. Respir. J. Off. J. Eur. Soc. Clin. Respir. Physiol.* **2,** 267–274 (1989).

10. West, A. R. *et al.* Airway contractility and remodeling: links to asthma symptoms. *Pulm. Pharmacol. Ther.* **26,** 3–12 (2013).

11. Sumi, Y. & Hamid, Q. Airway remodeling in asthma. *Allergol. Int.* **56,** 341–8 (2007).

12. Bergeron, C. & Boulet, L.-P. Structural Changes in Airway Diseases: Characteristics, Mechanisms, Consequences and Pharmacologic Modulation. *Chest* (2006).

13. Erle, D. J. & Sheppard, D. The cell biology of asthma. *J. Cell Biol.* **205,** 621–631 (2014).

14. Shifren, A., Witt, C., Christie, C. & Castro, M. Mechanisms of remodeling in asthmatic airways. *J. Allergy* **2012,** 1–12 (2011).

15. Soja, J. *et al.* The use of endobronchial ultrasonography in assessment of bronchial wall remodeling in patients with asthma. *Chest* **136,** 797–804 (2009).

16. Gleich, G. J. Mechanisms of eosinophil-associated inflammation. *J. Allergy Clin. Immunol.* **105,** 651–663 (2000).

17. Bates, J. H. T., Stevenson, C. A., Aliyeva, M. & Lundblad, L. K. A. Airway responsiveness depends on the diffusion rate of methacholine across the airway wall. *J. Appl. Physiol.* **112,** 1670–1677 (2012).

18. Assoian, R. K. *et al.* Transforming Growth Factor-β in Human Platelets. Identification of a Major Storage Site, Purification, and Characterization. *J. Biol. Chem.* (1983).

19. Khalil, N. TGF-β: from latent to active. *Microbes Infect.* **1,** 1255–1263 (1999).

20. Dubois, C. M., Laprise, M.-H., Blanchette, F., Gentry, L. E. & Leduc, R. Processing of Transforming Growth Factor β1 Precursor by Human Furin Convertase. *J. Biol. Chem.* **270,** 10618–10624 (1995).

21. Taipale, J. & Miyazono, K. Latent Transforming Growth Factor-β1 Associates to Fibroblast Extracellular Matrix via Latent TGF-β Binding Protein. *J. Cell Biol.* **124,** 171–181 (1994).

22. Annes, J. P. Making sense of latent TGFβ activation. *J. Cell Sci.* **116,** 217–224 (2003).

23. Dabovic, B. *et al.* Bone abnormalities in latent TGF-β binding protein (Ltbp)-3-null mice

indicate a role for Ltbp-3 in modulating TGF-β bioavailability. *J. Cell Biol.* **156,** 227–232 (2002).

24. Bossé, Y. & Rola-Pleszczynski, M. Controversy surrounding the increased expression of TGF beta 1 in asthma. *Respir. Res.* **8,** 66 (2007).

25. de Caestecker, M. The transforming growth factor-β superfamily of receptors. *Cytokine Growth Factor Rev.* **15,** 1–11 (2004).

26. Lopez-casillas, F., Wrana, J. L. & Massague, J. Betaglycan Presents Ligand to the TGFP Signaling Receptor. *Cell* **73,** 1435–1444 (1993).

27. De Crescenzo, G. *et al.* Three key residues underlie the differential affinity of the TGFβ isoforms for the TGFβ type II receptor. *J. Mol. Biol.* **355,** 47–62 (2006).

28. Koo, S. H., Cunningham, M. C., Arabshahi, B., Gruss, J. S. & Grant, J. H. 3rd. The transforming growth factor-beta 3 knock-out mouse: an animal model for cleft palate. *Plast. Reconstr. Surg.* **108,** 938–951 (2001).

29. Kulkarni, A. B. *et al.* Transforming growth factor β1 null mutation in mice causes excessive inflammatory response and early death. *Proc. Natl. Acad. Sci. U. S. A.* **90,** 770–774 (1993).

30. Sanford, L. P. *et al.* TGFβ2 knockout mice have multiple developmental defects that are non- overlapping with other TGFβ knockout phenotypes. *Development* **2670,** 2659–2670 (1997).

31. Sporn, M. B. & Roberts, A. B. Transforming Growth Factor-β: Recent Progress and New Challenges. *J. Cell Biol.* **119,** 1017–1021 (1992).

32. Feng, X.-H. & Derynck, R. Specificity and versatility in TGF-β signaling through Smads.

Annu. Rev. Cell Dev. Biol. **21,** 659–93 (2005).

33. Wrana, J. L., Attisano, L., Wieser, R., Ventura, F. & Massague, J. Mechanism of activation of the TGF-β receptor. *Nature* (1994).

34. Schmierer, B. & Hill, C. S. TGFβ-SMAD signal transduction: molecular specificity and functional flexibility. *Nat. Rev. Mol. Cell Biol.* **8,** 970–982 (2007).

35. Yu, L., Hébert, M. C. & Zhang, Y. E. TGF-β receptor-activated p38 MAP kinase mediates Smad-independent TGF-β responses. *EMBO J.* **21,** 3749–3759 (2002).

36. Itoh, S. *et al.* Elucidation of Smad requirement in transforming growth factor-β type I receptor-induced responses. *J. Biol. Chem.* **278,** 3751–3761 (2003).

37. Xu, J., Lamouille, S. & Derynck, R. TGF-beta-induced epithelial to mesenchymal transition. *Cell Res.* **19,** 156–172 (2009).

38. Xie, L. *et al.* Activation of the Erk pathway is required for TGF-beta1-induced EMT in vitro. *Neoplasia* **6,** 603–610 (2004).

39. Crawford, S. E. *et al.* Thrombospondin-1 is a major activator of TGF-β1 in vivo. *Cell* **93,** 1159–1170 (1998).

40. Yu, Q. & Stamenkovic, I. Cell surface-localized matrix mealloproteinase-9 proteolytically activates TGF-beta and promotes tumor invasion and angiogenesis. *Genes Dev.* **14,** 163–176 (2000).

41. Munger, J. S. *et al.* The integrin αvβ6 binds and activates latent TGFβ1: A mechanism for regulating pulmonary inflammation and fibrosis. *Cell* **96,** 319–328 (1999).

42. Yehualaeshet, T. *et al.* Activation of Rat Alveolar Macrophage-Derived Latent Transforming Growth Factor β-1 by Plasmin Requires Interaction with Thrombospondin-1

and its Cell Surface Receptor, CD36. *Am. J. Pathol.* **155,** 841–851 (1999).

43. Howat, W. J., Holgate, S. T. & Lackie, P. M. TGF-beta isoform release and activation during in vitro bronchial epithelial wound repair. *Am. J. Physiol. Lung Cell. Mol. Physiol.* **282,** L115-23 (2002).

44. Tatler, A. L. *et al.* Integrin αvβ5-mediated TGF-β activation by airway smooth muscle cells in asthma. *J. Immunol.* **187,** 6094–107 (2011).

45. Tatler, A. L. & Jenkins, G. TGF-β activation and lung fibrosis. *Proc. Am. Thorac. Soc.* **9,** 130–6 (2012).

46. Nomura, A. *et al.* Increases in collagen type I synthesis in asthma: the role of eosinophils and transforming growth factor-bbeta. *Clin. Exp. Allergy* **32,** 860–865 (2002).

47. Batra, V. *et al.* Bronchoalveolar lavage fluid concentrations of transforming growth factor (TGF)-β1 , TGF-β2 , interleukin (IL)-4 and IL-13 after segmental allergen challenge and their effects on a -smooth muscle actin and collagen III synthesis by primary human lung fibr. *Clin. Exp. Allergy* **34,** 437–444 (2004).

48. Tillie-Leblond, I. *et al.* Balance between proinflammatory cytokines and their inhibitors in bronchial lavage from patients with status asthmaticus. *Am. J. Respir. Crit. Care Med.* **159,** 487–94 (1999).

49. Matsunaga, K. *et al.* Airway cytokine expression measured by means of protein array in exhaled breath condensate: correlation with physiologic properties in asthmatic patients. *J. Allergy Clin. Immunol.* **118,** 84–90 (2006).

50. Torrego, A., Hew, M., Oates, T., Sukkar, M. & Fan Chung, K. Expression and activation of TGF-beta isoforms in acute allergen-induced remodelling in asthma. *Thorax* **62,** 307–313 (2007).

51. Sagara, H. *et al.* Activation of TGF-β/Smad2 signaling is associated with airway remodeling in asthma. *J. Allergy Clin. Immunol.* **110,** 249–254 (2002).

52. Phipps, S. *et al.* Acute allergen-induced airway remodeling in atopic asthma. *Am. J. Respir. Cell Mol. Biol.* **31,** 626–632 (2004).

53. Fixman, E. D., Tolloczko, B. & Lauzon, A. in *Physiologic Basis of Respiratory Disease* (eds. Hamid, Q., Shannon, J. & Martin, J.) (2005).

54. Ratz, P. H., Berg, K. M., Urban, N. H., Miner, A. S. & Paul, H. Regulation of smooth muscle calcium sensitivity : KCl as a calcium- sensitizing stimulus. *Am. J. Physiol. Cell Physiol.* **288,** C769-783 (2005).

55. Lodish, H. *et al. Molecular Cell Biology*. (Sara Tenny, W.H. Freeman and Company, 2008). at <http://www.amazon.com/Molecular-Biology-Lodish-Fifth-Edition/dp/B004GH8P6E>

56. Halayko, A. J. & Solway, J. Molecular Mechanisms of Phenotypic Plasticity in Smooth Muscle Cells. *J. Appl. Physiol.* **90,** 358–368 (2001).

57. Halayko, A. J., Tran, T. & Gosens, R. Phenotype and functional plasticity of airway smooth muscle: role of caveolae and caveolins. *Proc. Am. Thorac. Soc.* **5,** 80–88 (2008).

58. Seow, C. Y. & Solway, J. Mechanical and structural plasticity. *Compr. Physiol.* **1,** 283–293 (2011).

59. Johnson, P. R. *et al.* Airway smooth muscle cell proliferation is increased in asthma. *Am. J. Respir. Crit. Care Med.* **164,** 474–477 (2001).

60. Hassan, M. *et al.* Airway smooth muscle remodeling is a dynamic process in severe long-standing asthma. *J. Allergy Clin. Immunol.* **125,** 1037–1045 (2010).

61. Bossé, Y. & Paré, P. in *Lung Diseases - Selected State of the Art Reviews* (ed. Irusen, E. M.)

3–54 (2012). at <http://cdn.intechopen.com/pdfs/30242/InTech-Airway_smooth_muscle_in_asthma_symptoms_culprit_but_maybe_innocent.pdf>

62. McParland, B. E., Macklem, P. T. & Pare, P. D. Airway wall remodeling: friend or foe? *J. Appl. Physiol.* **95,** 426–434 (2003).

63. Solway, J. & Fredberg, J. J. Perhaps Airway Smooth Muscle Dysfunction Contributes to Asthmatic Bronchial Hyperresponsiveness After All. *Am. J. Respir. Cell Mol. Biol.* **17,** 144–146 (1997).

64. Léguillette, R. & Lauzon, A.-M. Molecular mechanics of smooth muscle contractile proteins in airway hyperresponsiveness and asthma. *Proc. Am. Thorac. Soc.* **5,** 40–46 (2008).

65. Bullimore, S. R. *et al.* Could an increase in airway smooth muscle shortening velocity cause airway hyperresponsiveness? *Am. J. Physiol. Lung Cell. Mol. Physiol.* **300,** L121–L131 (2011).

66. Ma, X. *et al.* Changes in biophysical and biochemical properties of single bronchial smooth muscle cells from asthmatic subjects. *Am. J. Physiol. Lung Cell. Mol. Physiol.* **283,** L1181-9 (2002).

67. Gerthoffer, W. T. & Murphy, R. a. Myosin phosphorylation and regulation of cross-bridge cycle in tracheal smooth muscle. *Am. J. Physiol.* **244,** C182–C187 (1983).

68. Gerthoffer, W. T. Dissociation of myosin phosphorylation and active tension during muscarinic stimulation of tracheal smooth muscle. *J. Pharmacol. Exp. Ther.* **240,** 8–15 (1987).

69. Léguillette, R. *et al.* Myosin, transgelin, and myosin light chain kinase expression and function in asthma. *Am. J. Respir. Crit. Care Med.* **179,** 194–204 (2009).

70. Babu, G. J. *et al.* Loss of SM-B myosin affects muscle shortening velocity and maximal force development. *Nat. Cell Biol.* **3,** 1025–1029 (2001).

71. Chen, G. & Khalil, N. TGF-beta1 increases proliferation of airway smooth muscle cells by phosphorylation of map kinases. *Respir. Res.* **7,** (2006).

72. Xie, S., Sukkar, M. B., Issa, R., Khorasani, N. M. & Chung, K. F. Mechanisms of induction of airway smooth muscle hyperplasia by transforming growth factor-beta. *Am. J. Physiol. Lung Cell. Mol. Physiol.* **293,** L245-53 (2007).

73. Bao, J. *et al.* Role of the short isoform of myosin light chain kinase in the contraction of cultured smooth muscle cells as examined by its down-regulation. *Proc. Natl. Acad. Sci. U. S. A.* **99,** 9556–9561 (2002).

74. Goldsmith, A. M. *et al.* Transforming growth factor-beta induces airway smooth muscle hypertrophy. *Am. J. Respir. Cell Mol. Biol.* **34,** 247–54 (2006).

75. Black, P. N., Young, P. G. & Skinner, S. J. Response of airway smooth muscle cells to TGF-beta 1: effects on growth and synthesis of glycosaminoglycans. *Am. J. Physiol. Lung Cell. Mol. Physiol.* **271,** L910–L917 (1996).

76. Coutts, A. *et al.* Release of biologically active TGF-beta from airway smooth muscle cells induces autocrine synthesis of collagen. *Am. J. Physiol. Lung Cell. Mol. Physiol.* **280,** L999–L1008 (2001).

77. Knight, D. A. & Holgate, S. T. The airway epithelium : Structural and functional properties in health and disease. *Respirology* **8,** 432–446 (2003).

78. Tam, A., Wadsworth, S., Dorscheid, D., Man, S. F. P. & Sin, D. D. The airway epithelium: more than just a structural barrier. *Ther. Adv. Respir. Dis.* **5,** 255–73 (2011).

79. Shahana, S. *et al.* Ultrastructure of bronchial biopsies from patients with allergic and non-allergic asthma. *Respir. Med.* **99,** 429–43 (2005).

80. Roth, H. M., Wadsworth, S. J., Kahn, M. & Knight, D. a. The airway epithelium in asthma: developmental issues that scar the airways for life? *Pulm. Pharmacol. Ther.* **25,** 420–6 (2012).

81. Hackett, T.-L. *et al.* Induction of epithelial-mesenchymal transition in primary airway epithelial cells from patients with asthma by transforming growth factor-beta1. *Am. J. Respir. Crit. Care Med.* **180,** 122–33 (2009).

82. Lamouille, S., Xu, J. & Derynck, R. Molecular mechanisms of epithelial-mesenchymal transition. *Nat. Rev. Mol. Cell Biol.* **15,** 178–96 (2014).

83. Kalluri, R. & Weinberg, R. A. The basics of epithelial-mesenchymal transition. *J. Clin. Invest.* **119,** 1420–1428 (2009).

84. Legrand, C. *et al.* Airway epithelial cell migration dynamics. MMP-9 role in cell-extracellular matrix remodeling. *J. Cell Biol.* **146,** 517–529 (1999).

85. Gilles, C., Newgreen, D. F., Sato, H. & Thompson, E. W. Matrix Metalloproteases and Epithelial-to-Mesenchymal Transition: Implications for Carcinoma Metastasis. *Madame Curie Bioscience Database* (2004). at <http://www.ncbi.nlm.nih.gov/books/NBK6387/>

86. Hackett, T.-L. Epithelial–mesenchymal transition in the pathophysiology of airway remodelling in asthma. *Curr. Opin. Allergy Clin. Immunol.* **12,** 53–59 (2012).

87. Johnson, J. R., Roos, A., Berg, T., Nord, M. & Fuxe, J. Chronic respiratory aeroallergen exposure in mice induces epithelial-mesenchymal transition in the large airways. *PLoS One* **6,** (2011).

88. Hackett, T.-L. *et al.* Characterization of side population cells from human airway epithelium. *Stem Cells* **26,** 2576–2585 (2008).

89. Vanhoutte, P. M. Airway epithelium-derived relaxing factor: myth, reality, or naivety? *Am. J. Physiol. Cell Physiol.* **304,** C813-20 (2013).

90. Folkerts, G. & Nijkamp, F. P. Airway epithelium: more than just a barrier! *Trends Pharmacol. Sci.* **19,** 334–41 (1998).

91. Matera, M. G. *et al.* Epithelium integrity is crucial for the relaxant activity of brain natriuretic peptide in human isolated bronchi. *Br. J. Pharmacol.* **163,** 1740–1754 (2011).

92. Gallos, G. *et al.* Endogenous γ-aminobutyric Acid Modulates Tonic Guinea Pig Airway Tone and Propofol-induced Airway Smooth Muscle Relaxation. *Anesthesiology* **110,** 748–758 (2009).

93. Zaidi, S. *et al.* Functional expression of γ-amino butyric acid transporter 2 in human and guinea pig airway epithelium and smooth muscle. *Am. J. Respir. Cell Mol. Biol.* **45,** 332–339 (2011).

94. Holgate, S. T. The airway epithelium is central to the pathogenesis of asthma. *Allergol. Int.* **57,** 1–10 (2008).

95. Heijink, I. H., Nawijn, M. C. & Hackett, T.-L. Airway epithelial barrier function regulates the pathogenesis of allergic asthma. *Clin. Exp. Allergy* **44,** 620–30 (2014).

96. Holgate, S. T. Airway epithelial–mesenchymal interactions in the pathogenesis of asthma. *Drug Discov. Today Dis. Mech.* **9,** e103–e110 (2012).

97. Zheng, X.-L. Myocardin and smooth muscle differentiation. *Arch. Biochem. Biophys.* **543,** 48–56 (2014).

98. Long, X., Creemers, E. E., Wang, D.-Z., Olson, E. N. & Miano, J. M. Myocardin is a bifunctional switch for smooth versus skeletal muscle differentiation. *Proc. Natl. Acad. Sci. U. S. A.* **104,** 16570–16575 (2007).

99. Mack, C. P. & Owens, G. K. Regulation of Smooth Muscle α-Actin Expression In Vivo Is Dependent on CArG Elements Within the 5' and First Intron Promoter Regions. *Circ Res* **84,** 852–861 (1999).

100. Manabe, I. & Owens, G. K. CArG elements control smooth muscle subtype-specific expression of smooth muscle myosin in vivo. *J. Clin. Invest.* **107,** 823–834 (2001).

101. Chen, M. *et al.* Regulation of 130-kDa smooth muscle myosin light chain kinase expression by an intronic CArG element. *J. Biol. Chem.* **288,** 34647–34657 (2013).

102. Long, X. *et al.* Smooth muscle calponin: An unconventional CArG-dependent gene that antagonizes neointimal formation. *Arterioscler. Thromb. Vasc. Biol.* **31,** 2172–2180 (2011).

103. Miano, J. M., Long, X. & Fujiwara, K. Serum response factor: master regulator of the actin cytoskeleton and contractile apparatus. *Am. J. Physiol. Cell Physiol.* **292,** C70–C81 (2007).

104. Wang, Z., Wang, D.-Z., Pipes, G. C. T. & Olson, E. N. Myocardin is a master regulator of smooth muscle gene expression. *Proc. Natl. Acad. Sci. U. S. A.* **100,** 7129–34 (2003).

105. Creemers, E. E., Sutherland, L. B., McAnally, J., Richardson, J. A. & Olson, E. N. Myocardin is a direct transcriptional target of Mef2, Tead and Foxo proteins during cardiovascular development. *Development* **133,** 4245–4256 (2006).

106. Miano, J. M. Myocardin in biology and disease. *J. Biomed. Res.* **29,** 3–19 (2015).

107. Lin, Q. *et al.* Requirement of the MADS-box transcription factor MEF2C for vascular

development. *Development* **125,** 4565–74 (1998).

108. Liu, Z. P., Wang, Z., Yanagisawa, H. & Olson, E. N. Phenotypic modulation of smooth muscle cells through interaction of Foxo4 and Myocardin. *Dev. Cell* **9,** 261–270 (2005).

109. Liu, F., Wang, X., Hu, G., Wang, Y. & Zhou, J. The transcription factor TEAD1 represses smooth Musclespecific gene expression by Abolishing Myocardin function. *J. Biol. Chem.* **289,** 3308–3316 (2014).

110. Imamura, M., Long, X., Nanda, V. & Miano, J. M. Expression and functional activity of four myocardin isoforms. *Gene* **464,** 1–10 (2010).

111. Long, X., Bell, R. D., Gerthoffer, W. T., Zlokovic, B. V. & Miano, J. M. Myocardin is sufficient for a smooth muscle-like contractile phenotype. *Arterioscler. Thromb. Vasc. Biol.* **28,** 1505–1510 (2008).

112. Eddinger, T. J. & Meer, D. P. Myosin II isoforms in smooth muscle: heterogeneity and function. *Am. J. Physiol. Cell Physiol.* **293,** C493–C508 (2007).

113. Lowey, S. & Trybus, K. M. Role of skeletal and smooth muscle myosin light chains. *Biophys J* **68,** 120S–126S; discussion 126S–127S (1995).

114. Deng, Z. *et al.* Smooth Muscle Myosin Heavy Chain Locus (MYH11) Maps to 16p13.13-p13.12 and Establishes a New Region of Conserved Synteny between Human 16p and Mouse 16.pdf. *Genomics* **18,** 156–159 (1993).

115. Yoon, S. J., Seiler, S. H., Kucherlapati, R. & Leinwand, L. Organization of the human skeletal myosin heavy chain gene cluster. *Proc. Natl. Acad. Sci. U. S. A.* **89,** 12078–82 (1992).

116. Schiaffino, S. & Reggiani, C. Myosin isoforms in mammalian skeletal muscle. *J Appl*

Physiol **77,** 493–501 (1994).

117. Fischer, R. *et al.* Multiple divergent mRNAs code for a single human calmodulin. *J. Biol. Chem.* **263,** 17055–17062 (1988).

118. Van Lierop, J. E. *et al.* Activation of smooth muscle myosin light chain kinase by calmodulin. Role of LYS30 and GLY40. *J. Biol. Chem.* **277,** 6550–6558 (2002).

119. Chin, D. & Means, A. R. Calmodulin: A prototypical calcium sensor. *Trends Cell Biol.* **10,** 322–328 (2000).

120. Johnson, J. D., Snyder, C., Walsh, M. & Flynn, M. Effects of Myosin Light Chain Kinase and Peptides on Ca 2 ⁒. Exchange with the N- and C-terminal Ca 2 ⁒. Binding Sites of Calmodulin *. **271,** 761–767 (1996).

121. Khapchaev, A. Y. & Shirinsky, V. P. Myosin Light Chain Kinase MYLK1 : Anatomy , Interactions , Functions , and Regulation. **81,** 1676–1697 (2016).

122. Blue, E. K. *et al.* 220- and 130-kDa MLCKs have distinct tissue distributions and intracellular localization patterns. *Clin. Lymphoma* **9,** 19–22 (2010).

123. Hirota, J. a, Nguyen, T. T. B., Schaafsma, D., Sharma, P. & Tran, T. Airway smooth muscle in asthma: phenotype plasticity and function. *Pulm. Pharmacol. Ther.* **22,** 370–8 (2009).

124. Halayko, A. J., Salari, H., Ma, X. & Stephens, N. L. Markers of airway smooth muscle cell phenotype. *Am. J. Physiol.* **270,** L1040-51 (1996).

125. Surks, H. K., Richards, C. T. & Mendelsohn, M. E. Myosin phosphatase-Rho interacting protein: A new member of the myosin phosphatase complex that directly binds RhoA. *J. Biol. Chem.* **278,** 51484–51493 (2003).

126. Surks, H. K., Riddick, N. & Ohtani, K. I. M-RIP targets myosin phosphatase to stress fibers

to regulate myosin light chain phosphorylation in vascular smooth muscle cells. *J. Biol. Chem.* **280,** 42543–42551 (2005).

127. Riddick, N., Ohtani, K. I. & Surks, H. K. Targeting by myosin phosphatase-RhoA interacting protein mediates RhoA/ROCK regulation of myosin phosphatase. *J. Cell. Biochem.* **103,** 1158–1170 (2008).

128. Liu, R. & Jin, J. P. Calponin isoforms CNN1, CNN2 and CNN3: Regulators for actin cytoskeleton functions in smooth muscle and non-muscle cells. *Gene* **585,** 143–153 (2016).

129. Mino, T., Yuasa, U., Nakamura, F., Naka, M. & Tanaka, T. Two distinct actin-binding sites of smooth muscle calponin. *Eur. J. Biochem.* **251,** 262–268 (1998).

130. Naka, M. *et al.* Modulation of smooth muscle calponin by protein kinase C and calmodulin. *Biochem. Biophys. Res. Commun.* **171,** 933–937 (1990).

131. Winder, S. J. & Walsh, P. Smooth Muscle Calponin: Inhibition of Actomyosin MgATPase and Regulation by Phosphorylation. *J. Biol. Chem.* **265,** (1990).

132. Winder, S. J., Walsh, M. P., Vasulka, C. & Johnson, J. D. Calponin-calmodulin interaction: Properties and effects on smooth and skeletal muscle actin binding and actomyosin ATPases. *Biochemistry* **32,** 13327–13333 (1993).

133. Samaha, F. F. *et al.* Developmental pattern of expression and genomic organization of the calponin-h1 gene: A contractile smooth muscle cell marker. *J. Biol. Chem.* **271,** 395–403 (1996).

134. Duband, J. L., Gimona, M., Scatena, M., Sartore, S. & Small, J. V. Calponin and Sm22 As Differentiation Markers of Smooth-Muscle - Spatiotemporal Distribution During Avian Embryonic-Development. *Differentiation* **55,** 1–11 (1993).

135. Ulmer, B. *et al.* Calponin 2 Acts As an Effector of Noncanonical Wnt-Mediated Cell Polarization during Neural Crest Cell Migration. *Cell Rep.* **3,** 615–621 (2013).

136. Hossain, M. M., Crish, J. F., Eckert, R. L., Lin, J. J.-C. & Jin, J.-P. H2-calponin is regulated by mechanical tension and modifies the function of actin cytoskeleton. *J. Biol. Chem.* **280,** 42442–42453 (2005).

137. Hossain, M. M., Hwang, D. Y., Huang, Q. Q. & Jin, J. P. Developmentally regulated expression of calponin isoforms and the role of H2-calponin in cell proliferation. *Biophys. J.* **82,** 417A--417A (2002).

138. Wu, H. Q. & Schwarcz, R. Seizure activity causes elevation of endogenous extracellular kynurenic acid in the rat brain. *Brain Res. Bull.* **39,** 155–162 (1996).

139. Fujii, T., Yabe, S., Nakamura, K. & Koizumi, Y. Functional analysis of rat acidic calponin. *Biol.Pharm.Bull.* **25,** 573–579 (2002).

140. Mendez, M. G., Kojima, S.-I. & Goldman, R. D. Vimentin induces changes in cell shape, motility, and adhesion during the epithelial to mesenchymal transition. *FASEB J.* **24,** 1838–51 (2010).

141. Song, Y., Washington, M. K. & Crawford, H. C. Loss of FOXA1/2 is essential for the epithelial-to-mesenchymal transition in pancreatic cancer. *Cancer Res.* **70,** 2115–2125 (2010).

142. Mani, S. A. *et al.* Mesenchyme Forkhead 1 (FOXC2) plays a key role in metastasis and is associated with aggressive basal-like breast cancers. *Proc. Natl. Acad. Sci. U. S. A.* **104,** 10069–74 (2007).

143. Ito, J. *et al.* Wound-induced TGF-β1 and TGF-β2 enhance airway epithelial repair via HB-EGF and TGF-α. *Biochem. Biophys. Res. Commun.* **412,** 109–14 (2011).

144. Rogel, M. R. *et al.* Vimentin is sufficient and required for wound repair and remodeling in alveolar epithelial cells. *FASEB J.* **25,** 3873–83 (2011).

145. Tian, X. *et al.* E-Cadherin/β-catenin complex and the epithelial barrier. *J. Biomed. Biotechnol.* **2011,** (2011).

146. Le, T. L., Yap, A. S. & Stow, J. L. Recycling of E-cadherin: A potential mechanism for regulating cadherin dynamics. *J. Cell Biol.* **146,** 219–232 (1999).

147. Biswas, K. H. & Zaidel-Bar, R. Early events in the assembly of E-cadherin adhesions. *Exp. Cell Res.* (2017). doi:10.1016/j.yexcr.2017.02.037

148. Deng, L., Fairbank, N. J., Cole, D. J., Fredberg, J. J. & Maksym, G. N. Airway smooth muscle tone modulates mechanically induced cytoskeletal stiffening and remodeling. *J Appl Physiol* **99,** 634–641 (2005).

149. Fairbank, N. J. Cytoskeletal Stress Alters Airway Smooth Muscle Cell Structure and Contractile Function. (Dalhousie University, 2008).

150. Puig-De-Morales, M. *et al.* Measurement of cell microrheology by magnetic twisting cytometry with frequency domain demodulation. *J. Appl. Physiol.* **91,** 1152–1159 (2001).

151. Valberg, P. A. & Butler, J. P. Magnetic particle motions within living cells. Physical theory and techniques. *Biophys. J.* **52,** 537–550 (1987).

152. Fabry, B. *et al.* Time course and heterogeneity of contractile responses in cultured human airway smooth muscle cells. *J. Appl. Physiol.* **91,** 986–94 (2001).

153. Fabry, B. *et al.* Scaling the Microrheology of Living Cells. *Phys. Rev. Lett.* **87,** 148102 (2001).

154. Maksym, G. N. *et al.* Mechanical properties of cultured human airway smooth muscle

cells from 0.05 to 0.4 Hz. *J. Appl. Physiol.* **89,** 1619–32 (2000).

155. An, S. S., Fabry, B., Trepat, X., Wang, N. & Fredberg, J. J. Do biophysical properties of the airway smooth muscle in culture predict airway hyperresponsiveness? *Am. J. Respir. Cell Mol. Biol.* **35,** 55–64 (2006).

156. Deng, L., Fairbank, N. J., Fabry, B., Smith, P. G. & Maksym, G. N. Localized mechanical stress induces time-dependent actin cytoskeletal remodeling and stiffening in cultured airway smooth muscle cells. *Am. J. Physiol. Cell Physiol.* **287,** C440-8 (2004).

157. Chen, Y. Epithelial cell modulation of airway smooth muscle cell contractile phenotype. (Dalhousie University, 2009).

158. Zaman, N. Influence of Loading and Matrix Stiffness on Airway Smooth Muscle Contractile Function and Phenotype in a Novel 3D Microtissue Culture Model. (Dalhousie University, 2013).

159. Cozens, A. L. *et al.* CFTR expression and chloride secretion in polarized immortal human bronchial epithelial cells. *Am. J. Respir. Cell Mol. Biol.* **10,** 38–47 (1994).

160. Ahuja, D., Saenz-Robles, M. T. & Pipas, J. M. SV40 large T antigen targets multiple cellular pathways to elicit cellular transformation. *Oncogene* **24,** 7729–7745 (2005).

161. Ehrhardt, C. *et al.* Influence of apical fluid volume on the development of functional intercellular junctions in the human epithelial cell line 16HBE14o-: implications for the use of this cell line as an in vitro model for bronchial drug absorption studies. *Cell Tissue Res.* **308,** 391–400 (2002).

162. Eberhard, L. HVM-3000 Magnetizer manual. EOL Eberhard, CH-4104. (2002).

163. Smith, P. G., Roy, C., Zhang, Y. N. & Chauduri, S. Mechanical stress increases RhoA

activation in airway smooth muscle cells. *Am. J. Respir. Cell Mol. Biol.* **28,** 436–442 (2003).

164. Shahana, S., Jaunmuktane, Z., Stenkvist Asplund, M. & Roomans, G. M. Ultrastructural investigation of epithelial damage in asthmatic and non-asthmatic nasal polyps. *Respir. Med.* **100,** 2018–2028 (2006).

165. Xiao, C. *et al.* Defective epithelial barrier function in asthma. *J. Allergy Clin. Immunol.* **128,** (2011).

166. Heijink, I. H., Postma, D. S., Noordhoek, J. a., Broekema, M. & Kapus, A. House dust mite-promoted epithelial-to-mesenchymal transition in human bronchial epithelium. *Am. J. Respir. Cell Mol. Biol.* **42,** 69–79 (2010).

167. Oida, T. & Weiner, H. L. Depletion of TGF-β from fetal bovine serum. *J. Immunol. Methods* **362,** 195–198 (2010).

168. Zhang, M. *et al.* TGF-beta1 induces human bronchial epithelial cell-to-mesenchymal transition in vitro. *Lung* **187,** 187–94 (2009).

169. Câmara, J. & Jarai, G. Epithelial-mesenchymal transition in primary human bronchial epithelial cells is Smad-dependent and enhanced by fibronectin and TNF-alpha. *Fibrogenesis Tissue Repair* **3,** 2 (2010).

170. Redington, A. E., Roche, W. R., Holgate, S. T. & Howarth, P. H. Co-localization of Immunoreactive Transforming Growth Factor-Beta1 and Decorin in Bronchial Biopsies from Asthmatic and Normal Subjects. *J. Pathol.* **186,** 410–415 (1998).

171. Clarke, D. C., Brown, M. L., Erickson, R. A., Shi, Y. & Liu, X. Transforming growth factor beta depletion is the primary determinant of Smad signaling kinetics. *Mol Cell Biol* **29,** 2443–2455 (2009).

172. Massague, J. & Kelly, B. Internalization of Transforming Growth Factor-β and Its Receptor in BALB/c 3T3 Fibroblasts. *J. Cell. Physiol.* **128,** 216–222 (1986).

173. Jinesh G., G., Chunduru, S. & Kamat, a. M. Smac mimetic enables the anticancer action of BCG-stimulated neutrophils through TNF- but not through TRAIL and FasL. *J. Leukoc. Biol.* **92,** 233–244 (2012).

174. Masieri, F. Online Forum 'Does anyone have experience in using conditioned media in cell lines? What are your experiences and recommendations?' *ResearchGate* (2013). at <https://www.researchgate.net/post/Does_anyone_have_experience_in_using_conditioned_media_in_cell_lines_What_are_your_experiences_and_recommendations>

175. Wang, N. *et al.* Cell prestress. I. Stiffness and prestress are closely associated in adherent contractile cells. *Am. J. Physiol. Cell Physiol.* **282,** C606–C616 (2002).

176. Vanhoutte, P. M. Epithelium derived relaxing factor: myth or reality? *Thorax* **43,** 665–668 (1988).

177. Flavahan, N. a, Abbiss, C. R., Rimele, T. J. & Vanhoutte, P. M. Respiratory epithelium inhibits bronchial smooth muscle tone. *J. Appl. Physiol.* **58,** 834–838 (1985).

178. Aizawa, H., Miyazaki, N., Shigematsu, N. & Tomooka, M. A possible role of airway epithelium in modulating hyperresponsiveness. *Br. J. Pharmacol.* **93,** 139–145 (1988).

179. Barnes, P. J., Cuss, F. M. & Palmer, J. B. The effect of airway epithelium on smooth muscle contractility in bovine trachea. *Br. J. Pharmacol.* **86,** 685–691 (1985).

180. Oenema, T. a *et al.* Bronchoconstriction Induces TGF-β Release and Airway Remodelling in Guinea Pig Lung Slices. *PLoS One* **8,** e65580 (2013).

181. Du, K. L. *et al.* Myocardin Is a Critical Serum Response Factor Cofactor in the

Transcriptional Program Regulating Smooth Muscle Cell Differentiation. *Mol. Cell. Biol.* **23,** 2425–2437 (2003).

182. Yoshida, T., Kawai-Kowase, K. & Owens, G. K. Forced expression of myocardin is not sufficient for induction of smooth muscle differentiation in multipotential embryonic cells. *Arterioscler. Thromb. Vasc. Biol.* **24,** 1596–1601 (2004).

183. Panettieri, R. A., Murray, R. K., DePalo, L. R., Yadvish, P. A. & Kotlikoff, M. I. A human airway smooth muscle cell line that retains physiological responsiveness. *Am J Physiol Cell Physiol* **256,** C329-335 (1989).

184. Damera, G. & Panettieri, R. a. Does airway smooth muscle express an inflammatory phenotype in asthma? *Br. J. Pharmacol.* **163,** 68–80 (2011).

185. An, S. S. *et al.* An inflammation-independent contraction mechanophenotype of airway smooth muscle in asthma. *J. Allergy Clin. Immunol.* **138,** 294–297.e4 (2016).

186. Vignola, A. M. *et al.* Transforming Growth Factor-β Expression in Mucosal Biopsies in Asthma and Chronic Bronchitis. *Am. J. Respir. Crit. Care Med.* **156,** 591–599 (1997).

187. Hershenson, M. B., Brown, M., Camoretti-Mercado, B. & Solway, J. Airway Smooth Muscle in Asthma. *Annu. Rev. Pathol. Dis.* **3,** 523–555 (2008).

188. Millipore. Millicell® -ERS User Guide P17304, Rev. A, 2/96. (1996).

189. Shuler, L. & Hickman, J. J. *TEER Measurement Techniques for in vitro barrier model systems*. **20,** (2016).

190. Chi, R. J., Simon, A. R., Bienkiewicz, E. A., Felix, A. & Keller, T. C. S. Smooth muscle titin Zq domain interaction with the smooth muscle ??-actinin central rod. *J. Biol. Chem.* **283,** 20959–20967 (2008).

191. Stamenović, D., Mijailovich, S. M., Tolić-Nørrelykke, I. M., Chen, J. & Wang, N. Cell prestress. II. Contribution of microtubules. *Am. J. Physiol. Cell Physiol.* **282,** C617–C624 (2002).

192. Dekkers, B. G. J., Bos, I. S. T., Zaagsma, J. & Meurs, H. Functional consequences of human airway smooth muscle phenotype plasticity. *Br. J. Pharmacol.* **166,** 359–367 (2012).

193. SANTA CRUZ BIOTECHNOLOGY. Calponin 1/2/3 (FL-297): sc-28545. 1 (2015).

194. SANTA CRUZ BIOTECHNOLOGY. MYLK (H-195): sc-25428. (2015).

195. Malavia, N. K. *et al.* Airway epithelium stimulates smooth muscle proliferation. *Am. J. Respir. Cell Mol. Biol.* **41,** 297–304 (2009).

196. Damera, G. & Panettieri, R. A. Airway Smooth Muscle : Is There a Phenotype Associated with Asthma ? (2006).

197. Page, K., Li, J. & Hershenson, M. B. p38 MAP kinase negatively regulates cyclin D1 expression in airway smooth muscle cells. *Am. J. Physiol. Lung Cell. Mol. Physiol.* **280,** L955-64 (2001).

198. Forbes, B., Shah, A., Martin, G. P. & Lansley, A. B. The human bronchial epithelial cell line 16HBE14o− as a model system of the airways for studying drug transport. *Int. J. Pharm.* **257,** 161–167 (2003).

Appendix

A.

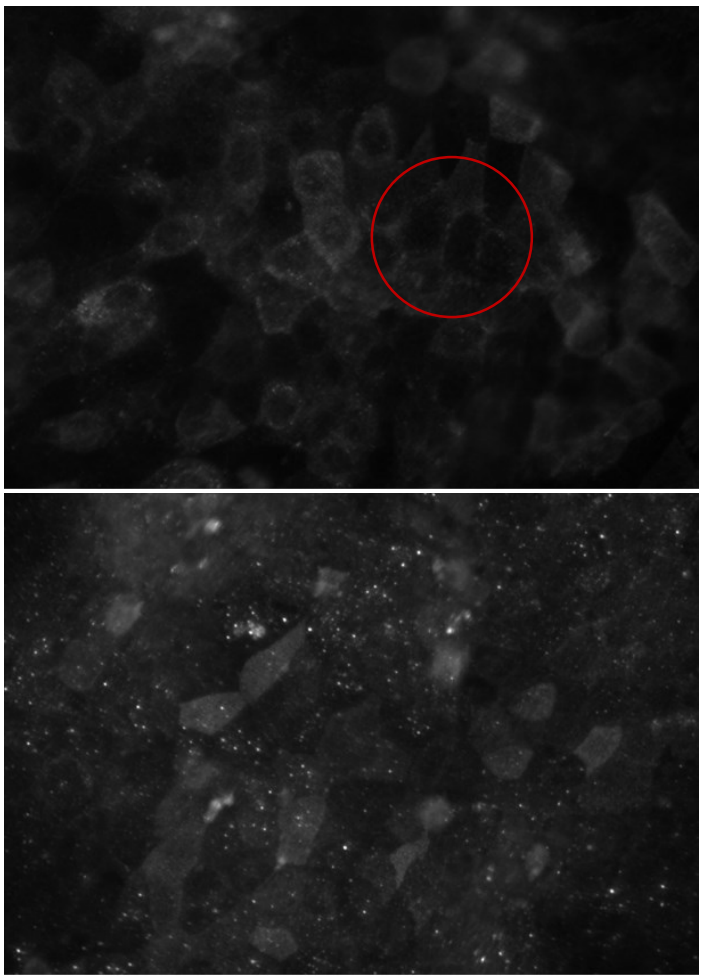

Appendix A: 16HBE14o- cells immunostained for E-cadherin. Top photograph shows cells that were not permeabilized prior to the immunostaining. E-cadherin on the cell surface is visible here. Some more differentiated cells show E-cadherin staining only at the cell-cell boundaries (red circle). Bottom photograph shows cells that were permeabilized prior to immunostaining. Staining appears more diffuse, some cell boundaries are difficult to distinguish, and significant speckling artifacts from undetermined source are visible.